NONDESTRUCTIVE VIBRATORY TESTING OF AIRPORT PAVEMENTS. VOLUME II: THEORETICAL STUDY OF THE DYNAMIC STIFFNESS AND ITS APPLICATION TO THE VIBRATORY NONDESTRUCTIVE METHOD OF TESTING PAVEMENTS

Richard A. Weiss

Army Engineer Waterways Experiment Station

Prepared for:

Federal Aviation Administration

April 1975

Report No. FAA-RD-73-205-II

NONDESTRUCTIVE VIBRATORY TESTING OF AIRPORT PAVEMENTS

VOLUME II

Theoretical Study of the Dynamic Stiffness and Its Application to the Vibratory Nondestructive Method of Testing Pavements

Richard A. Weiss

U. S. Army Engineer Waterways Experiment Station
Soils and Pavements Laboratory
Vicksburg, Miss. 39180

APRIL 1975
FINAL REPORT

Prepared for

U.S. DEPARTMENT OF TRANSPORTATION
FEDERAL AVIATION ADMINISTRATION
Systems Research & Development Service
Washington, D.C. 20590

NOTICES

This document is disseminated under the sponsorship of the Department of Transportation in the interest of information exchange. The United States Government assumes no liability for its contents or use thereof.

The United States Government does not endorse products or manufacturers. Trade or manufacturers' names appear herein solely because they are considered essential to the object of this report.

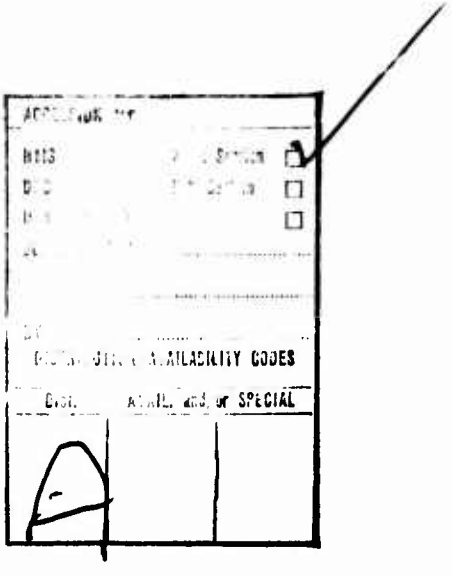

Technical Report Documentation Page

1. Report No.	2 Government Accession No.	3 Recipient's Catalog No
FAA-RD-73-205-II		

4. Title and Subtitle	5. Report Date
NONDESTRUCTIVE VIBRATORY TESTING OF AIRPORT PAVEMENTS VOLUME II: THEORETICAL STUDY OF THE DYNAMIC STIFFNESS AND ITS APPLICATION TO THE VIBRATORY NONDESTRUCTIVE METHOD OF TESTING PAVEMENTS	April 1975
	6. Performing Organization Code
7. Author(s) Richard A. Weiss	8. Performing Organization Report No. Technical Report S-75-Volume II
9. Performing Organization Name and Address U. S. Army Engineer Waterways Experiment Station Soils and Pavements Laboratory, P. O. Box 631 Vicksburg, Miss. 39180	10 Work Unit No. (TRAIS)
	11. Contract or Grant No. FA71-WAI-218
	13. Type of Report and Period Covered Final report
12. Sponsoring Agency Name and Address Department of Transportation Federal Aviation Administration Systems Research and Development Service Washington, D. C. 20591	14. Sponsoring Agency Code

15. Supplementary Notes

16. Abstract

A theoretical and experimental study of the dynamic load-deflection curves of pavements was conducted to determine the dependence of the measured dynamic stiffness values of a pavement on the type of vibrator that is used to make the measurements, and to correlate dynamic stiffness measurements obtained from different vibrators at the same pavement location. Experimental tests were conducted to verify the theoretical results. The dynamic load-deflection curves of pavements are found to be nonlinear, and a nonlinear vibration theory of pavements is developed to describe these curves. This study gives a method of determining the shear modulus and thickness of each pavement layer directly from the measured values of dynamic stiffness for a series of vibrator baseplate sizes. This method may be of practical value for nondestructively determining the subsurface structure of a pavement.

Volume I, "Experimental Test Results and Development of Evaluation Methodology and Procedure" is being prepared and will be released soon.

PRICES SUBJECT TO CHANGE

17. Key Words	18. Distribution Statement
Airfield pavements Load distribution Nondestructive tests Pavements Vibration tests	Document is available to the public through the National Technical Information Service, Springfield, Va. 22151

19. Security Classif. (of this report)	20. Security Classif. (of this page)	21. No. of Pages	22. Price
Unclassified	Unclassified	111	525-225

Form DOT F 1700.7 (8-72) Reproduction of completed page authorized

PREFACE

This study was conducted during the period April 1972-October 1974 by personnel of the U. S. Army Engineer Waterways Experiment Station (WES). It was sponsored by the Federal Aviation Administration through part of Inter-Agency Agreement FA71-WAI-218, "Development of Airport Pavement Criteria."

The study was done under the general supervision of Messrs. J. P. Sale and R. G. Ahlvin, Chief and Assistant Chief, respectively, of the Soils and Pavements Laboratory, Mr. R. L. Hutchinson, Special Assistant to the Soils and Pavements Laboratory, and Mr. H. H. Ulery, Jr., Chief, Pavement Design Division, and under the direct supervision of Messrs. A. H. Joseph and J. W. Hall, Jr., Chiefs, respectively, of the Pavement Investigations Division and the Evaluation Branch. The programming for this study was done in part by Mr. A. P. Park, Soils Testing Branch. Significant contributions were made by Mr. J. L. Green, Evaluation Branch. This report was written by Dr. R. A. Weiss.

BG E. D. Peixotto and COL G. H. Hilt were Directors of WES during the conduct of this study and the preparation of this report. The Technical Director was Mr. F. R. Brown.

TABLE OF CONTENTS

LIST OF ILLUSTRATIONS

LIST OF TABLES

LIST OF SYMBOLS

a	Contact radius of vibrator baseplate
$a_{c1}, a_{c2}, \ldots a_{ci}$	Critical contact radius of vibrator baseplate
A	Amplitude of dynamic deflection of pavement surface directly beneath vibrator baseplate
b	Third-order nonlinear elastic parameter
B	Function of Poisson's ratio for the homogeneous half-space
$B_1, B_2, \ldots B_i$	Values of B for each pavement layer
C	Damping constant of the pavement-vibrator system
C_H	Damping constant for homogeneous linear elastic half-space
D	Algebraic discriminant
e	Fifth-order nonlinear elastic parameter
$e^{i(\omega t-\Lambda)}$	Complex number notation for a sinusoidal time dependence
$\mathcal{E}$	Elastic strain energy density
$F_D(t)$	Dynamic load of vibrator
$F_D \equiv F_D(\omega)$	Magnitude of the sinusoidal dynamic force applied to the pavement surface
$F_P(x)$	Pavement-restoring force
F_s	Static load of vibrator
F_{sc}	Critical static load of vibrator
$F_V(t)$	Total force applied to the pavement surface (static plus dynamic)
g	Acceleration due to gravity
G	Shear modulus of homogeneous elastic half-space
G_s	Shear modulus of subgrade
G_s^0	Shear modulus at the very top of the subgrade
$G_1, G_2, G_3, \ldots G_i$	Shear moduli of pavement layers
$h_1, h_2, h_3, \ldots h_i$	Thickness of the pavement layers
$H_1, H_2, H_3, \ldots H_i$	Sums of pavement layer thicknesses
i	$\sqrt{-1}$
k	Effective spring constant of a nonlinear pavement

k_H	Spring constant of a homogeneous linear elastic half-space
k_0	Effective quasi-static spring constant
k_{00}	Linear elastic parameter of a nonlinear pavement
ℓ	Finite depth of influence of the static strain field
$\ell_0, \ell_2, \ell_4, \ldots \ell_i$	Coefficients of the power series expansion of the finite depth of influence
m	Lumped mass of pavement and soil
n	Number of layers of pavement
Q	Function of Poisson's ratio
$Q_1, Q_2, Q_3, \ldots Q_i$	Value of Q for each pavement layer
Q_s	Value of Q for the subgrade
Q_s^0	Value of Q at very top of subgrade
$\overline{QG}$	Value of QG averaged over the depth of influence ℓ
$\overline{Q_s G_s}$	Average value of $Q_s G_s$ in the interval $\ell - H_3$
S	Dynamic stiffness of pavement
S_c	Critical value of dynamic stiffness
S_0	Value of the dynamic stiffness obtained from S by taking $k = k_0$ (or $A = 0$).
t	Time
U	Elastic strain energy
$U_2, U_4, U_6, \ldots U_i$	Coefficients of the power series expansion of the elastic strain energy
V	Volume of the frustum of a cone having a depth equal to the finite depth of influence in the pavement
W	Work done during elastic deflection of the pavement under the action of the static load F_s
W_2, W_4, W_6	Coefficients in the series expansion of W
x	Total elastic deflection of the pavement surface under the vibrator baseplate
$\dot{x}$	Velocity of pavement surface
$\ddot{x}$	Acceleration of pavement surface
x_e	Static elastic deflection of pavement surface beneath the vibrator baseplate
z	Depth below surface of the pavement
$\alpha_1, \alpha_2, \ldots \alpha_n$	Coefficients appearing in the power series expansion of the amplitude of the dynamic deflection

$\beta_1, \beta_2, \ldots \beta_n$	Coefficients appearing in the power series expansion of the dynamic stiffness
γ	Weight density of the half-space
δ	Function of the expansion coefficients of the finite depth of influence
Δb	Value of the discontinuity of b for $\ell_0 = H_i$
Δe	Value of the discontinuity of e for $\ell_0 = H_i$
$\Delta \ell$	Increment of finite depth of influence
ΔV	Increment of the volume of the frustum of the cone containing the strain field
ε	Vertical strain in pavement (assumed constant)
$\varepsilon_2, \varepsilon_4, \varepsilon_6$	Expansion coefficients appearing in the expressions for k_{00}, b, and e
η	5/8
θ	Elastic volume dilation
κ	Ratio of the radius of the lower base to the radius of the upper area of the frustum of the cone of stress
$\kappa_2, \kappa_4, \kappa_6$	Expansion coefficients appearing in the expressions for k_{00}, b, and e
λ	Lame elastic constant
μ	3/4
ν	Poisson's ratio for homogeneous elastic material
ν_s	Poisson's ratio for subgrade
$\nu_1, \nu_2, \nu_3, \ldots \nu_i$	Poisson's ratios for pavement layers
ξ	Dynamic elastic deflection of pavement surface beneath the vibrator baseplate measured from the static equilibrium deflection
ρ	Function of the expansion coefficients of the finite depth of influence
ϕ	Angle which appears in the solution of the cubic equation for calculating x_e in terms of F_s
ϕ_D	Angle of stress distribution
$\phi_2(a), \phi_3(a), \phi_4(a)$	Functions of the baseplate radius and Poisson's ratio of the successive pavement layers
ψ	$F_D^2 S_0^{-4}$, expansion parameter
Ψ	Volume factor for the frustum of the cone
ω	Angular frequency

ω_c Critical angular frequency

ω_R Resonance angular frequency

Λ Phase angle between the dynamic load applied to the pavement surface and the dynamic deflection of the pavement surface

CONVERSION FACTORS, BRITISH TO METRIC UNITS OF MEASUREMENT

British units of measurement used in this report can be converted to metric units as follow:

Multiply	By	To Obtain
inches	2.54	centimeters
feet	0.3048	meters
square inches	6.4516	square centimeters
pounds (force) per inch	175.1268	newtons/meter
pounds (force) per square inch	0.6894757	newtons per square centimeters
pounds (force) per cubic inch	27,679.91	kilograms per cubic meter
kips (force)	4,448.222	newtons
kips (force) per inch	1.7512685	kilonewtons per centimeters
kip-second per inch	1.7512685	kilonewtons-second per centimeter
kip-second^2 per inch	1.7512685	kilonewtons-second^2 per inch

1. INTRODUCTION

1.1 BACKGROUND

Nondestructive vibratory testing of pavements may be of importance toward predicting the performance of airfield pavements and may be used for the rapid evaluation of pavement strength.[1-3] To be useful, the physical quantities measured by the nondestructive testing technique must be related to pavement performance. Pavement performance is measured by number of aircraft coverages on the pavement required to reach some defined condition of failure. The U. S. Army Engineer Waterways Experiment Station (WES) was requested to perform experimental and theoretical investigations to determine if the physical quantities measured by the nondestructive technique can be used for pavement evaluation and can be related to pavement performance. Some of the quantities that are measurable by the nondestructive vibratory technique are:

a. The dynamic deflection of the pavement surface versus the frequency of vibratory loading for a series of fixed static and dynamic loads.

b. The stress and strain distribution in the pavement around the vibrator measured on instrumented pavement sections.

c. Rayleigh wave dispersion curves giving phase velocity versus wavelength measured with the wave propagation techniques.

d. The dynamic deflection of the pavement surface versus the dynamic force for a series of fixed static loads and fixed frequencies.

Most of the previous work on the nondestructive testing of pavements has treated the mechanical quantities listed in Subparagraphs a, b, and c. This report concentrates primarily on the nonlinear response exhibited by pavements through the measurements listed in Subparagraph d. Further study of the physical quantities mentioned in Subparagraphs a, b, and c should be made in the light of the new results obtained from the study of nonlinear effects in pavements.

1.2 OBJECTIVES

The overall objectives of this pavement study are:

a. The development of a mechnical model which describes the

measured response of pavements to a sinusoidal dynamic loading that is applied to the pavement surface.

b. The development of a method for determining the subsurface structure of the pavement in terms of the measured dynamic response of the pavement.

The development of the pavement response model includes the following specific objectives:

a. To determine the effects of intrinsic pavement properties and structure on the dynamic load-deflection curves.

b. To determine the effects of such vibrator characteristics as dynamic load, static load, and contact area on the dynamic load deflection curves.

c. To calculate the dynamic stiffness and determine its dependence on the intrinsic properties of the pavement and on the characteristics of the vibrator used to measure this quantity.

d. To develop a theory of the nonlinear dynamic response of pavements which enables the comparison of dynamic stiffness measurements obtained from different vibrators at the same pavement location.

The theoretical work done in this report may have applications for the nondestructive testing of roads and airport pavements. The possible practical applications of this work are twofold: (a) the use of the dynamic stiffness measurement for determining the subsurface structure of the pavement, i.e., the shear modulus and thickness for each pavement layer, and (b) the development of the capability of comparing the values of the dynamic stiffness measured by different vibrators at the same pavement location.

1.3 SCOPE

To achieve the objectives listed above, both theoretical and experimental studies were conducted.

1.3.1 THEORETICAL STUDIES

The theoretical studies included:

a. The formulation of a nonlinear mechanical model to describe the response of a pavement to static and dynamic loading.

b. The determination of effects of the structure of the pavement-soil system on the parameters which appear in the nonlinear vibration model.

c. A numerical evaluation of the parameters that appear in the nonlinear model.

d. The development of formulas giving the shear modulus and layer thickness of each pavement layer in terms of quantities that are obtained directly from the measured dynamic load-deflection curves.

1.3.2 EXPERIMENTAL STUDIES

The experimental studies performed on both actual airport pavements and especially constructed test sections included:

a. The measurement of dynamic load-deflection curves using a vibrator developed at WES which can generate dynamic loads up to 16 kips* (WES 16-kip vibrator) with a constant 16-kip static load and a constant frequency of 15 Hz.

b. The measurement of dynamic load-deflection curves at a constant static load of 16 kips for a series of fixed frequencies in the range from 10-40 Hz.

c. The measurement of dynamic load-deflection curves at a constant static load of 16 kips and a constant frequency of 15 Hz for a series of baseplates whose diameters ranged from 5-18 in.

d. The measurement of dynamic load-deflection curves at constant frequency and constant baseplate size for a range of static loads from 5-50 kips.

---

* A table of factors for converting U. S. customary units of measurement to metric (SI) units is given on page 11.

2. LINEAR OSCILLATOR MODEL OF PAVEMENT RESPONSE

2.1 GENERAL CONSIDERATIONS

Nondestructive vibratory testing of pavements uses a mechanical vibrator operating at a known frequency and dynamic force applied to the pavement surface to produce a time-dependent sinusoidal deflection of the pavement surface directly beneath the vibrator baseplate. The magnitude of the dynamic deflection of the pavement surface for a series of dynamic force levels and frequencies is considered to be a measure of the strength of a pavement. This section discusses a linear oscillator model used to describe the motion of the surface of a linear elastic half-space and then shows how this model fails to account for the measured values of the dynamic deflection of the pavement for a series of frequencies and dynamic loadings generated by the vibrator. The concepts of dynamic stiffness and deflection are introduced, and the separation of static and dynamic displacements is demonstrated.

2.2 HOMOGENEOUS LINEAR ELASTIC HALF-SPACE

The equation of motion of a mass of pavement or soil undergoing vertical oscillations on the surface of a homogeneous elastic half-space is

$$m\ddot{x} + C_H\dot{x} + k_H x = F_V(t) \qquad (2.1)$$

where

m = lumped mass of pavement and soil

$\ddot{x}$ = acceleration of pavement surface

C_H = damping constant $(3 \cdot 4a^2\sqrt{G\gamma/g}/(1 - \nu)$, where a is the contact radius of the vibrator baseplate, G is the shear modulus of the half-space, γ is the density by weight of the half-space, g is the acceleration due to gravity, and ν is Poisson's ratio, Reference 4)

$\dot{x}$ = velocity of pavement surface

k_H = spring constant $(4Ga/(1 - \nu)$, Reference 4)

x = total elastic deflection of the pavement surface under the vibrator baseplate

$F_V(t)$ = total force applied to the pavement surface (static plus dynamic)

t = time

The values of k_H and C_H are chosen to construct a damped spring model for the vertical vibrations of an elastic half-space; therefore C_H represents the radiation damping of the system. If viscous friction is present, the value of the actual damping constant may be considerably larger than the value of C_H.

The total force applied by the vibrator is written as

$$F_V(t) = F_s + F_D(t) \tag{2.2}$$

where F_s equals static load and $F_D(t)$ equals dynamic load. The total displacement can be written as

$$x = x_e + \xi \tag{2.3}$$

where x_e is the static elastic deflection of the pavement surface beneath the vibrator baseplate, F_s/k_H, and ξ is the dynamic elastic deflection of pavement surface beneath the vibrator baseplate measured from the static equilibrium deflection. Combining Equations 2.1, 2.2, and 2.3 gives the equation of motion as

$$m\ddot{\xi} + C_H\dot{\xi} + k_H\xi = F_D(t) \tag{2.4}$$

wherein all static forces and displacements have canceled. Therefore, for a linear system, the static deflection does not affect the dynamic response of the vibrator mass; only the reference point is changed by the static load.

2.3 DYNAMIC LOAD-DEFLECTION CURVES

For a sinusoidal driving force, the dynamic deflection obtained from Equation 2.4 is[5]

$$\xi = \frac{F_D(\omega)e^{i(\omega t-\Lambda)}}{\sqrt{\left(k_H - m\omega^2\right)^2 + C_H^2\omega^2}} \qquad (2.5)$$

where:

$F_D(\omega)$ = magnitude of the sinusoidal dynamic force applied to pavement surface

$e^{i(\omega t-\Lambda)}$ = complex number notation for a sinusoidal time dependence where $i = \sqrt{1}$, ω = angular frequency, and Λ = phase angle between the dynamic load applied to the pavement surface and the dynamic deflection of the pavement surface.

Two kinds of dynamic response curves of physical interest can be obtained from Equation 2.5:

a. Dynamic deflection versus frequency.

b. Dynamic deflection versus dynamic force.

For a linear system, the magnitude of the maximum dynamic deflection is a simple linear function of $F_D(\omega)$ as shown in Figure 1a. The magnitude of the peak dynamic deflection as a function of frequency appears in Figure 1b for a constant force vibrator and for an eccentric mass vibrator (where the dynamic force is frequency-dependent in the manner $F_D(\omega) \sim \omega^2$). The WES 16-kip vibrator is a constant force vibrator. Therefore, for a linear system the dependence of ξ on ω is rather complicated, but the dependence of ξ on $F_D(\omega)$ is given simply by a straight line whose slope is the dynamic stiffness. The phase angle Λ is assumed to be the same for all of the elements of the mass of pavement and subgrade which enter into motion with the vibrator mass. This is the lumped mass assumption, which requires that m be interpreted as an effective mass which vibrates in phase with the vibrator mass and has a value which is determined by requiring that the theoretical frequency response curves agree with the measured frequency response curves.

2.4 DYNAMIC STIFFNESS

Equation 2.5 shows that for a linear system, the dynamic stiffness is given by

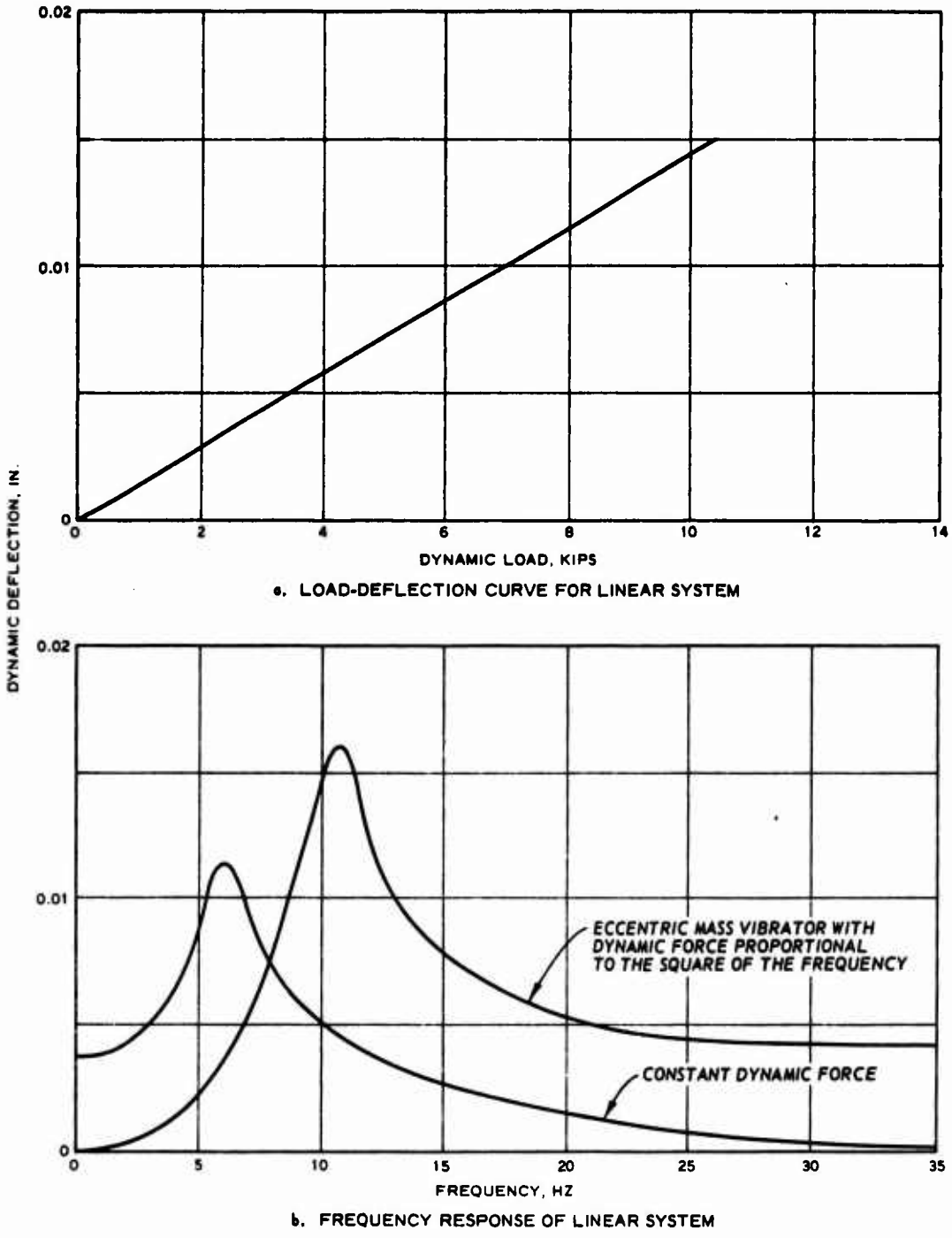

Figure 1. Typical dynamic response of the linear spring model

$$S = \sqrt{\left(k_H - m\omega^2\right)^2 + C_H^2\omega^2} \qquad (2.6)$$

and depends only on the following quantities:

a. Frequency.

b. Spring constant.

c. Damping constant.

d. Lumped mass of pavement and soil.

The elastic parameters of the pavement, G and ν, and the radius of the contact area of the vibrator with the pavement enter the dynamic stiffness through k_H and C_H as seen from Equation 2.6 and the expressions for the spring constant and damping constant. For a linear oscillator model, the dynamic stiffness does not depend on the dynamic load or on the equilibrium elastic deflection, i.e., ξ is a linear function of $F_D(\omega)$. However, the experimental values of the dynamic stiffness of pavements, as given in Section 4.1, indicate a strong dependence of the dynamic stiffness on the dynamic load and on the static elastic equilibrium displacement of the pavement surface. Therefore, the linear oscillator model is insufficient to describe the response of pavements to dynamic loadings, and a nonlinear oscillator model is required to explain the experimental data.

3. THE NONLINEAR MECHANICAL MODEL

3.1 INTRODUCTION TO THE NONLINEAR MODEL

In this section, a nonlinear mechanical model is developed to describe the response of a pavement-subgrade system to a sinusoidal dynamic loading applied to the surface of the pavement by a vibrator. The model is developed in three basic steps:

a. The determination of the nonlinear pavement-restoring force in terms of three parameters: the linear elastic parameter of a nonlinear pavement, the third-order nonlinear elastic parameter, and the fifth-order nonlinear elastic parameter.

b. The solution of the motion equation (2.4) for the case of the nonlinear pavement-restoring force and the subsequent calculation of the dynamic stiffness and deflection of the pavement as a function of the static and dynamic loads exerted by the vibrator.

c. The determination of the parameters k_{00}, b, and e in terms of the elastic constants of the layered pavement-subgrade system and in terms of the finite depth of influence that a static surface load produces in this system.

If for a fixed frequency the dynamic deflection of the pavement surface is not directly proportional to the dynamic force, the system is said to be nonlinear. The experimental data of Section 4.1 indicate that this is the case for most asphaltic concrete (AC) pavements and for some portland cement concrete (PCC) pavements. It will be shown in Section 3.8.2 that the nonlinear behavior of a pavement undergoing forced sinusoidal vibrations can produce very different values of dynamic stiffness such as those measured at the same location by different mechanical vibrators. Therefore, it is important to be able to account for the nonlinear effects by a simple physical model.

A physical and mathematical model for the nonlinear response of pavements can be derived which will account for the dependence of the impedance values on the type of vibrator used to determine them, i.e., on the static weight, dynamic load, and contact area of the vibrator. This report will show that it is possible to describe the dependence of the measured values of pavement dynamic stiffness on the physical

characteristics of the vibrator by introducing three parameters to describe the nonlinear pavement-restoring force.

3.2 NONLINEAR PAVEMENT-RESTORING FORCE

The pavement-restoring force is the force that the bulk pavement exerts on the lumped pavement mass from below. In linear Equation 2.1, the pavement-restoring force is simply $k_H x$. In general, the pavement-restoring force is not equal to the force generated by the vibrator; only for the static case are these two forces equal. The first task to be accomplished is the development of a mathematical expression for the pavement-restoring force which satisfies the following two very general criteria:

a. The mathematical form of the pavement-restoring force will be sufficiently general so that the nonlinear dynamic response of the pavement that is calculated from this restoring force will be adequate to describe the experimental nonlinear dynamic load-deflection curves.

b. Only terms based on sound physical theory are included in the mathematical form of the pavement-restoring force.

The form of the nonlinear elastic pavement-restoring force used in the nonlinear model is determined by requiring the restoring force to be antisymmetric in the deflection of the pavement surface, i.e.,

$$F_p(x) = -F_p(-x) \tag{3.1}$$

where $F_p(x)$ equals the pavement-restoring force. Equation 3.1 is satisfied for the linear case, $F_p = k_H x$. A simple nonlinear pavement-restoring force which satisfies Equation 3.1, and which is found to be adequate to describe the dynamic load-deflection curves for pavements, is

$$F_p(x) = k_{00}x + bx^3 + ex^5 \tag{3.2}$$

where k_{00} equals the linear elastic parameter of a nonlinear pavement while b and e equal respectively the third- and fifth-order nonlinear parameters. The experimental data of Section 4.1 indicate that at least two nonlinear elastic parameters, b and e , are required to

describe AC and PCC pavements. The linear spring constant k_{00} which appears in Equation 3.2 is not in general equal to the spring constant k_H which describes the homogeneous linear elastic half-space.

3.3 EQUATION OF MOTION FOR THE NONLINEAR SYSTEM

The equation of motion of the oscillating lumped pavement and soil mass can now be written using the expression for the nonlinear pavement-restoring force derived in the previous section. This equation of motion cannot be completely separated into static and dynamic parts as was the case for the linear elastic system.

The equation of motion for the nonlinear spring is given by

$$m\ddot{x} + C\dot{x} + k_{00}x + bx^3 + ex^5 = F_V(t) \tag{3.3}$$

where C is the damping constant of the pavement-vibrator system, and m is the in-phase lumped mass of the pavement and subgrade. The value of C is larger than the value of the radiation damping constant C_H which appears in Equation 2.6 because C describes several material damping processes in addition to the dissipation of energy by mechanical radiation. Equation 3.3 can be greatly simplified by choosing a new origin of coordinates as in Equation 2.3, such that the motion is described in terms of coordinates measured relative to the static equilibrium deflection. By itself the static load produces a static deflection given by

$$F_s = k_{00}x_e + bx_e^3 + ex_e^5 \tag{3.4}$$

Substituting Equation 3.4 into Equation 3.3 enables the equation of motion to be written as

$$m\ddot{x} + C\dot{x} + k_{00}(x - x_e) + b\left(x^3 - x_e^3\right) + e\left(x^5 - x_e^5\right) = F_D(t) \tag{3.5}$$

Using Equation 2.3 and the following algebraic identities:

$$x^3 - x_e^3 = (x - x_e)\left(x^2 + xx_e + x_e^2\right) \tag{3.6}$$

$$x^5 - x_e^5 = (x - x_e)\left(x^4 + x^3x_e + x^2x_e^2 + xx_e^3 + x_e^4\right) \qquad (3.7)$$

allows Equation 3.5 to be rewritten as

$$m\ddot{\xi} + C\dot{\xi} + k_0\xi + b\xi^3 + e\xi^5 = F_D(t) \qquad (3.8)$$

where k_0 is the effective quasi-static spring constant and is defined by

$$k_0 = k_{00} + 3bx_e^2 + 5ex_e^4 + g(x_e\xi) \qquad (3.9)$$

and

$$g(x_e\xi) = 3bx_e\xi + 10ex_e^3\xi + 10ex_e^2\xi^2 + 5ex_e\xi^3 \qquad (3.10)$$

Equation 3.8 is a generalization of the Duffing Equation.[6]

3.4 EFFECTIVE SPRING CONSTANT

In this section, the equation which determines the amplitude of the sinusoidal dynamic deflection of the pavement surface beneath the vibrator mass is developed. The amplitude equation is expressed in terms of an effective spring constant which in turn depends on the static and dynamic deflections of the pavement surface. The dynamic stiffness for the nonlinear system will eventually be expressed in terms of this effective spring constant.

The functions $k_0(x_e\xi)$ and $g(x_e\xi)$ are time-dependent, and therefore Equation 3.8 is very difficult to solve exactly. Under special conditions to be described, the coefficient which appears in Equation 3.8 may be taken to be independent of time, thereby making this equation somewhat easier to solve. For harmonic motion, the dynamic force applied to the pavement surface by the vibrator can be written as

$$F_D(t) = F_D(\omega)e^{i\omega t} \qquad (3.11)$$

$$\xi(t) = Ae^{i(\omega t - \Lambda)} \tag{3.12}$$

where A equals the amplitude of the dynamic deflection of the pavement surface directly beneath the vibrator baseplate. The dynamic deflection of the lumped mass is assumed to be equal to the dynamic deflection of the pavement surface. For the case in which the dynamic deflection amplitude is much less than the static equilibrium deflection, $A << x_e$, $g(x_e\xi) \approx 0$ can be used in Equation 3.9, while for the case where $A \approx x_e$, the time-averaged value of $g(x_e\xi) \approx 10ex_e^4$ can be used in Equation 3.7. For the two special cases, the coefficient k_0 can be written as

$$k_0 = k_{00} + 3bx_e^2 + 5ex_e^4 \qquad A << x_e \tag{3.13}$$

$$k_0 = k_{00} + 3bx_e^2 + 15ex_e^4 \qquad A \approx x_e \tag{3.14}$$

A simple linear interpolation formula for k_0 is given by

$$k_0 = k_{00} + 3bx_e^2 + 5\left(1 + 2\frac{A}{x_e}\right)ex_e^4 \tag{3.15}$$

It should be noted that the choice of k_0 as time-independent is an approximation which becomes invalid for large dynamic deflections.

Even with the coefficient k_0 assumed to be time-independent, Equation 3.8 is a nonlinear equation. However, it can be shown that Equation 3.8 can be cast into the form of an equivalent linear system whose amplitude equation is [6]

$$A^2\left[\left(k - m\omega^2\right)^2 + C^2\omega^2\right] = F_D^2(\omega) \tag{3.16}$$

provided an effective spring constant is introduced which is defined by

$$k = k_0 + \mu bA^2 + \eta eA^4 \tag{3.17}$$

where k_0 is given by Equation 3.15, $\mu = 3/4$, and $\eta = 5/8$. The

effective spring constant, k, is seen to be a function of the amplitude of the dynamic deflection and also depends on the static equilibrium deflection through the coefficient k_0. If the static load applied to the pavement by the vibrator were zero, then $x_e = 0$, $g(x_e\xi) = 0$, and $k_0 = k_{00}$. For this case, there could be no coupling of terms between x_e and ξ and the effective spring constant would depend only on the amplitude of the dynamic deflection. On the other hand, if the dynamic load were zero, the effective spring constant would be $k = k_0$ and would depend only on the static equilibrium deflection.

3.5 CALCULATION OF THE DYNAMIC STIFFNESS AND THE DEFLECTION AMPLITUDE FOR NONLINEAR PAVEMENTS

This section considers the calculation of the dynamic stiffness and the dynamic deflection of the pavement surface and dynamic forces generated by the vibrator. The deflection amplitude equation (3.16) derived in the previous section is expanded in powers of the deflection amplitude, A, to give a tenth-order algebraic equation for the determination of A. Infinite series expansions for the dynamic amplitude and the dynamic stiffness are obtained as solutions to this equation. These solutions express the dynamic stiffness and deflection as functions of the dynamic load generated by the vibrator and the static deflection of the pavement surface. The static deflection is then expressed in terms of the static load, so that finally the dynamic stiffness and deflection are expressed in terms of the static and dynamic loads at which the vibrator is operated.

3.5.1 EQUATION FOR THE DYNAMIC DEFLECTION AMPLITUDE

The explicit equation for the dynamic deflection amplitude will now be calculated. The dynamic stiffness of the pavement which is described by a nonlinear oscillator is given by

$$S^2 = \left(k - m\omega^2\right)^2 + C^2\omega^2 \tag{3.18}$$

where the effective spring constant is given by Equation 3.17. The

dynamic stiffness depends on the amplitude of the dynamic displacement and the static equilibrium deflection. The amplitude of the dynamic deflection is determined by Equation 3.16, which may be written as

$$A^2S^2 = F_D^2(\omega) \tag{3.19}$$

Using Equations 3.17 and 3.18, the amplitude equation (3.19) can be written as

$$S_0^2A^2 + 2\mu b\left(k_0 - m\omega^2\right)A^4 + \left[2\eta\left(k_0 - m\omega^2\right)e + \mu^2b^2\right]A^6 + 2\mu\eta beA^8 + \eta^2e^2A^{10} = F_D^2(\omega) \tag{3.20}$$

where S_0 is the value of the dynamic stiffness obtained from S by taking $k = k_0$ (or equivalently $A = 0$ in Equation 3.17) and is defined by the equation:

$$S_0^2 = \left(k_0 - m\omega^2\right)^2 + c^2\omega^2 \tag{3.21}$$

Whereas the simple linear system produces a linear equation for the calculation of the dynamic displacement in terms of the dynamic force, the nonlinear system appropriate to describe dynamic pavement response produces a fifth-order equation for calculating A^2 in terms of $F_D(\omega)$. The value S_0 appearing in Equation 3.21 is the dynamic stiffness in the limit of zero dynamic loading.

3.5.2 POWER SERIES EXPANSION

The tenth-order equation (3.20) will now be solved for the dynamic amplitude A which will take the form of an infinite series expansion. The dynamic stiffness is calculated in terms of A by Equation 3.19 so that S also will have the form of an infinite series expansion.

The solution of Equation 3.20 for the amplitude of the dynamic displacement in terms of the amplitude of the dynamic force is, in

general, difficult to obtain analytically. For the case in which the dynamic force is not very large, the amplitude of motion and the dynamic stiffness are easily obtained from Equation 3.20 in the form of

$$A = \frac{F_D(\omega)}{S_0}\left(1 + \alpha_1\psi + \alpha_2\psi^2 + \ldots\right) \tag{3.22}$$

$$S = S_0\left(1 + \beta_1\psi + \beta_2\psi^2 + \ldots\right) \tag{3.23}$$

where

α_1, α_2 = coefficient appearing in the power series expansion of the amplitude of the dynamic deflection

ψ = expansion parameter

β_1, β_2 = coefficients appearing in the power series expansion of the dynamic stiffness

The values of ψ, α_1, α_2, β_1, and β_2 can be obtained by combining Equations 3.20 and 3.22 with the following results:

$$\psi = \frac{F_D^2(\omega)}{S_0^4} \tag{3.24}$$

and

$$\alpha_1 = -\mu b\left(k_0 - m\omega^2\right) \tag{3.25}$$

$$\alpha_2 = \frac{7}{2}\mu^2b^2\left(k_0 - m\omega^2\right)^2 - S_0^2\left[\eta e\left(k_0 - m\omega^2\right) + \frac{\mu^2b^2}{2}\right] \tag{3.26}$$

$$\beta_1 = \mu b\left(k_0 - m\omega^2\right) \tag{3.27}$$

$$\beta_2 = S_0^2\left[\eta e\left(k_0 - m\omega^2\right) + \frac{\mu^2b^2}{2}\right] - \frac{5}{2}\mu^2b^2\left(k_0 - m\omega^2\right)^2 \tag{3.28}$$

The solutions given in Equations 3.22 and 3.23 are valid provided the dynamic load is not so large as to prevent the convergence of these power series solutions. Equations 3.22-3.23 have been derived from Equation 3.19 and give the fundamental description of the nonlinear dynamic load-deflection curves. These equations will be fitted to

experimental dynamic load-deflection curves in Section 4.2.2.

Equation 3.22 shows that the amplitude of the dynamic deflection is not a linear function of F_D but approaches the linear condition for small F_D or large S_0. The linear system can be regained by setting $b = e = 0$ in Equations 3.22-3.28. When $F_D = 0$, $A = 0$ and $S = S_0$, and the dynamic stiffness depends only on the static equilibrium deflection. If $F_s = 0$, the deflection and stiffness are given by Equations 3.22-3.28 with the provision that k_0 be replaced by the constant k_{00}. The static equilibrium deflection can always be expressed in terms of the static load through Equation 3.4. Therefore, in general, the dynamic stiffness of a nonlinear system will depend on the magnitude of F_D and F_s. The dependence of S on F_D enters through the expansion parameter ψ given in Equation 3.24, while the dependence of S on F_s enters through the function S_0 given by Equation 3.21.

3.5.3 FIRST-ORDER NONLINEAR TERM

The expression for the dynamic amplitude A given in Equation 3.22 shows that A does not depend linearly on F_D. The departure from linearity is due to the terms $\alpha_1\psi$, $\alpha_2\psi^2$,..., that appear in Equation 3.22. It is desirable to determine the physical quantities which determine the degree of departure from the linear condition, $A = F_D/S_0$. In the range of small F_D, the predominant term describing the nonlinear behavior of the deflection of the pavement mass is obtained from Equations 3.22, 3.24, and 3.25 as follows:

$$\alpha_1\psi = -\mu b\left(k_0 - m\omega^2\right)\frac{F_D^2}{S_0^4} \tag{3.29}$$

In general the degree of nonlinearity depends on four quantities:

a. The magnitude of the nonlinear parameters b and e.

b. The relative magnitudes of F_s and F_D.

c. The frequency at which the vibrator is operated.

d. The static stiffness S_0 of the pavement-vibrator system.

The parameter ψ, which appears in the infinite series expansion for A and S in Equations 3.22-3.24, depends inversely on S_0 in the

form S_0^{-4}, and therefore it follows that the dynamic load-deflection curves of stiff pavements are more linear than those of the more flexible pavements. Thus concrete pavements are expected to have a more linear response to a dynamic loading than do the more flexible asphalt pavements. The value of S_0 includes the effects of the subgrade as well as the effects of each layer in the pavement.

3.5.4 CRITICAL FREQUENCY

It is clear from Equations 3.22 and 3.29 that the degree of departure from the linear condition expected for the response of a pavement to an applied vibratory load at the pavement surface depends on the frequency at which the vibrator is operated. In particular, it is apparent from Equation 3.29 that the first-order nonlinear term is frequency-dependent and that this first-order term will vanish at a special critical frequency for which $k_0 - m\omega^2 = 0$.

It is a characteristic property of the first-order nonlinear term (Equation 3.29) that there is a critical frequency for which this term vanishes; the critical frequency is defined by

$$\omega_c^2 = \frac{k_0}{m} \tag{3.30}$$

where ω_c is the critical angular frequency. In terms of the critical frequency, the first-order nonlinear coefficient can be written as

$$\alpha_1 = -\mu bm\left(\omega_c^2 - \omega^2\right) \tag{3.31}$$

At the critical frequency, the departure from a linear system occurs only through the second-order and higher terms in ψ, i.e., $\alpha_2\psi^2 + \alpha_3\psi^3 + \ldots$. Therefore at the critical frequency, the pavement response for small dynamic loads should be nearly linear. The critical frequency depends on the vibrator characteristics as well as on pavement properties. The connection between the resonance frequency and the critical frequency is obtained from Equation 3.17 as follows:

$$\omega_R^2 = \omega_c^2 + \frac{\mu b A^2 + \eta e A^4}{m} - 2\left(\frac{C}{2m}\right)^2 \qquad (3.32)$$

where ω_R is the resonance angular frequency. In general $\omega_R < \omega_c$.

3.5.5 CRITICAL STATIC FORCE

In addition to a critical frequency, $\omega_c(F_s)$ which depends on the static load of the vibrator, there is a critical static load F_{sc} for each operating frequency of the vibrator, which is defined from Equation 3.29 by $\alpha_1 = 0$ or

$$k_0(F_{sc}) = m\omega^2 \qquad (3.33)$$

Using Equations 3.15, 3.31, and 3.33, the first-order coefficient α_1 can be written as

$$\alpha_1 = \mu b\left[k_0(F_s) - k_0(F_{sc})\right] \qquad (3.34)$$

$$\alpha_1 = + \frac{3\mu b^2}{k_{00}^2}\left(F_{sc}^2 - F_s^2\right) + \ldots \qquad (3.35)$$

It is possible to operate a vibrator at the critical condition by adjusting either the frequency or the static load of the vibrator.

3.5.6 SHAPE OF THE DYNAMIC LOAD-DEFLECTION CURVES

An approximately linear dynamic deflection versus dynamic force curve occurs at the critical frequency. For an arbitrary frequency, the departure from this approximately linear curve is positive or negative depending on the sign of the parameter α_1 in Equations 3.22 and 3.31. The sign of the parameter α_1 depends on the sign of the parameter b and whether $\omega \gtrless \omega_c$ or $F_s \gtrless F_{sc}$. It will be shown in Section 3.7 that b is generally negative. For the case $b < 0$, which corresponds to the case in which the shear modulus of the half-space is constant with depth, or to the case of a layered system which has G decreasing with depth, as is usually the case with pavements, the dynamic stiffness and deflection versus dynamic force curves are shown schematically in

Figure 2a. For the case $b > 0$, which may be possible for the situation in which the shear modulus of a layered system increases rapidly with depth, the dynamic stiffness and displacement versus dynamic force curves are shown schematically in Figure 2b. Therefore the choice of sign $b < 0$ has physical relevance to pavement problems. For the choice $b < 0$, the sign of the parameter α_1 can be positive or negative depending on whether $\omega < \omega_c$ or $\omega > \omega_c$, respectively. The value of ω_c can be determined by observing the frequency which produces the most linear load-deflection curve. The algebraic signs of b and e can be determined from the manner in which the dynamic load-deflection curves bend away (as in Figures 2a and 2b) from the approximately linear load-deflection curve which occurs at $\omega = \omega_c$. It should be pointed out that the definition of dynamic stiffness as being equal to the ratio of the dynamic load to the dynamic deflection for each point on the dynamic load-deflection curve is different from that used in Volume I of this report in which the dynamic stiffness is taken to be a single number determined from the portion of the dynamic load-deflection curve where F_D is large.

3.5.7 STATIC EQUILIBRIUM DISPLACEMENT

The explicit dependence of the dynamic stiffness on F_D is given by Equations 3.22-3.28. These equations will also give the explicit dependence of S on F_s, provided that the static equilibrium displacement x_e is expressed explicity as a function of F_s by using Equation 3.4. Because Equation 3.4 is an equation of fifth degree, numerical methods are generally required for its solution. However, in the extremes of very large and very small values of F_s, analytical solutions of this equation are possible. For a very small static load, the equilibrium elastic displacement is given by

$$x_e = \frac{F_s}{k_{00}} \tag{3.36}$$

For somewhat larger values of F_s, the cubic term manifests itself and x_e may be obtained from the approximate equation:

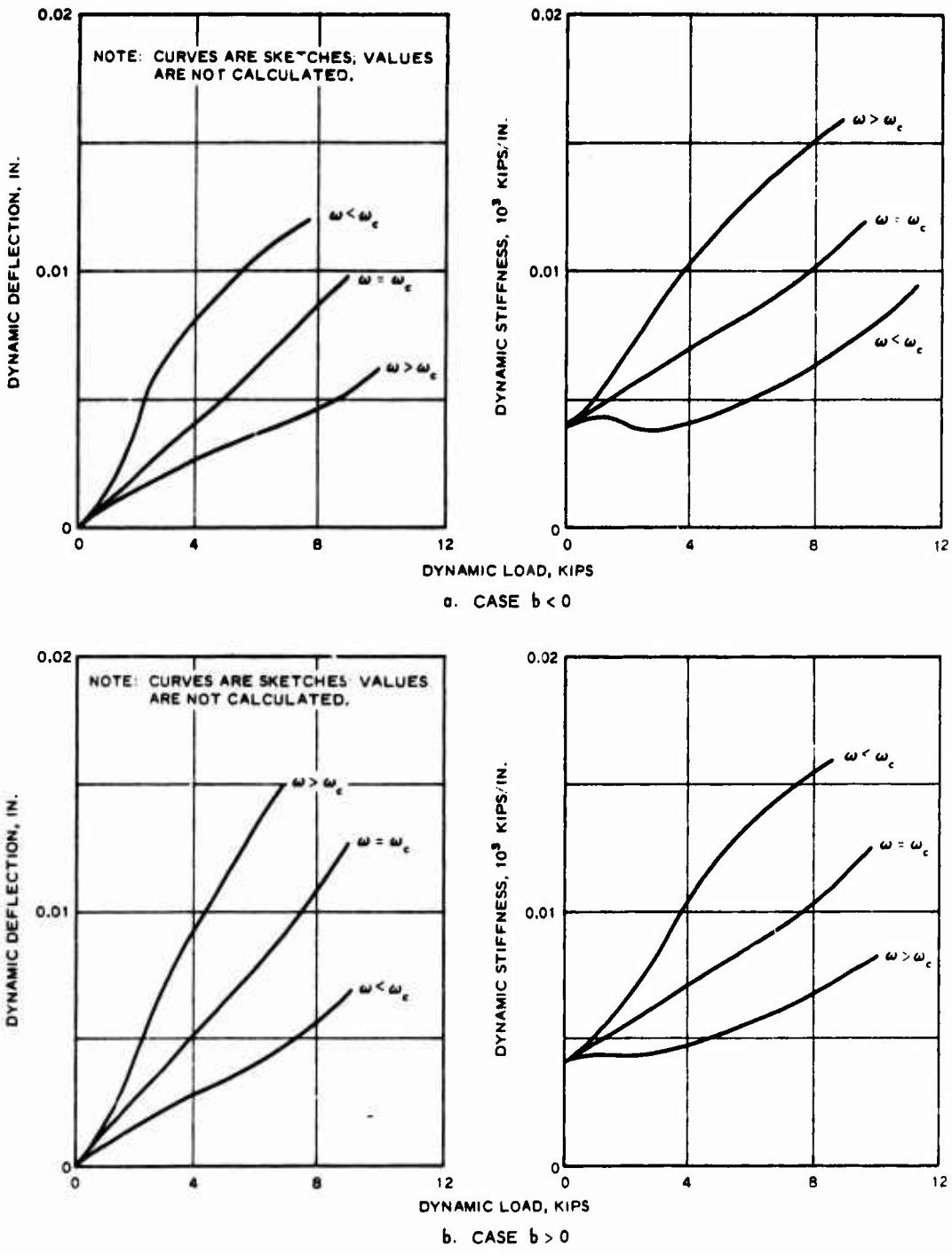

Figure 2. Theoretical dynamic load-deflection curves and dynamic stiffness curves predicted by the nonlinear spring model

$$x_e^3 + \frac{k_{00}}{b} x_e - \frac{F_s}{b} = 0 \qquad (3.37)$$

The discriminant of this cubic equation is

$$D = \frac{F_s^2}{4b^2} + \frac{k_{00}^3}{27b^3} \qquad (3.38)$$

and is negative for small F_s when $b < 0$. For the condition $D < 0$, the solution of the cubic equation can be written as[7]

$$x_e = \sqrt{-\frac{4k_{00}}{3b}} \cos\left(\frac{\phi}{3}\right) \qquad (3.39)$$

$$\cos \phi = -\frac{F_s}{\sqrt{-\frac{4k_{00}^3}{27b}}} \qquad (3.40)$$

where ϕ is the angle which appears in the solution of this cubic equation. In the limit of small F_s (or small b), the cosine term in Equation 3.39 has the value

$$\cos\left(\frac{\phi}{3}\right) = \frac{F_s}{\sqrt{-\frac{4k_{00}^3}{3b}}} + \frac{F_s^3}{\left(-\frac{4k_{00}^3}{3b}\right)^{3/2}} + \ldots \qquad (3.41)$$

Combining Equations 3.39 and 3.41 gives

$$x_e = \frac{F_s}{k_{00}} - \frac{bF_s^3}{k_{00}^4} + \ldots \qquad (3.42)$$

The solutions of Equations 3.39 and 3.42 have been derived for $b < 0$ and are therefore applicable to pavements. It can be shown that Equation 3.42 is also valid for $b > 0$.

With increasing values of F_s, the fifth-order terms become dominant, and in this region the approximate solution for x_e is

$$x_e = \left[\frac{F_s}{e} - \frac{k_{00}}{e}\left(\frac{F_s}{e}\right)^{1/5} - \frac{b}{e}\left(\frac{F_s}{e}\right)^{3/5}\right]^{1/5} \qquad (3.43)$$

Equation 3.4 is easily solved for the general case of an arbitrary value of F_s by using a digital computer. A schematic graph of x_e versus F_s for pavements ($b < 0$) is given in Figure 3a while the corresponding graph for a $b > 0$ formation is given in Figure 3b.

3.5.8 DEPENDENCE OF THE SPRING CONSTANT ON THE STATIC FORCE

The spring constant k_0 given by Equations 3.13-3.15 has a conventional interpretation only when the dynamic deflection amplitude satisfies $A << x_e$. For $A \neq 0$ the spring constant has the approximate value given by Equation 3.15. Using Equations 3.13, 3.42, and 3.43, the value of k_0 for zero dynamic amplitude and for small F_s is

$$k_0 = k_{00} + 3b\left(\frac{F_s}{k_{00}} - \frac{bF_s^3}{k_{00}^4}\right)^2 + 5e\left(\frac{F_s}{k_{00}} - \frac{bF_s^3}{k_{00}^4}\right)^4 \qquad (3.44)$$

while for large F_s

$$k_0 = k_{00} + 3b\left[\frac{F_s}{e} - \frac{b}{e}\left(\frac{F_s}{e}\right)^{3/5} - \frac{k_{00}}{e}\left(\frac{F_s}{e}\right)^{1/5}\right]^{2/5} + 5e\left[\frac{F_s}{e} - \frac{b}{e}\left(\frac{F_s}{e}\right)^{3/5} - \frac{k_{00}}{e}\left(\frac{F_s}{e}\right)^{1/5}\right]^{4/5} \qquad (3.45)$$

For very small F_s, Equation 3.44 can be rewritten as

$$k_0 = k_{00} + 3b\left(\frac{F_s}{k_{00}}\right)^2 + \left(5e - 6\frac{b^2}{k_{00}}\right)\left(\frac{F_s}{k_{00}}\right)^4 \qquad (3.46)$$

while for very large F_s, Equation 3.45 can be rewritten as

$$k_0 = 5e\left(\frac{F_s}{e}\right)^{4/5} \qquad (3.47)$$

Equations 3.4 and 3.15 are easily solved simultaneously on a digital computer to give the general solution, $k_0 = k_0(F_s)$. Figures 4a and b

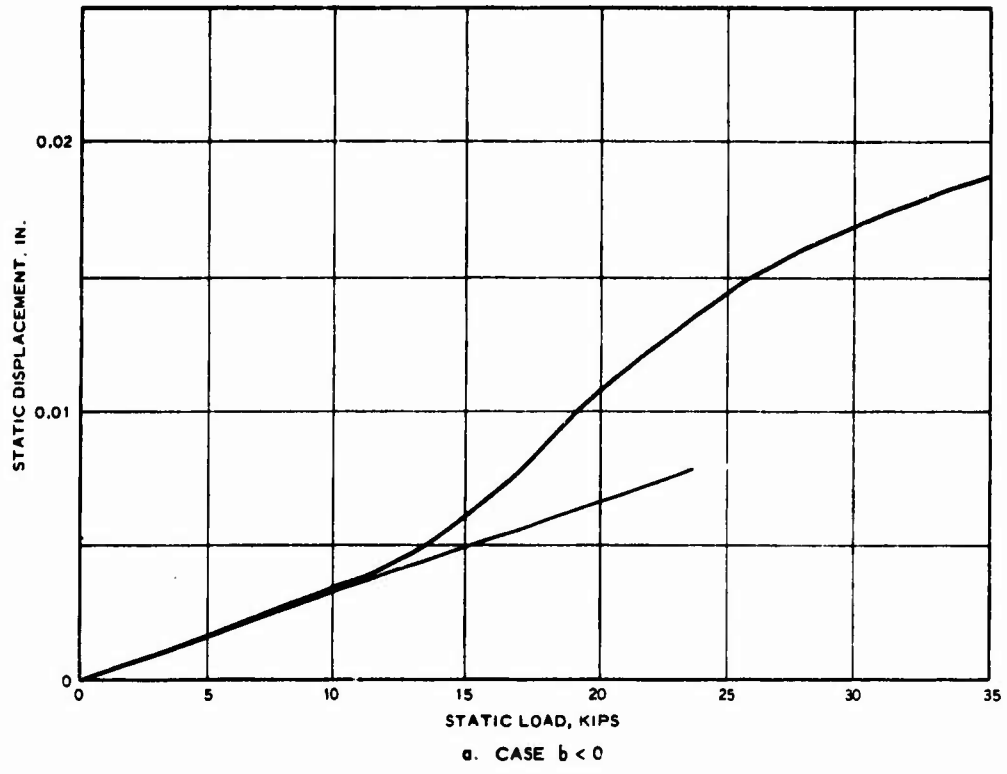

a. CASE $b < 0$

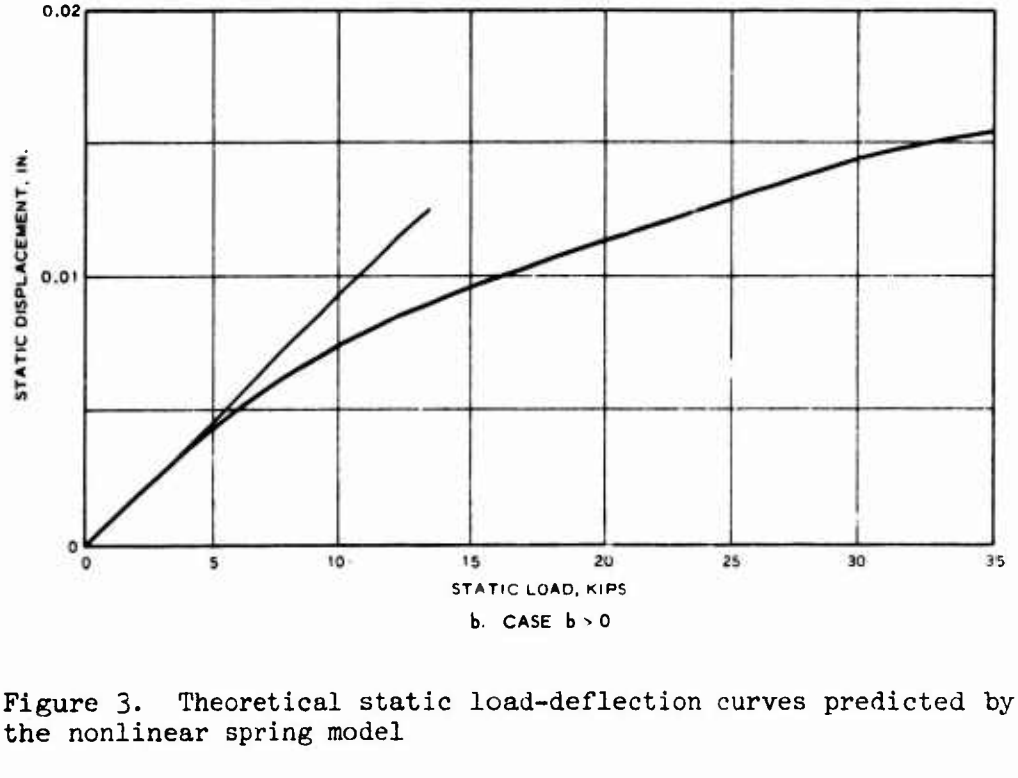

b. CASE $b > 0$

Figure 3. Theoretical static load-deflection curves predicted by the nonlinear spring model

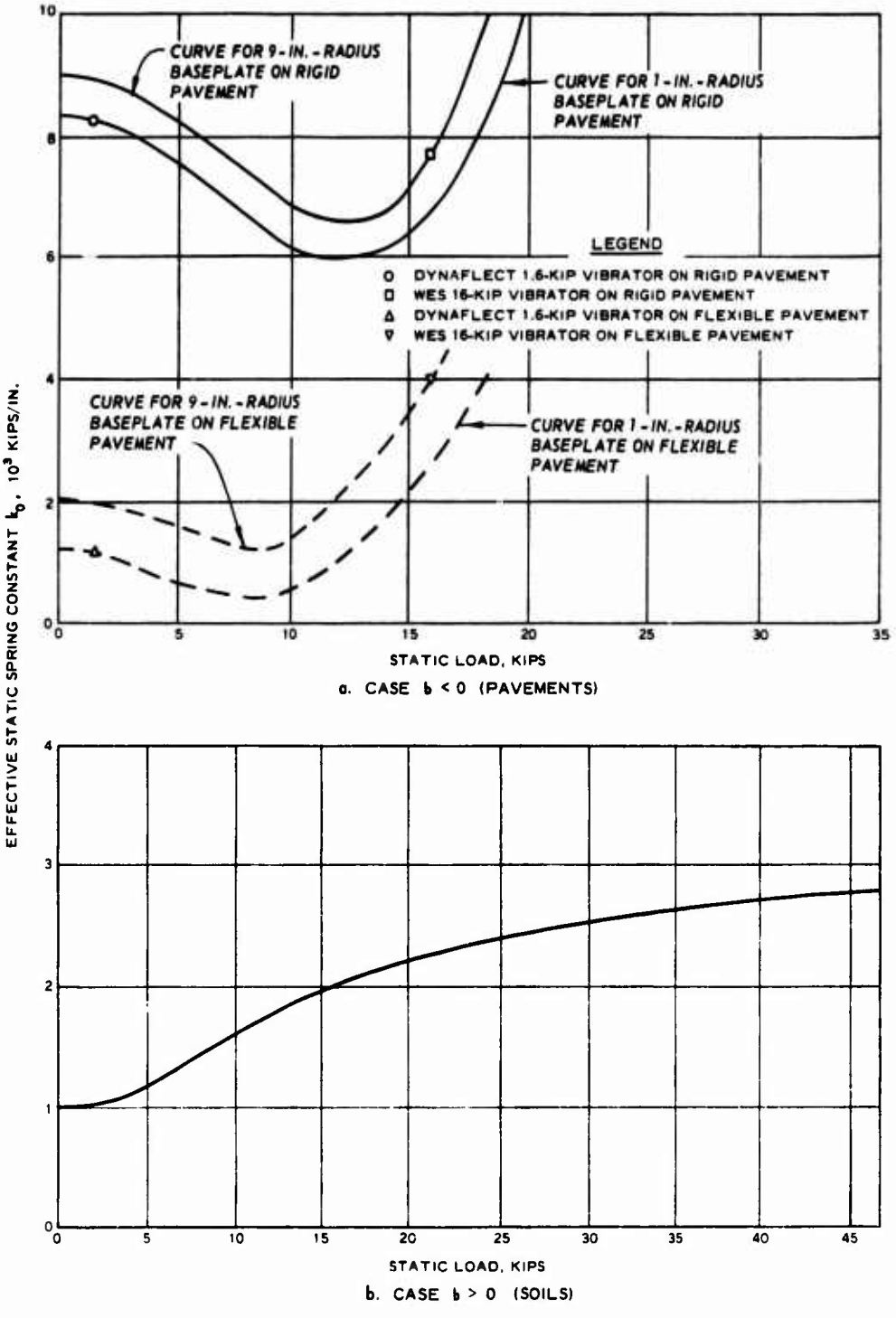

Figure 4. Theoretical dependence of the effective static spring constant on the static load

show respectively the dependence of k_0 on F_s for pavements ($b < 0$) and for $b > 0$ formations. For the case $b < 0$, the function k_0 exhibits a local minimum value for some value of F_s (or x_e).

3.5.9 DAMPING CONSTANT

The dynamic stiffness defined by Equation 3.18 depends on the damping constant C of the pavement as well as on the effective spring constant k. This damping constant is not in general equal to the damping constant for the homogeneous linear elastic half-space, C_H, that was defined in the damping constant expression. A theoretical calculation of C was not made in this report; however, the nonlinear elastic nature of flexible pavements gives rise to a simple method of estimating the value of the damping constant. Equations 3.17, 3.18, and 3.30 show that when $\omega = \omega_c$, the dynamic stiffness has the critical value:

$$S_c = \sqrt{\left(\mu b A^2 + \eta e A^4\right)^2 + C^2\omega_c^2}$$

$$\approx \sqrt{2C\omega_c} \qquad (3.48)$$

Therefore a measure of the damping constant can be determined directly from the dynamic load versus deflection curves by measuring the critical value of the dynamic stiffness. An approximation to the value of the damping constant is thus given by

$$C = \frac{S_c}{\sqrt{2\omega_c}} \qquad (3.49)$$

3.6 PHYSICAL ORIGIN OF THE NONLINEAR PAVEMENT PARAMETERS

3.6.1 INTRODUCTION OF THE FINITE DEPTH OF INFLUENCE

This part of the report examines the physical origin of the parameters k_{00}, b, and e that were introduced in Section 3.2 as part of a model developed to account for the observed nonlinear vibration

data that will be presented in Section 4.1. It is the departure from perfect linear elasticity that is responsible for the nonlinear response of vibrators operating at the surface of pavements and soil formations. Over a large depth in the half-space, the departure from a perfectly linear constitutive equation for soils and pavements has the effect of introducing a finite range of influence of the elastic stress and strain due to a static surface loading on an elastic half-space. In this report the finite range of influence of the static stress and strain is assumed to produce the experimentally observed nonlinear dynamic load deflection curves.

3.6.2 DEPARTURE FROM LINEAR ELASTICITY

Many authors have studied the problem of the static embedding of a circular punch into a linear elastic half-space.[8] Layered elastic half-spaces have been considered and so has the case in which G has a power law variation with depth.[8-10] The case in which G has a simple linear variation with depth has been worked out completely.[11] All of these theories are insufficient to explain the experimental data appearing in Section 4.1 because these theories are based on the assumption of a perfect linear elasticity. One of the characteristics of a nonhomogeneous perfectly linear elastic half-space is that the static load-deflection curve and the dynamic load-deflection curve are straight lines. For instance, a stack of perfectly linear elastic layers of different values of ν and G produces a linear load-deflection curve for a load applied to the surface of the stack. This is so because the static stress and strain in a perfectly linear elastic half-space extend to an infinite depth and to an infinite radial distance, and theoretically the entire stack of elastic layers contributes to the deflection of the load at the surface of the stack. In a perfectly linear theory of elasticity, the static load-deflection curve for a stack of layers can always be reproduced by an equivalent homogeneous three-dimensional half-space with an equivalent spring constant. Therefore, a nonhomogeneous linear elastic system exhibits a linear load-deflection curve, and nonhomogeneity by itself is insufficient to explain the

nonlinear load-deflection curves observed on pavements and soils. A basic departure from linear elasticity is required to account for the observed nonlinear response of vibrators which are operated on the surface of airfield pavements. The nonlinear behavior of pavements is an example of the inadequacy of linear elasticity to explain the dynamic response of real materials.

The static stress and strain field has a finite range of influence in real systems such as PCC, AC, or soil. This is a fundamental characteristic of real media. If a static load is placed on the surface of a soil formation or a pavement, the static stress and strain attenuate rapidly with depth and radial distance and go to zero at some finite depth below the surface and at some finite radial distance from the load. The stress and strain field in a real half-space does not extend to infinite depth as it does for the case of the Boussinesq and Terazawa treatment of the static load applied to the surface of a linear elastic half-space.[12,13] For real materials, the depth of influence depends on the size of the loaded area, the magnitude of the static load, and the intrinsic nonlinear properties of the material. For a dynamic load, there is also a finite range of influence in real media where the dynamic amplitude of the three-dimensional elastic waves emanating from a source goes to zero. For the dynamic source, the finite range of influence is generally thousands of feet or often miles; but for the static source, the finite influence distance is generally a few feet or inches. Both homogeneous and nonhomogeneous materials exhibit a finite range of influence, and in this report it is assumed that the finite static depth of influence combined with the variation of the elastic properties of a pavement with depth determines the magnitude of the nonlinear response of a pavement to static and dynamic loads applied to the surface.

Only a small departure from the linear stress-versus-strain constitutive equation is required to produce a finite range of influence of several feet. A small specimen of this solid would exhibit essentially linear characteristics during laboratory load-deflection tests or standing wave tests. Only over a distance of several feet in an actual soil

formation or pavement would the nonlinear constitutive equation manifest itself by the finite range of the stress and strain field. The spring constant for a real elastic half-space depends on the static range of influence and on the values of ν and G which are contained within the static range of influence. In this chapter, the foregoing arguments are placed on a quantitative basis by a calculation of the nonlinear response of a one-dimensional representation of an elastic half-space for any distribution of ν and G with depth.

The four calculations required to determine the three parameters k_{00}, b, and e are:

a. Work done by the static elastic deflection of the pavement surface beneath the vibrator baseplate (Section 3.6.3).

b. Static strain energy in the pavement (Section 3.6.4).

c. Calculation of average elastic parameters for a one-dimensional layered system (Sections 3.6.5 and 3.6.6).

d. Representation of the finite depth of influence by an infinite series (Section 3.6.7).

3.6.3 WORK ASSOCIATED WITH STATIC ELASTIC DEFLECTION

The dynamic load applied at the surface is determined by the three parameters k_{00}, b, and e. A general method of calculating these three parameters in terms of the variation of ν and G with depth is required. The static elastic indentation as a function of static load can then be calculated from Equation 3.4 using these three parameters. The method used to calculate k_{00}, b, and e is an energy method which equates the work done during the indentation of a rigid punch into the surface of an elastic half-space to the increase of the potential strain energy of the half-space. The work done by the static load is obtained from Equation 3.4 to be

$$W = \frac{k_{00}x_e^2}{2} + \frac{bx_e^4}{4} + \frac{ex_e^6}{6}$$

$$\equiv W_2x_e^2 + W_4x_e^4 + W_6x_e^6 \qquad (3.50)$$

where W_2 , W_4 , and W_6 are the coefficients in the power series expansion of W . Only a static approach to the calculation of k_{00} , b , and e is undertaken in this report, and it should be realized that a fully dynamic calculation of these parameters may introduce a frequency dependence.

3.6.4 STRAIN ENERGY OF AN ELASTIC HALF-SPACE WITH A FINITE DEPTH OF INFLUENCE

The elastic strain energy of a pavement-soil system can be expressed in terms of the equilibrium static elastic displacement x_e . A complete three-dimensional calculation of the strain energy of a nonhomogeneous nonlinear half-space is very complicated. The calculation of the static strain energy that is done in this chapter is a one-dimensional approximation of the actual physical situation. In this calculation it is assumed that the strain in the half-space is in the vertical direction only and is confined to a frustum of a cone whose upper area is equal to the area of the vibrator baseplate. The height of the frustum of a cone is taken to be equal to the finite depth of influence in the pavement, and the area of the lower base is chosen to make the theoretical values of the finite depth of influence agree with the experimental values.

The frustum of the cone in which the strain is assummed to be confined is shown in Figure 5. The volume of the frustum is given by

$$V = \pi a^2 \ell \Psi \tag{3.51}$$

where

V = volume of the frustum of a cone having a depth equal to the finite depth of influence in the pavement

ℓ = finite depth of influence of the static strain field

Ψ = the volume factor for the frustum of the cone which is calculated as follows:

$$\Psi = \frac{1 + \kappa + \kappa^2}{3} \tag{3.52}$$

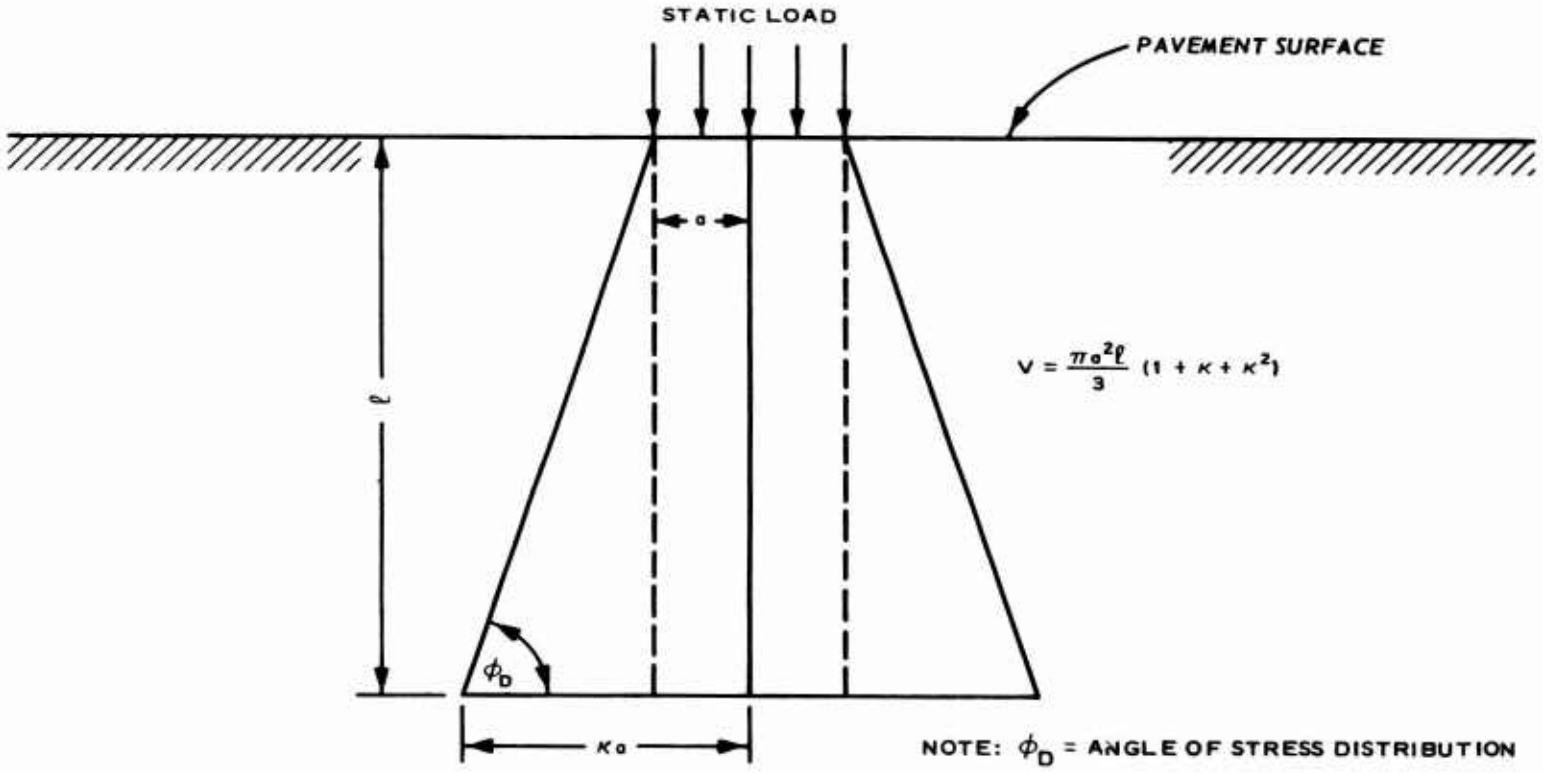

Figure 5. Frustum of cone in which stress and strain in the pavement are assumed to be confined

where κ equals the ratio of the radius of the lower base of the frustum to the radius of the upper area of the frustum. Experimental tests show that $\Psi \approx 4$ and $\kappa \approx 3$ for AC pavements.

It is assumed that the strain energy can be written in a form analogous to that for a perfectly linear elastic system except that the depth of influence is taken to be finite. The elastic strain energy density for a homogeneous solid is[14]

$$\mathfrak{E} = G\varepsilon^2 + \frac{\lambda\theta^2}{2} \tag{3.53}$$

where

$\mathfrak{E}$ = energy density

ε = strain in vertical direction

λ = Lame elastic constant

θ = elastic volume dilation

The validity of Equation 3.53 for a material with a finite depth of influence arises from the essentially linear elastic behavior of most solids including PCC and AC under a small, uniformly disturbed stress. This implies that G and λ have a physical meaning even for real solids. It is only over a long distance from a static surface source on a half-space (which produces a nonuniform distribution of stress and strain) that the nonlinear effects manifest themselves by producing a definite cutoff range for the stress and strain.

An approximation to the strain energy density of a real half-space is given by Equation 3.52 if the finite depth of influence is introduced through ε and θ. For a one-dimensional representation of an elastic half-space, the strain and dilation can be approximated by

$$\varepsilon = \frac{\Delta\ell}{\ell} = \frac{x_e}{\ell} \tag{3.54}$$

$$\theta = \frac{\Delta V}{V} = \frac{\pi a^2 x_e \Psi}{\pi a^2 \ell \Psi} = \frac{x_e}{\ell} \tag{3.55}$$

where

$\Delta\ell$ = increment of the finite depth of influence

ΔV = increment of the volume of the frustum of the cone containing the strain field

Therefore within the limits of the vertical strain approximation, ϵ and θ are equal, and the strain energy density for a homogeneous half-space can be written as

$$\mathfrak{E} = \left(G + \frac{\lambda}{2}\right)\left(\frac{x_e}{\ell}\right)^2 \tag{3.56}$$

The total strain energy for the homogeneous material in the cylinder of influence can be written as

$$U = \mathfrak{E}V = \pi a^2 \Psi \left(G + \frac{\lambda}{2}\right)\frac{x_\epsilon^2}{\ell} \tag{3.57}$$

where U is the elastic strain energy. In engineering practice it is customary to use Poisson's ratio in place of the Lame elastic constant. In terms of Poisson's ratio, Equation 3.57 is written as

$$U = \frac{\pi a^2 Q G x_e^2 \Psi}{\ell} \tag{3.58}$$

where Q, the function of Poisson's ratio, is expressed as

$$Q = \frac{1 - \nu}{1 - 2\nu} \tag{3.59}$$

For a nonhomogeneous half-space for which ν and G vary with depth, the strain energy is written as

$$U = \frac{\pi a^2 \overline{QG} x_e^2 \Psi}{\ell} \tag{3.60}$$

where $\overline{QG}$ equals the value of QG averaged over the depth of influence ℓ.

3.6.5 LAYERED ELASTIC MODEL OF PAVEMENT AND SOIL SYSTEM

A pavement-soil system generally consists of a layer of PCC or AC

overlying several layers of crushed rock base and subbase, all of which rest on the subgrade which is the natural soil foundation. A model representing the pavement-soil system consists of a series of elastic layers, with ν and G constant in each layer to represent the pavement, base, and subbase overlying an elastic half-space. This half-space represents the subgrade and therefore has ν and G increasing continuously with depth because the overburden pressure increases continuously with depth. This variation of ν and G with depth is represented in Figure 6.

3.6.6 AVERAGED ELASTIC PARAMETERS

The average value, $\overline{QG}$, required in Equation 3.60 is calculated by averaging over the depth of influence ℓ as follows:

$$\overline{QG} = Q_1G_1 , \qquad \ell < h_1 \quad (3.61)$$

$$\overline{QG} = \frac{1}{\ell}\left[Q_1G_1h_1 + Q_2G_2(\ell - h_1)\right], \qquad h_1 < \ell < H_2 \quad (3.62)$$

$$\overline{QG} = \frac{1}{\ell}\left[Q_1G_1h_1 + Q_2G_2h_2 + Q_3G_3(\ell - H_2)\right], \qquad H_2 < \ell < H_3 \quad (3.63)$$

where Q_1G_1, Q_2G_2, and Q_3G_3 equal respectively the value of QG in layers 1, 2, and 3, h_1, h_2, and h_3 equal respectively the thicknesses of layers 1, 2, and 3, H_1, H_2, and H_3 equal the sums of pavement layer thicknesses, and where

$$H_2 = h_1 + h_2 \quad (3.64)$$

$$H_3 = h_1 + h_2 + h_3 \quad (3.65)$$

Equation 3.61 is valid if the depth of influence extends only into the upper layer, while Equation 3.62 is valid if ℓ extends into the second layer, and finally Equation 3.63 is valid if ℓ extends into the third layer. The generalization of Equations 3.61-3.63 to more than three layers is obvious. Equations 3.61-3.63 are valid only if the depth of

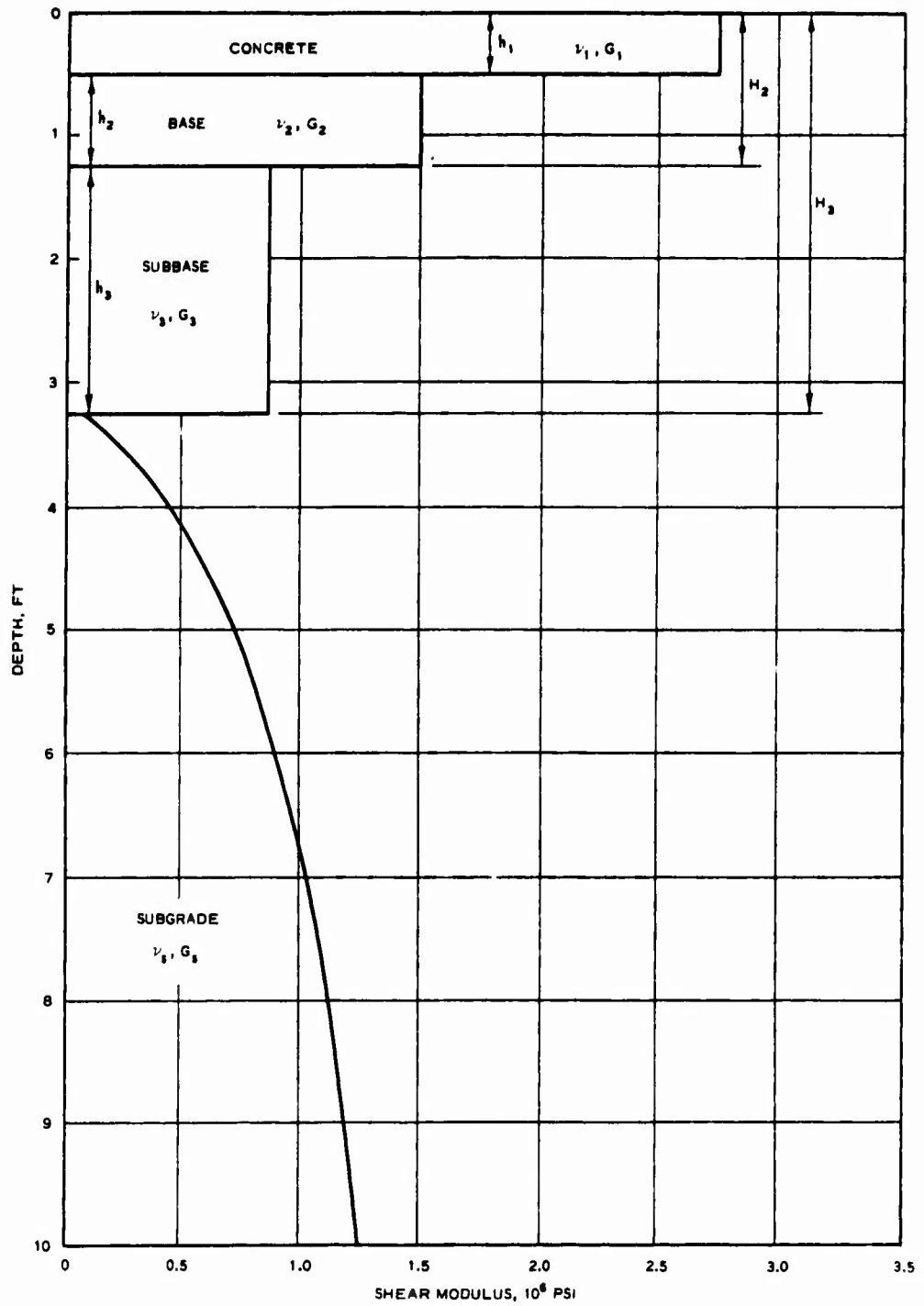

Figure 6. Layered model of pavement

influence is contained within the pavement, base, and subbase, i.e., the layers in which ν and G are constant. If the depth of influence extends into the subgrade, then the proper average is

$$\overline{QG} = \frac{1}{\ell}\left[Q_1G_1h_1 + Q_2G_2h_2 + Q_3G_3h_3 + \overline{Q_sG_s}\,(\ell - H_3)\right], \quad \ell > H_3 \tag{3.66}$$

where G_s equals the shear modulus of the subgrade, Q_s equals the value of Q given by Equation 3.59 but for the subgrade, and $\overline{Q_sG_s}$ equals the average value of Q_sG_s in the interval $\ell - H_3$. The product Q_sG_s for soil at a depth z below the surface of the pavement can be written as a Taylor series expansion as follows:

$$Q_s(z)G_s(z) = Q_s^0G_s^0 + \left.\frac{d(Q_sG_s)}{dz}\right|_{H_3}(z - H_3) + \frac{1}{2}\left.\frac{d^2(Q_sG_s)}{dz^2}\right|_{H_3}(z - H_3)^2 + \ldots \tag{3.67}$$

where $Q_s^0G_s^0$ equals the product Q_sG_s for the soil at the very top of the subgrade, i.e., the value of Q_sG_s at $\ell = H_3$. The average value $\overline{Q_sG_s}$ appearing in Equation 3.66 is assumed to be given as

$$\overline{Q_sG_s} = \frac{1}{\ell - H_3}\int_{H_3}^{\ell} Q_sG_s\,dz \tag{3.68}$$

Using Equation 3.67, the average becomes

$$\overline{Q_sG_s} = Q_s^0G_s^0 + \frac{1}{2}\left.\frac{d(Q_sG_s)}{dz}\right|_{H_3}(\ell - H_3) + \frac{1}{6}\left.\frac{d^2(Q_sG_s)}{dz^2}\right|_{H_3}(\ell - H_3)^2 + \ldots \tag{3.69}$$

and this value is used in Equation 3.66.

3.6.7 SERIES EXPANSION OF THE FINITE DEPTH OF INFLUENCE

The physics of pavements and soils enters through a calculation of the depth of influence, ℓ, from a fundamental knowledge of the molecular structure of pavement and soil materials and from a knowledge of the cracks, voids, dislocations, and other microscopic flaws in these materials. A basic calculation of ℓ from a theoretical physics point of view has not been carried out in this study. In this report, the static depth of influence is assumed to be given by

$$\ell = \ell_0 + \ell_2 x_e^2 + \ell_4 x_e^4 + \ldots \tag{3.70}$$

where ℓ_0, ℓ_2, and ℓ_4 are coefficients of the power series expansion of the finite depth of influence, and depend on the radius of the contact area of the load with the pavement surface and on the values of ν and G of the pavement-soil system. The choice of the form of Equation 3.70 is dictated by the even powers of the work function in Equation 3.50. A rigorous calculation of the values of ℓ_0, ℓ_2, and ℓ_4 has not been accomplished theoretically. In this report the values of ℓ_0, ℓ_2, and ℓ_4 are estimated from the experimental values of k_{00}, b, and e.

3.7 CALCULATION OF THE NONLINEAR PARAMETERS

All of the quantities required for the determination of k_{00}, b, and e have been calculated in the previous five sections. Now the energy principle, that the static potential strain energy must equal the work done during the static elastic deflection of the vibrator into the pavement surface, is applied to the one-dimensional pavement model. This condition gives the connection between the parameters k_{00}, b, and e and the corresponding elastic and inelastic pavement parameters. In this section the parameters k_{00}, b, and e are calculated for a pavement system consisting of a series of layers overlying a subgrade.

3.7.1 GENERAL EXPRESSION FOR THE PAVEMENT PARAMETERS

The potential strain energy is calculated using Equations 3.60-3.70 and can be put in the form:

$$U = U_2 x_e^2 + U_4 x_e^4 + U_6 x_e^6 \tag{3.71}$$

where U_2 , U_4 , and U_6 are the coefficients of the power series expansion of the elastic strain energy. The particular mathematical form for the potential strain energy given by Equation 3.71 is chosen in order to agree with the form of the work function in Equation 3.50. The values of U_2 , U_4 , and U_6 are calculated by substituting the value of ℓ given by Equation 3.70 into the expression $\overline{QG}$ in Equation 3.60 and expanding in a power series in x_e^2 . The values of U_2 , U_4 , and U_6 will depend on the magnitude of the depth of influence, which is determined by ℓ_0 , ℓ_2 , and ℓ_4 , and on the ν and G values within the depth of influence. The coefficients k_{00} , b , and e are obtained by setting $W = U$ or equivalently

$$\begin{aligned} W_2 &= U_2 \\ W_4 &= U_4 \\ W_6 &= U_6 \end{aligned} \tag{3.72}$$

from which it follows that

$$\begin{aligned} k_{00} &= 2U_2 \\ b &= 4U_4 \\ e &= 6U_6 \end{aligned} \tag{3.73}$$

The values of k_{00} , b , and e will depend on ℓ_0 , ℓ_2 , and ℓ_4 .

In the following sections, the general expressions for the parameters k_{00} , b , and e given by Equation 3.73 are evaluated for specific cases of layered systems and layered systems overlying a

subgrade whose shear modulus increases uniformly with depth.

3.7.2 ONE ELASTIC LAYER

For $\ell < h_1$, the stress and strain extend only into the upper pavement layer. Equations 3.60, 3.61, and 3.70 give:

$$k_{00} = \frac{2\pi a^2 Q_1 G_1 \Psi}{\ell_0} \tag{3.74}$$

$$b = -\frac{4\pi a^2 Q_1 G_1 \ell_2 \Psi}{\ell_0^2} \tag{3.75}$$

$$e = \frac{6\pi a^2 Q_1 G_1 \delta \Psi}{\ell_0} \tag{3.76}$$

where δ is the function of the expansion coefficients of the finite depth of influence and

$$\delta = \left(\frac{\ell_2}{\ell_0}\right)^2 - \frac{\ell_4}{\ell_0} \tag{3.77}$$

The results of Equations 3.74-3.77 are valid for the homogeneous half-space.

3.7.3 TWO ELASTIC LAYERS

For $h_1 < \ell < H_2$, the stress and strain extend into the second layer and Equations 3.60, 3.62, and 3.70 give:

$$k_{00} = \frac{2\pi a^2 \Psi}{\ell_0^2}\left[h_1\left(Q_1 G_1 - Q_2 G_2\right) + Q_2 G_2 \ell_0\right] \tag{3.78}$$

$$b = -\frac{4\pi a^2 \ell_2 \Psi}{\ell_0^3}\left[2h_1(Q_1 G_1 - Q_2 G_2) + Q_2 G_2 \ell_0\right] \tag{3.79}$$

$$e = \frac{6\pi a^2 \Psi}{\ell_0^2}\left[\rho h_1(Q_1 G_1 - Q_2 G_2) + \delta Q_2 G_2 \ell_0\right] \tag{3.80}$$

where ρ is the function of the expansion coefficients of the finite depth of influence and

$$\rho = 3\left(\frac{\ell_2}{\ell_0}\right)^2 - 2\frac{\ell_4}{\ell_0} \tag{3.81}$$

Equations 3.78-3.80 reduce to Equations 3.74-3.76 when $Q_1G_1 = Q_2G_2$, as they should because this condition reproduces the homogeneous half-space.

3.7.4 THREE-LAYER SYSTEM AND THE GENERALIZATION TO n LAYERS

For the three-layer case with $H_2 < \ell < H_3$ corresponding to the case where the stress and strain extend into the third layer, Equations 3.60, 3.63, and 3.70 give:

$$k_{00} = \frac{2\pi a^2\psi}{\ell_0^2}\left[h_1(Q_1G_1 - Q_3G_3) + h_2(Q_2G_2 - Q_3G_3) + Q_3G_3\ell_0\right] \tag{3.82}$$

$$b = -\frac{4\pi a^2\ell_2\psi}{\ell_0^3}\left\{2\left[h_1(Q_1G_1 - Q_3G_3) + h_2(Q_2G_2 - Q_3G_3)\right] + Q_3G_3\ell_0\right\} \tag{3.83}$$

$$e = \frac{6\pi a^2\psi}{\ell_0^2}\left\{\rho\left[h_1(Q_1G_1 - Q_3G_3) + h_2(Q_2G_2 - Q_3G_3)\right] + \delta Q_3G_3\ell_0\right\} \tag{3.84}$$

The generalization to the case of more than three layers is simple. Consider a system of n layers where $H_{n-1} < \ell < H_n$ and which corresponds to the case in which the finite influence depth extends into the n^{th} layer. For this case the coefficients are

$$k_{00} = \frac{2\pi a^2\psi}{\ell_0^2}\left[\sum_{i=1}^{n-1} h_i(Q_iG_i - Q_nG_n) + Q_nG_n\ell_0\right] \tag{3.85}$$

$$b = -\frac{4\pi a^2\ell_2\psi}{\ell_0^3}\left[2\sum_{i=1}^{n-1} h_i(Q_iG_i - Q_nG_n) + Q_nG_n\ell_0\right] \tag{3.86}$$

$$e = \frac{6\pi a^2 \psi}{\ell_0^2}\left[\rho \sum_{i=1}^{n-1} h_i(Q_i G_i - Q_n G_n) + \delta Q_n G_n \ell_0\right] \tag{3.87}$$

3.7.5 LAYERED SYSTEM WITH SUBGRADE

If the n layered pavement overlies a subgrade and $\ell > H_n$ so that the stress and strain extend into the soil medium, then Equations 3.60 and 3.66-3.70 give

$$k_{00} = \frac{2\pi a^2 \psi}{\ell_0^2}\left[\sum_{i=1}^{n} h_i\left(Q_i G_i - Q_s^0 G_s^0\right) + Q_s^0 G_s^0 \ell_0 + \varepsilon_2 \left.\frac{d(Q_s G_s)}{dz}\right|_{H_n} + \kappa_2 \left.\frac{d^2(Q_s G_s)}{dz^2}\right|_{H_n}\right] \tag{3.88}$$

$$b = -\frac{4\pi a^2 \ell_2 \psi}{\ell_0^3}\left[2 \sum_{i=1}^{n} h_i\left(Q_i G_i - Q_s^0 G_s^0\right) + Q_s^0 G_s^0 \ell_0 + \varepsilon_4 \left.\frac{d(Q_s G_s)}{dz}\right|_{H_n} + \kappa_4 \left.\frac{d^2(Q_s G_s)}{dz^2}\right|_{H_n}\right] \tag{3.89}$$

$$e = \frac{6\pi a^2 \psi}{\ell_0^2}\left[\rho \sum_{i=1}^{n} h_i\left(Q_i G_i - Q_s^0 G_s^0\right) + \delta Q_s^0 G_s^0 \ell_0 + \varepsilon_6 \left.\frac{d(Q_s G_s)}{dz}\right|_{H_n} + \kappa_6 \left.\frac{d^2(Q_s G_s)}{dz^2}\right|_{H_n}\right] \tag{3.90}$$

where ε_2, ε_4, ε_6, κ_2, κ_4, and κ_6 are the expansion coefficients appearing in the expressions for k_{00}, b, and e and

$$\varepsilon_2 = \frac{\ell_0}{2}(\ell_0 - H_n) \tag{3.91}$$

$$\kappa_2 = \frac{\ell_0^2}{6}(\ell_0 - H_n) \tag{3.92}$$

$$\varepsilon_4 = -\frac{1}{2}\ell_0 H_n \tag{3.93}$$

$$\kappa_4 = -\frac{1}{6}\ell_0^3 \tag{3.94}$$

$$\varepsilon_6 = -\frac{1}{2}\delta\ell_0 H_0 \tag{3.95}$$

$$\kappa_6 = \frac{1}{6}\ell_4\ell_0^2 \tag{3.96}$$

For a soil formation by itself, $h_i = 0$ and $H_n = 0$ so that

$$k_{00} = \frac{2\pi a^2 \Psi}{\ell_0}\left[Q_s^0 G_s^0 + \frac{\ell_0}{2}\frac{d(Q_s G_s)}{dz}\bigg|_0 + \frac{\ell_0^2}{6}\frac{d^2(Q_s G_s)}{dz^2}\bigg|_0 + \ldots\right] \tag{3.97}$$

$$b = -\frac{4\pi a^2 \ell_2 \Psi}{\ell_2^0}\left[Q_s^0 G_s^0 - \frac{\ell_0^2}{6}\frac{d^2(Q_s G_s)}{dz^2}\bigg|_0 + \ldots\right] \tag{3.98}$$

$$e = \frac{6\pi a^2 \Psi}{\ell_0}\left[\delta Q_s^0 G_s^0 + \frac{\ell_4\ell_0}{6}\frac{d^2(Q_s G_s)}{dz^2}\bigg|_0 + \ldots\right] \tag{3.99}$$

where $Q_s^0 G_s^0$ depends on the values of ν_s, Poisson's ratio for the subgrade, and G_s at the soil surface.

3.7.6 ALGEBRAIC SIGNS OF THE NONLINEAR PARAMETERS b AND e

The minus sign appearing in the expression for the nonlinear coefficient b arises from the inverse dependence of U on ℓ. From Equation 3.75 it follows that $b < 0$ for a homogeneous half-space. For a nonhomogeneous half-space, the sign of the coefficient b depends on the variation of ν and G with depth in the pavement and in the soil. Consider first the case where the depth of influence extends only into the pavement, $\ell < H_n$, and Equation 3.86 is valid. Then Equation 3.86 shows that if the values of $Q_i G_i$ decrease with depth, as is the general case with pavements, then $b < 0$. If $Q_i G_i$ increases with depth, then $b < 0$ or $b > 0$, depending on the rate of increase of $Q_i G_i$ with depth. If the rate of increase of $Q_i G_i$ with depth is sufficiently rapid, then there is a possibility that $b > 0$. The same results are valid when the depth of influence extends into the subgrade. Most cases of interest to soil and pavement engineers will have $b < 0$.

3.7.7 CALCULATION OF THE FINITE DEPTH OF INFLUENCE AND THE DETERMINATION OF LAYER THICKNESS

It has been shown in Sections 3.7.2-3.7.5 that different expressions for the coefficients k_{00}, b, and e must be chosen according to the magnitude of the depth of influence, i.e., depending on the particular pavement layer into which the static depth of influence extends. The static finite depth of influence is expected to depend on the baseplate radius of the vibrator and the static load that the vibrator applies to the pavement surface. Therefore different expressions for the coefficients k_{00}, b, and e must be used if a series of baseplate radii are selected for the vibrator. Equations 3.74-3.99 show that the change in the equations describing k_{00}, b, and e occurs when $\ell_0 = H_i$, i.e., when ℓ_0 passes through the successive interfaces of the pavement system. The values of the baseplate radius for which $\ell_0 = H_i$ will be called the critical radii. Therefore the critical radii are defined by

$$\ell_0(a_{ci}) = H_i \tag{3.100}$$

where a_{c1}, a_{c2}, ...a_{ci} are the critical contact radii of the vibrator baseplate corresponding to the interface at the depths H_i.

The zeroth-order coefficient, ℓ_0, of the static finite depth of influence can be calculated in terms of the radius of the vibrator baseplate, the critical radii for the layered system, and the elastic constants of each layer of the system. The value of ℓ_0 for a homogeneous elastic half-space can be obtained by equating the value of k_{00} given by Equation 3.74 with the value of the spring constant for a linear elastic half-space, with the result:

$$\ell_0 = \frac{1}{2}\pi a \Psi B \tag{3.101}$$

where B is a function of Poisson's ratio for the homogeneous half-space and is defined by:

$$B = \frac{(1 - \nu)^2}{1 - 2\nu} \tag{3.102}$$

Equation 3.101 shows that ℓ_0 is proportional to the radius of the contact area of the vibrator which is exerting the static load on the surface of the half-space.

For a layered pavement system, ℓ_0 is given by the following expressions:

$$\ell_0 = \frac{1}{2}\pi\Psi B_1 a, \qquad 0 < \ell_0 < H_1 \tag{3.103}$$

$$\ell_0 = \frac{1}{2}\pi\Psi[B_2 a + (B_1 - B_2)a_{c1}], \qquad H_1 < \ell_0 < H_2 \tag{3.104}$$

$$\ell_0 = \frac{1}{2}\pi\Psi\left[B_3 a + (B_2 - B_3)a_{c2} + (B_1 - B_2)a_{c1}\right], \qquad H_2 < \ell_0 < H_3 \tag{3.105}$$

$$\ell_0 = \frac{1}{2}\pi\Psi[B_n a + (B_{n-1} - B_n)a_{c,n-1} + (B_{n-2} - B_{n-1})a_{c,n-2} + \ldots(B_1 - B_2)a_{c1}\Big], \quad H_{n-1} < \ell_0 < H_n \tag{3.106}$$

where the values of B for each pavement layer are given by:

$$B_i = \frac{(1 - \nu_i)^2}{1 - 2\nu_i} \tag{3.107}$$

and ν_1, ν_2, ...ν_i are the values of Poisson's ratio for the 1, 2,...i layers of the pavement.

In Section 4.1 it will be shown that the critical radii of a pavement system can be measured experimentally using a mechanical vibrator, so that in principle the function $\ell_0(a,a_{ci})$ can be evaluated The value of the first critical radius is related to the thickness of the first layer in the following manner:

$$h_1 = \frac{1}{2}\pi\Psi B_1 a_{c1} \tag{3.108}$$

In a similar manner it is easy to show from Equations 3.103-3.105 that the thicknesses of the second and third layers are given by:

$$h_2 = \frac{1}{2}\pi\Psi B_2(a_{c2} - a_{c1}) \tag{3.109}$$

$$h_3 = \frac{1}{2}\pi\Psi B_3(a_{c3} - a_{c2}) \tag{3.110}$$

Therefore the thickness of each pavement layer can be determined if the values of the critical radii can be measured.

The values of ℓ_2 and ℓ_4 can be obtained in terms of the values of ℓ_0, b, and e using Equations 3.75, 3.76, 3.79, 3.80, 3.83, 3.84, 3.86, 3.87, 3.89, and 3.90. Therefore measurements of b, e, and the critical radii are necessary for the complete determination of the finite depth of influence. A theoretical calculation of ℓ_0, ℓ_2, and ℓ_4 would probably involve either a molecular theory to describe the nonlinear behavior of the molecular bonds in AC and PCC or a semiempirical nonlinear elastic theory, which has not been considered in this report. Numerical values of ℓ_0, ℓ_2, and ℓ_4 can be obtained from measured values of k_{00}, b, and e, provided that the elastic constants and the layer thicknesses of the pavement are known. The

numerical values of the coefficients ℓ_0 , ℓ_2 , and ℓ_4 that are described in Section 4.2.2 were estimated in this manner.

3.7.8 EFFECT OF BASEPLATE RADIUS

The coefficients k_{00} , b , and e depend on the following quantities:

a. The elastic parameters ν_i and G_i of the pavement layers.

b. The elastic parameters ν_s and G_s of the subgrade.

c. The coefficients ℓ_0 , ℓ_2 , and ℓ_4 , which describe the departure from the linear stress-strain constitutive equation.

The coefficients ℓ_0 , ℓ_2 , and ℓ_4 are functions of the radius of the loaded area on the surface, and therefore k_{00} , b , and e also depend on this radius. The values of k_{00} , b , and e can be obtained as a function of baseplate radius by combining Equations 3.74-3.87 with the equations giving ℓ_0 as a function of baseplate radius. The basic forms of the parameters k_{00} , b , and e and the dynamic stiffness, S , are given in Figures 7, 8, 9, and 10, respectively, for the cases where QG decreases with depth (as in pavements) and for the cases where QG increases with depth. The measured degree of nonlinearity of a pavement-soil system should depend on the radius of the vibrator baseplate. For very large values of the radius, the slopes of the parameters k_{00} , b , and e with respect to the baseplate radius are determined by the deeper pavement or soil layers, whereas the values of these three parameters are determined by the elastic properties of all of the layers which are contained in the depth of influence ℓ_0 . For very small values of the baseplate radius, the slopes of k_{00} , b , and e with respect to the baseplate radius are determined by the elastic properties of the surface and near-surface layers. The parameters b and e are discontinuous functions of the radius of the loaded area; the discontinuities occur when ℓ_0 passes through the boundary between two layers, i.e., when $\ell_0 = H_i$ where H_i is the total thickness of i layers. The value of the discontinuities at $\ell_0 = H_i$ are

$$\Delta b = - \frac{4\pi a^2 \ell_2 \Psi}{\ell_0^3} H_i \left(Q_i G_i - Q_{i+1} G_{\quad} \right) \qquad (3.111)$$

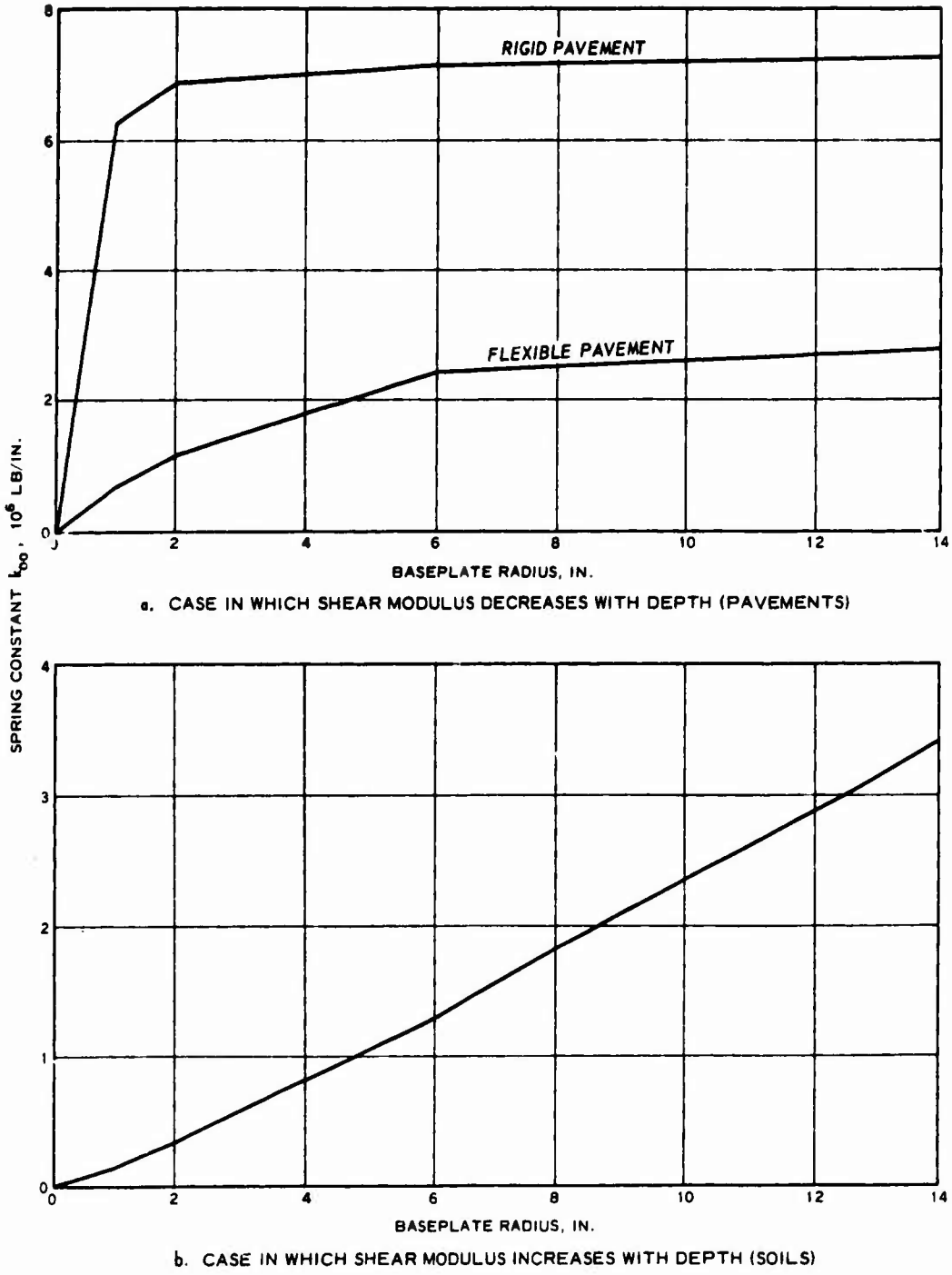

Figure 7. Theoretical dependence of the spring constant, k_{00}, on the radius of the vibrator baseplate

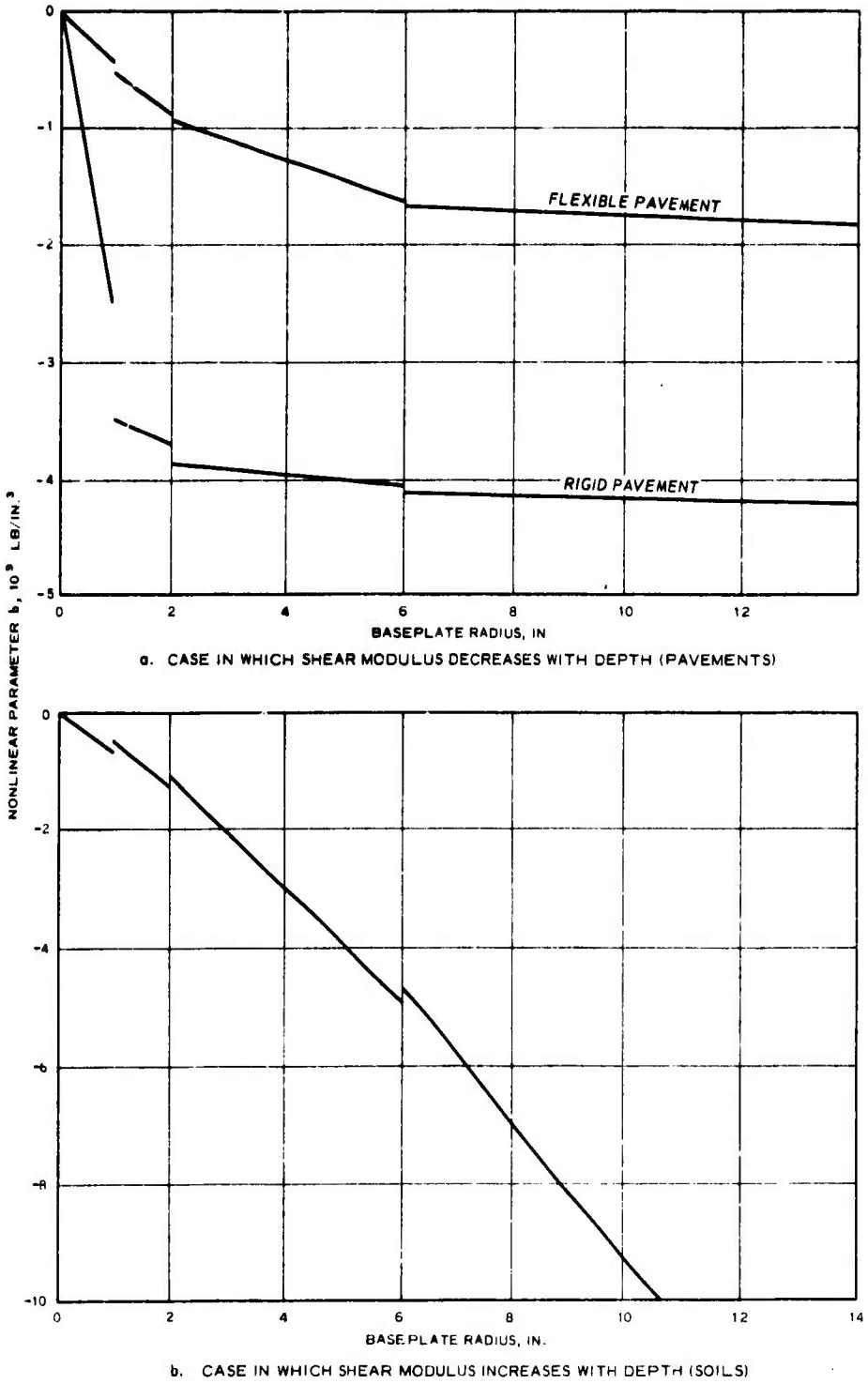

Figure 8. Theoretical dependence of the third-order nonlinear parameter, b , on the radius of the vibrator baseplate

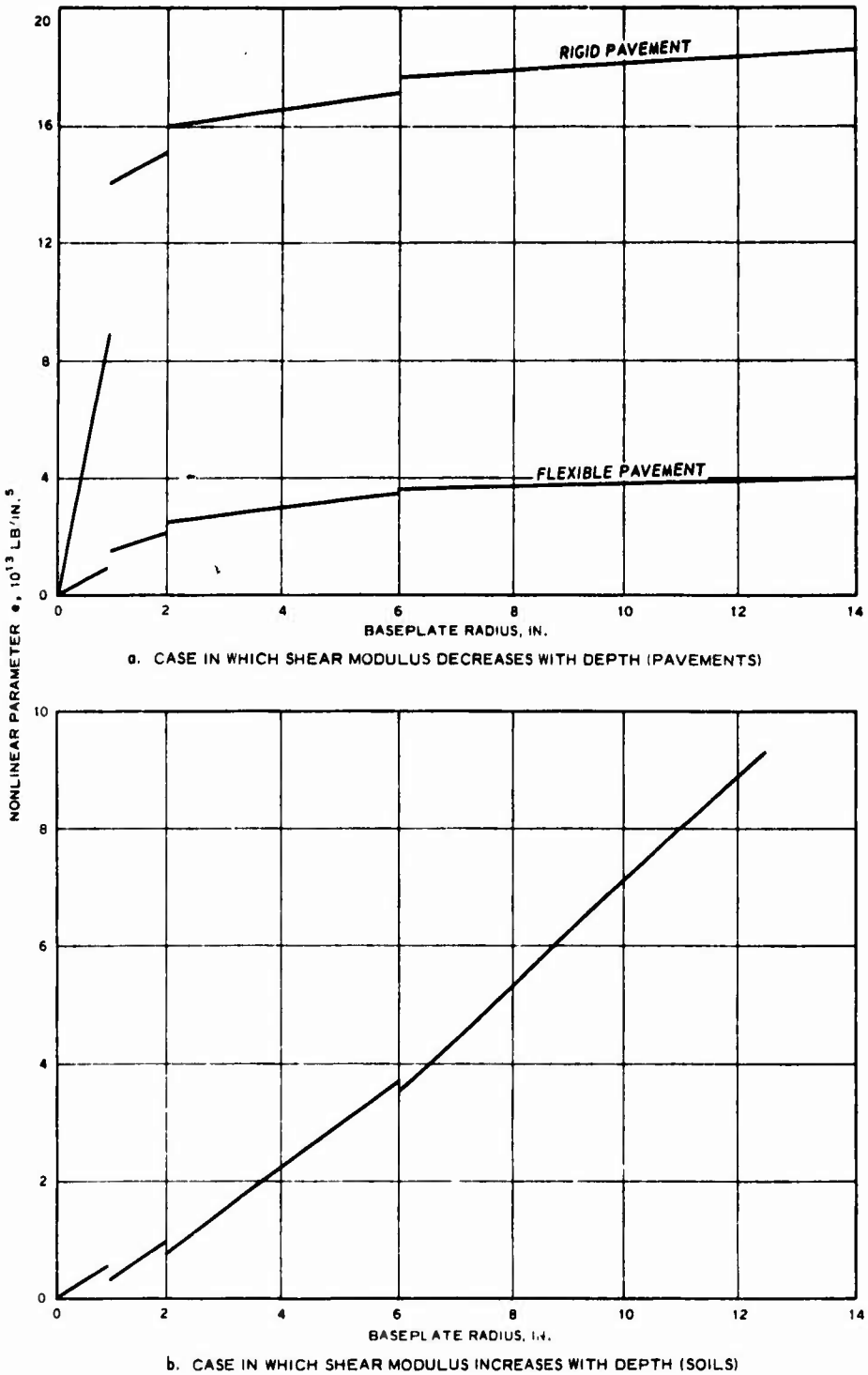

Figure 9. Theoretical dependence of the fifth-order nonlinear parameter, e , on the radius of the vibrator baseplate

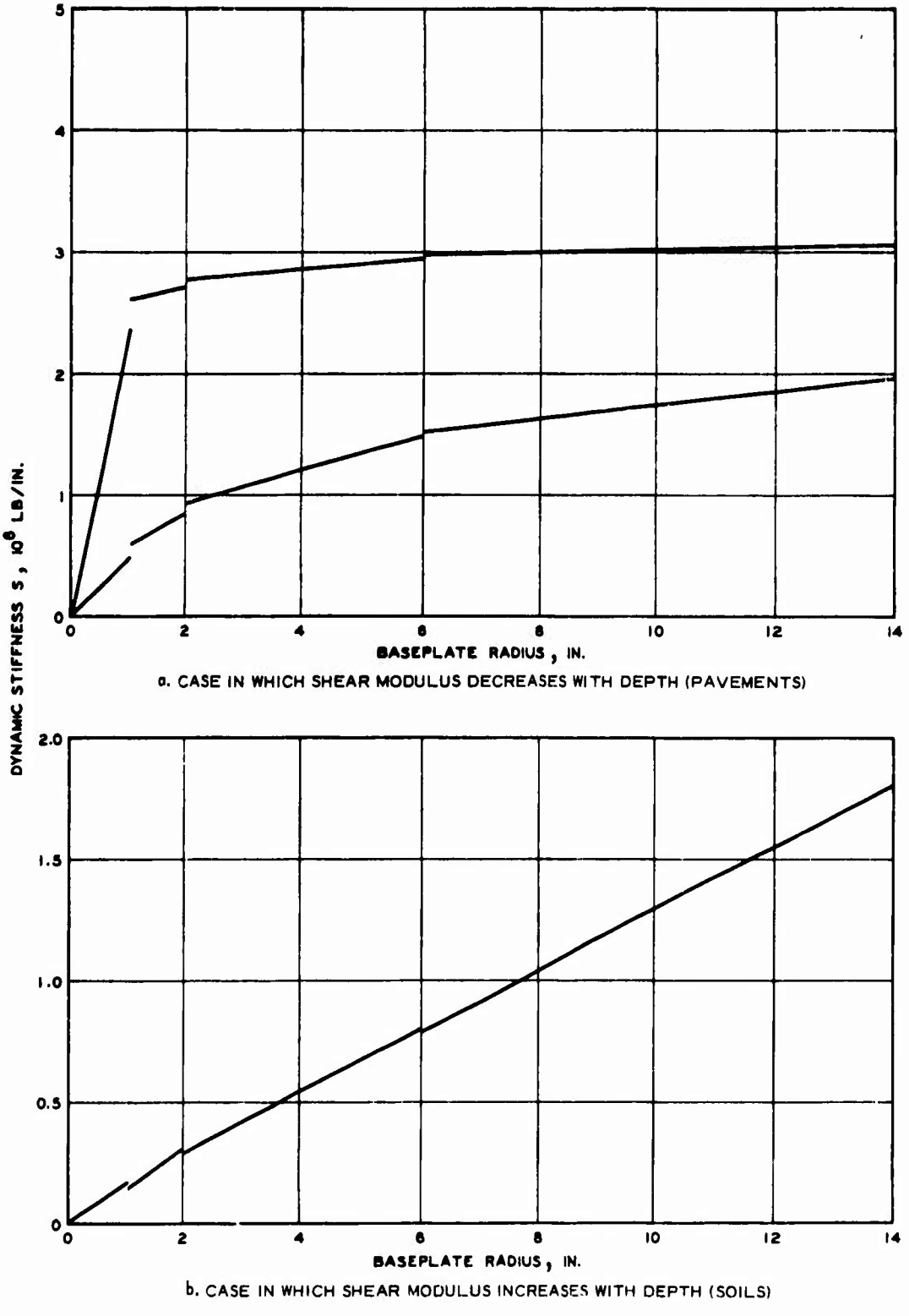

Figure 10. Theoretical dependence of the dynamic stiffness, S , on the radius of the vibrator baseplate

$$\Delta e = \frac{6\pi a^2 \Psi}{\ell_0^2} (\rho - \delta) H_i (Q_i G_i - Q_{i+1} G_{i+1}) \qquad (3.112)$$

The values of the discontinuities in b and e can be positive or negative depending on whether QG is a decreasing or an increasing function of depth, as indicated in Figures 8 and 9.

3.7.9 DETERMINATION OF THE SHEAR MODULI OF THE PAVEMENT LAYERS

The shear modulus of each pavement layer can be obtained from the values of k_{00} for a series of baseplate radii. Computer programs have been developed for calculating the values of k_{00} from the measured dynamic load-deflection curves. Therefore, if dynamic load-deflection curves are measured for a series of vibrator baseplate radii, it is possible to obtain k_{00} as a function of baseplate radius. The elastic shear modulus of each pavement layer is expressed in terms of k_{00} by using Equations 3.74-3.89 with the result:

$$G_1 = \frac{\ell_0 k_{00}(a)}{2\pi a^2 \Psi Q_1}, \qquad 0 < \ell_0 < H_1 \qquad (3.113)$$

$$G_2 = \frac{1}{Q_2(\ell_0 - H_1)} \left[\frac{\ell_0^2 k_{00}(a)}{2\pi a^2 \Psi} - h_1 Q_1 G_1 \right], \qquad H_1 < \ell_0 < H_2 \qquad (3.114)$$

$$G_3 = \frac{1}{Q_3(\ell_0 - H_2)} \left[\frac{\ell_0^2 k_{00}(a)}{2\pi a^2 \Psi} - h_2 Q_2 G_2 - h_1 Q_1 G_1 \right], \quad H_2 < \ell_0 < H_2 \qquad (3.115)$$

$$G_4 = \frac{1}{Q_4(\ell_0 - H_3)} \left[\frac{\ell_0^2 k_{00}(a)}{2\pi a^2 \Psi} - h_3 Q_3 G_3 - h_2 Q_2 G_2 - h_1 Q_1 G_1 \right], \qquad \ell_0 > H_3 \qquad (3.116)$$

These expressions for the shear moduli can be expressed in terms of the baseplate radius and the critical baseplate radii by using Equations 3.103-3.110, with the result:

$$G_1 = \frac{(1 - \nu_1)}{4a} k_{00}(a) , \qquad 0 < a \leq a_{c1} \qquad (3.117)$$

$$G_2 = \frac{(1 - \nu_2)}{4(a - a_{c1})} \phi_2(a) k_{00}(a) - \frac{1 - \nu_2}{1 - \nu_1} \frac{a_{c1}}{a - a_{c1}} \left(\frac{B_1}{B_2}\right)^2 G_1 ,$$

$$a_{c1} < a \leq a_{c2} \qquad (3.118)$$

$$G_3 = \frac{(1 - \nu_3)}{4(a - a_{c2})} \phi_3(a) k_{00}(a) - \frac{1 - \nu_3}{1 - \nu_2} \frac{a_{c2} - a_{c1}}{a - a_{c2}} \left(\frac{B_2}{B_3}\right)^2 G_2$$

$$- \frac{1 - \nu_3}{1 - \nu_1} \frac{a_{c1}}{a - a_{c2}} \left(\frac{B_1}{B_3}\right)^2 G_1 , \qquad a_{c2} < a \leq a_{c3} \qquad (3.119)$$

$$G_4 = \frac{1 - \nu_4}{4(a - a_{c3})} \phi_4(a) k_{00}(a) - \frac{1 - \nu_4}{1 - \nu_3} \frac{a_{c3} - a_{c2}}{a - a_{c3}} \left(\frac{B_3}{B_4}\right)^2 G_3 - \frac{1 - \nu_4}{1 - \nu_2}$$

$$\times \frac{a_{c2} - a_{c1}}{a - a_{c3}} \left(\frac{B_2}{B_4}\right)^2 G_2 - \frac{1 - \nu_4}{1 - \nu_1} \frac{a_{c1}}{a - a_{c3}} \left(\frac{B_1}{B_4}\right)^2 G_1 , \qquad a < a_{c3} \qquad (3.120)$$

where $\phi_2(a)$, $\phi_3(a)$, and $\phi_4(a)$ are functions of the baseplate radius and Poisson's ratio of the successive pavement layers. These functions are given by

$$\phi_2(a) = \left(1 + \frac{B_1 - B_2}{B_2} \frac{a_{c1}}{a}\right)^2 \qquad (3.121)$$

$$\phi_3(a) = \left(1 + \frac{B_2 - B_3}{B_3} \frac{a_{c3}}{a} + \frac{B_1 - B_2}{B_3} \frac{a_{c1}}{a}\right)^2 \qquad (3.122)$$

$$\phi_4(a) = \left(1 + \frac{B_3 - B_4}{B_4} \frac{a_{c3}}{a} + \frac{B_2 - B_3}{B_4} \frac{a_{c2}}{a} + \frac{B_1 - B_2}{B_4} \frac{a_{c1}}{a}\right)^2 \qquad (3.123)$$

Therefore the values of the shear modulus of each layer of the pavement system can be calculated if the values of Poisson's ratio are assumed to be known for each pavement layer and if the function $k_{00}(a)$ is known for a series of values of the baseplate radius. This series must include a baseplate radius sufficiently large to make the static finite depth of influence penetrate into the deepest layer whose shear modulus is to be determined. The function $k_{00}(a)$ can be obtained from measured values of the dynamic stiffness $S(a,F_s,F_d)$. The shear modulus of the subgrade can be determined by this method if a sufficiently large vibrator baseplate is used. It is clear also from Equations 3.97-3.99 that this method is also applicable to soil formations and may prove to be a useful method of shallow subsurface geophysical exploration.

The unique feature of this method of determining the variation of the shear modulus with depth is the one-to-one correspondence between the vibrator baseplate radius and the finite depth of influence in the pavement. Each pavement layer can be detected individually by choosing a proper baseplate size. This one-to-one correspondence does not exist in the wave propagation method of determining subsurface structure, because in this case a single point on a measured Rayleigh wave dispersion curve is influenced by the values of the shear modulus at all depths beneath the surface.

The basic purpose of applying pavement layers over a subgrade is to distribute the load which is applied to the pavement surface in such a way as to protect the comparatively weak subgrade. A measure of the load distribution characteristics of a pavement is given by the angle of the frustum of the cone in which the strain (and stress) in the pavement system is assumed to be confined. This angle is shown in Figure 5 and is defined as follows:

$$\tan \phi_D = \frac{\ell}{(\kappa - 1)a} \sim \frac{\ell_0}{(\kappa - 1)a} \qquad (3.124)$$

where ϕ_D is the angle of stress distribution. For a homogeneous elastic half-space this angle is given by

$$\tan \phi_D \sim \frac{\pi B(1 + \kappa + \kappa^2)}{6(\kappa - 1)} \qquad (3.125)$$

Similar expressions for the layered pavement system can be obtained by using Equations 3.104-3.106. For the homogeneous elastic half-space, ϕ_D is independent of the baseplate radius; but for layered systems, this angle does depend somewhat on the baseplate radius. The values of κ are determined experimentally by requiring that Equations 3.108-3.110 correctly predict the pavement layer thicknesses. This requirement gives a value of Ψ from which the value of κ is immediately obtained by using Equation 3.52. A typical value of ϕ_D for pavements is $\phi_D \approx 70$ deg.

3.8 EFFECTS OF THE MECHANICAL CHARACTERISTICS OF THE VIBRATOR ON THE MEASURED VALUES OF DYNAMIC STIFFNESS

3.8.1 VIBRATOR AND PAVEMENT PARAMETERS INFLUENCING THE DYNAMIC STIFFNESS

The dynamic stiffness of a pavement is measured by using a mechanical vibrator to determine the load-deflection curves. The shape of these curves depends on the values of the nonlinear parameters b and e . The experimental results of Section 4.1 and the theoretical results of Section 3.5 indicate that the nonlinear parameters b and e are not zero for pavements. In this case, Equations 3.22-3.28 show that in addition to the quantities listed in Section 2.4 pertaining to the linear oscillator, the dynamic stiffness of a pavement measured by a vibrator also depends on the following quantities:

a. Two nonlinear elastic parameters describing the pavement.

b. The static load (or static equilibrium displacement).

c. The dynamic force generated by the vibrator.

d. The baseplate radius of the vibrator.

Because various vibrators have different values of F_s and F_D , it follows that the dynamic stiffness value measured by different vibrators at the same locality will in general be different. The dynamic stiffness measured by a vibrator thus depends on the physical characteristics of the vibrator used for the measurements. For flexible pavement it is

in part the dependence of the dynamic stiffness on F_D that produces the discrepancy in the measured values of dynamic stiffness using two different vibrators with different values of F_D at the same pavement location. All other factors being equal, two vibrators operating at different levels of dynamic force will not yield the same value of dynamic stiffness. The lower value will occur in the region of large dynamic load.

3.8.2 THEORY OF THE ANOMALOUS BEHAVIOR OF THE DYNAMIC STIFFNESS

The spring constant expression shows that the linear theory of elasticity implies a value of the dynamic stiffness which is essentially proportional to the baseplate radius of the vibrator mass. Experimental results presented in Section 4.1 contradict this basic conclusion of linear elasticity. Some of the experimental data in Section 4.1 indicate that for the same vibrator (same static and dynamic loads), the measured values of dynamic stiffness are roughly independent of baseplate radius. In fact, some of the data in Section 4.1 show that for different vibrators (different static loads), it is sometimes possible to measure smaller values of the dynamic stiffness with a large baseplate than with a small baseplate at the same location. This conflict between the experimental results and the predictions of linear elastic theory will be referred to as the anomalous behavior of the dynamic stiffness.

The anomalous behavior of the dynamic stiffness can be explained in terms of the nonlinear response of a pavement to a static and dynamic load. The anomalous result, that the dynamic stiffness does not appear to vary directly with the radius of the baseplate (as it does for a linear homogeneous half-space), is due to the finite depth of influence which makes k_{00} only a very slowly increasing function of baseplate radius except for really small radii (see Figure 7a). This is especially true for the case of a concrete pavement where a very strong upper layer overlies considerably weaker layers of base and subbase. In this case, the value of k_{00} is determined primarily by the strong upper layer, and the major part of this value can be obtained with a

very small baseplate radius as shown in Figure 7a. The weaker lower layers tend to flatten out the k_{00}-versus-baseplate-radius curve. Thus, measurements of k_{00} using different sized baseplates would yield values of k_{00} considerably less different than they would be if the pavement were a homogeneous half-space with elastic parameters equal to those of the upper layer of the layered system. According to the nonlinear theory, k_{00} is a very slowly increasing function of baseplate radius for baseplate radii larger than the first critical radius. Therefore, for sufficiently large baseplate radii, the values of dynamic stiffness of rigid pavements measured for fixed static and dynamic loads should be essentially independent of the baseplate radius.

The fact that the values of k_{00} are similar for different baseplate radii which are sufficiently large implies that the values of two $k_0(F_s,a)$ functions corresponding to two different baseplate sizes are also similar for some pavements. In this case it is possible, due to a local minimum of the function $k_0(F_s,a)$ for some value of F_s, for $k_0(F_s,a)$ for a small baseplate radius and small static load to be larger than $k_0(F_s,a)$ for a large radius and a large static load as shown in the rigid pavement curve in Figure 4a. If the values of k_{00} are very different for two baseplate radii, the corresponding two values of the function $k_0(F_s,a)$ will also be very different. In particular, the function $k_0(F_s,a)$ for the larger radius will be larger than the corresponding function for the smaller radius for all values of F_s, as shown in the flexible pavement curves of Figure 4a. This case would then represent the normal situation in which large baseplates produce slightly larger values of dynamic stiffness than do smaller baseplates. This normal situation is expected to occur for weak pavements where there is not a great difference between the elastic parameters of the upper and lower pavement layers. The anomalous behavior of the dynamic stiffness measurements on pavements can be explained in terms of the relative constancy of the function $k_{00}(a)$, which implies that the values of the dynamic stiffness measured on rigid pavements by vibrators with large and small baseplates will be roughly the same. On the other hand, linear elastic theory implies that the value of the dynamic

stiffness should be directly proportional to the baseplate radius. The experimental results, then, contradict some of the predictions of the linear elastic theory.

4. EVALUATION OF THEORETICAL RESULTS OF THE DYNAMIC STIFFNESS STUDY

4.1 EXPERIMENTAL PROGRAM

The basic goal of the experimental program was to provide data to establish the use of the nondestructive evaluation method for airport pavements. Nondestructive pavement evaluation methodology based on correlations between nondestructive data and existing Federal Aviation Administration evaluation criteria is given in Volume I of this report.[15] The specific objectives of the experimental program were:

a. Determination of the dynamic stiffness as a function of frequency, dynamic load, static load, and vibrator baseplate radius.

b. Validation of the theoretical procedures and predictions of the nonlinear mechanical model of pavements.

4.1.1 MECHANICAL VIBRATORS USED FOR NONDESTRUCTIVE TESTING OF PAVEMENTS

Dynamic stiffness data were obtained from several vibrators including:

a. The WES 16-kip hydraulic vibrator

b. The Dynaflect

c. The Road Rater

d. The Civil Engineering Research Facility (CERF) vibrator

e. The WES 9-kip eccentric mass vibrator

Each vibrator has its own basic dynamic characteristics including weight, maximum dynamic force, and baseplate radius. A comparison of these four vibrators is made in Table 1. According to the nonlinear vibration theory of pavements developed in Section 3.5, the dynamic characteristics of a vibrator will be reflected in the value of the dynamic stiffness measured on a given pavement.

The experimental measurements of the dynamic load-deflection curves measured by WES were made primarily at a frequency of 15 Hz, but also in the range of 10-25 Hz. Most of the data taken were for a static load of 16 kips and for a dynamic load which varied from 5-14 kips. Some dynamic stiffness measurements were performed using a different

Table 1

Mechanical Characteristics of Vibrators

Vibrator	Static Load kips	Maximum Dynamic Load kips	Effective Baseplate Radius, in.	Contact Area sq in.	Operating Frequency Hz
WES 16-kip	16	15	9	245	5-100
Dynaflect	1.6	0.5	≈0.9 (concrete)*	2.54	8
			≈3.2 (asphaltic concrete	32.0	
Road Rater					
400	1.5	0.75			20-30
505	1.5	0.75	4.22**	56	20-30
510	2.0	1.5			10-40
550	4.0	3.0			10-40
CERF	6.75	5	6	113.1	15,25
WES 9-kip	9	8	9.5	283.5	5-60

* Road Rater applies load through two 4- by 7-in. rectangular steel pads spaced 6 in. apart.

** Dynaflect applies load through two 4-in. wide and 16-in.-diam steel wheels.

vibrator arrangement which allowed for a variation of the static load in the range of 5-50 kips by the addition of a series of lead weights to the vibrator load.

4.1.2 EFFECTS OF DYNAMIC LOAD

Typical dynamic load-deflection curves for AC pavements appear in Figure 11, while Figure 12 gives these curves for PCC pavements. These load-deflection curves correspond to a frequency of 15 Hz and a static load of 16 kips. The dynamic stiffness is the ratio of the dynamic load to the corresponding value of the dynamic deflection, and can be evaluated for each point on the dynamic load-deflection curve. The value of the dynamic stiffness corresponding to $F_D = 0$ has been designated by S_0 in Equation 3.21 and can be obtained from Figures 11 and 12 by measuring the slope of the load-deflection curves at the origin. The dynamic stiffness values corresponding to the dynamic load-deflection curves presented in Figures 11 and 12 are given in Figures 13a and b. For the WES 16-kip vibrator operating on AC pavements, the dynamic stiffness is generally a decreasing function of the dynamic load, while for rigid pavements the dynamic stiffness is essentially independent of the dynamic load. However, the 10-Hz dynamic load-deflection curves shown in Figure 14 indicate that it is possible under certain conditions for the dynamic stiffness to be an increasing function of the dynamic load and to have a local minimum value at a specific value of the dynamic load. The results in Figures 11 and 12 show that stiff pavements have dynamic load-deflection curves which are more linear than the dynamic load-deflection curves for the more flexible pavements.

4.1.3 CRITICAL FREQUENCIES

The dynamic load-deflection curves for a given pavement have been measured for a series of frequencies, from which an estimate of the critical frequency for a vibrator-pavement system can be made. The critical frequency has been defined as the frequency for which the dynamic load-deflection curves are nearly linear for small values of F_D. Figures 14 and 15 indicate that the critical frequency of the WES 16-kip vibrator operating on medium strength AC pavements is about 15.5 Hz,

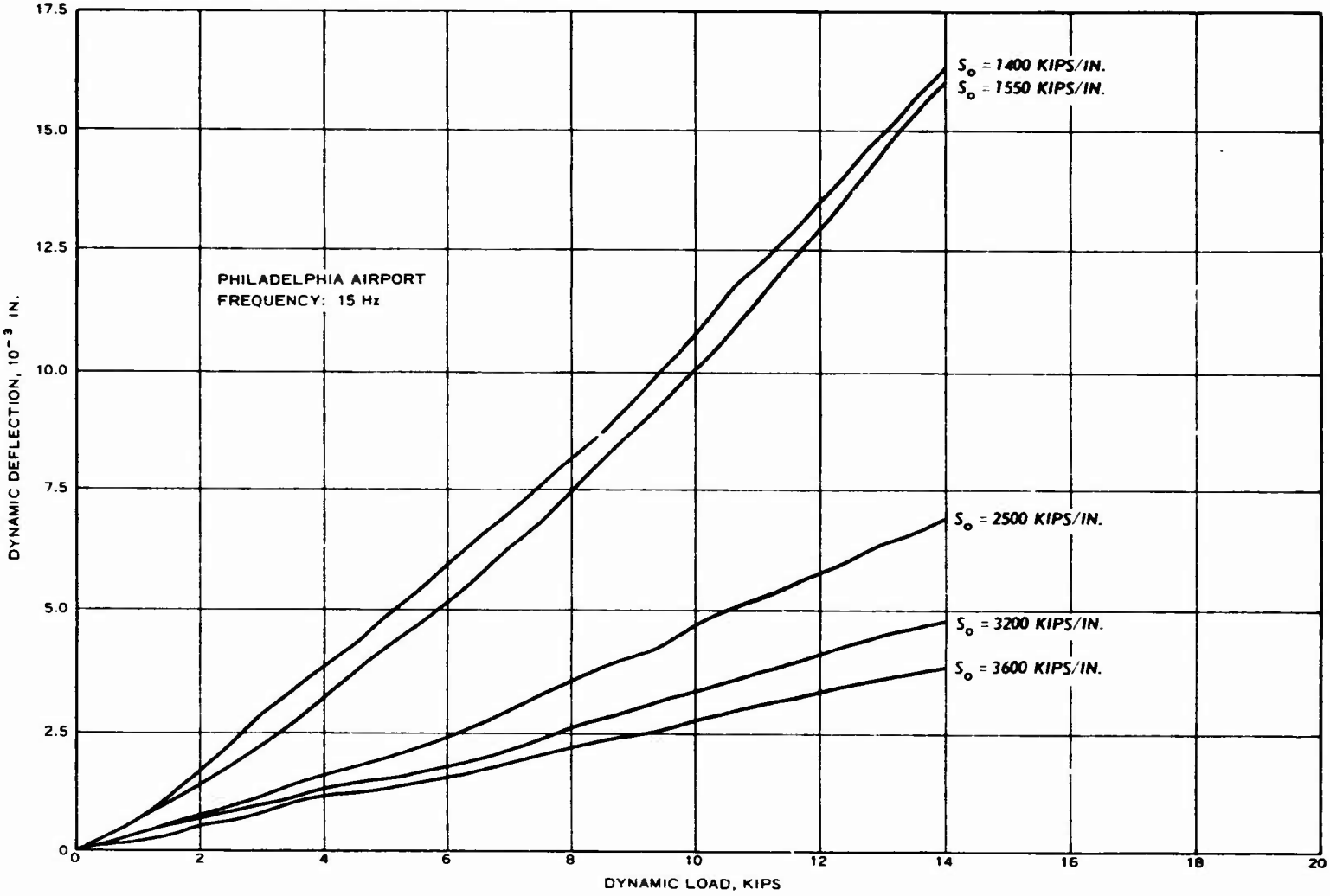

Figure 11. Dynamic load-deflection curves for different locations on AC pavements showing strong pavements to be more linear than weak pavements

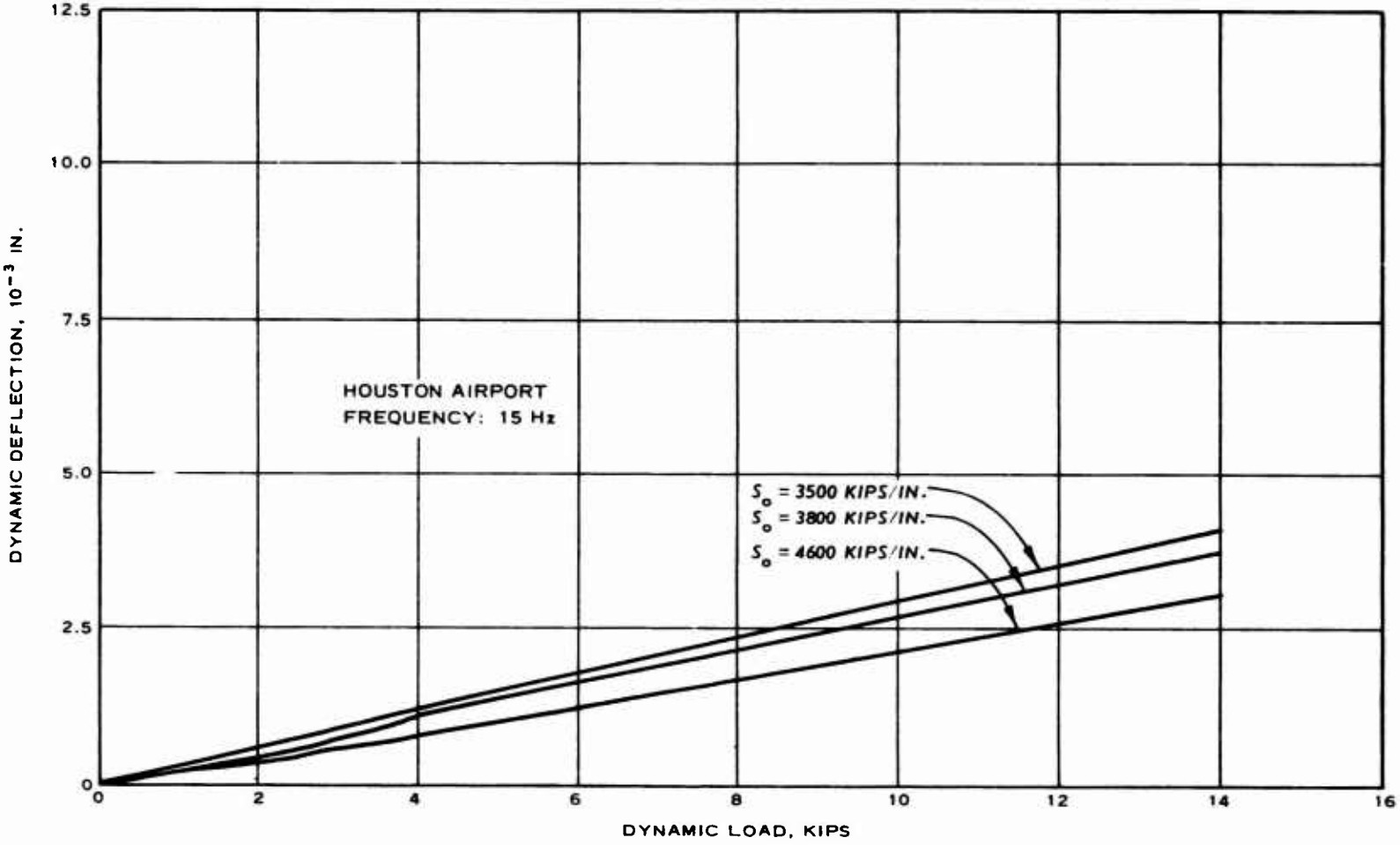

Figure 12. Dynamic load-deflection curves for different locations on PCC pavements showing extreme linearity of curves

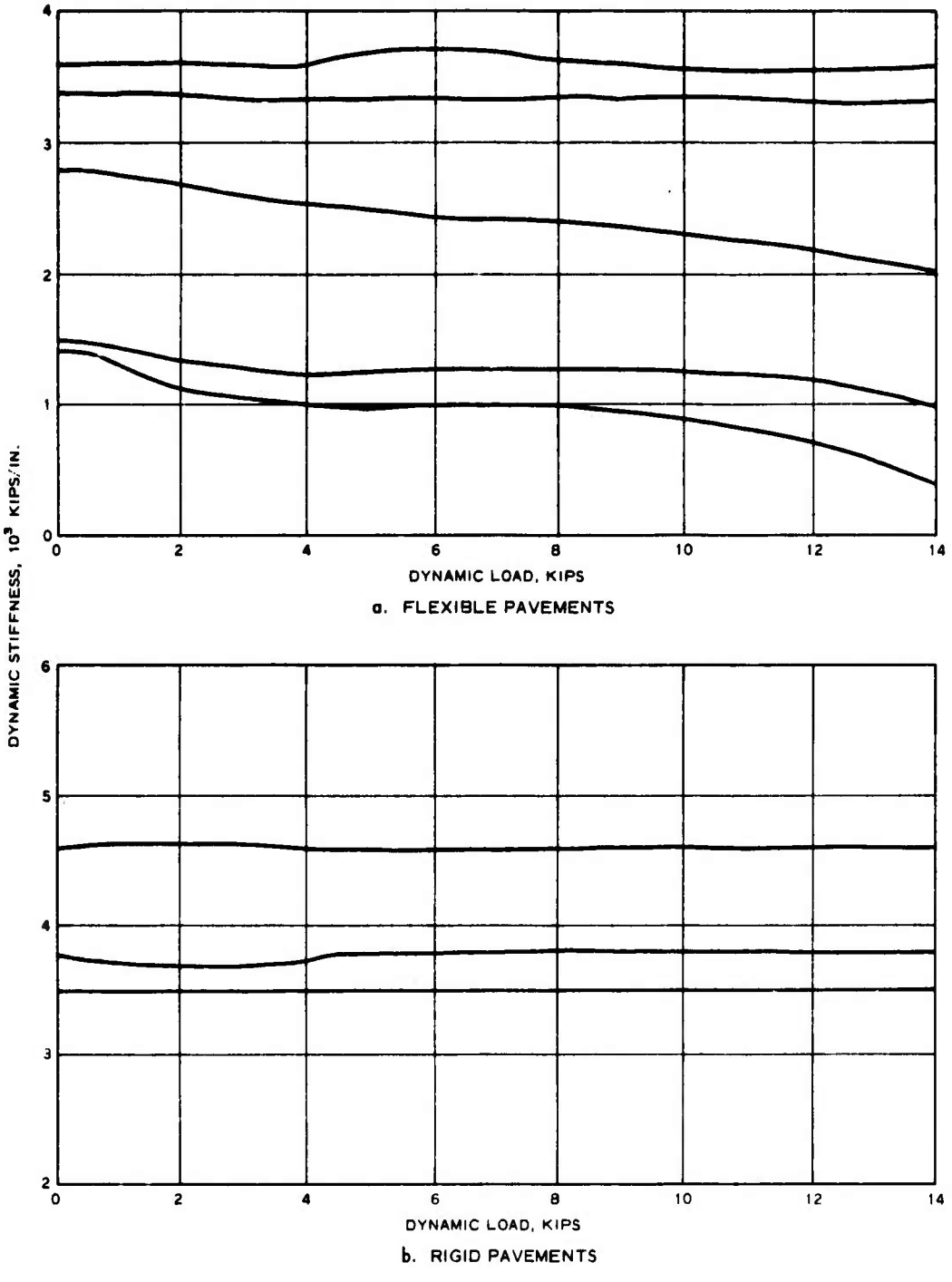

Figure 13. Measured values of dynamic stiffness versus dynamic load (15 Hz)

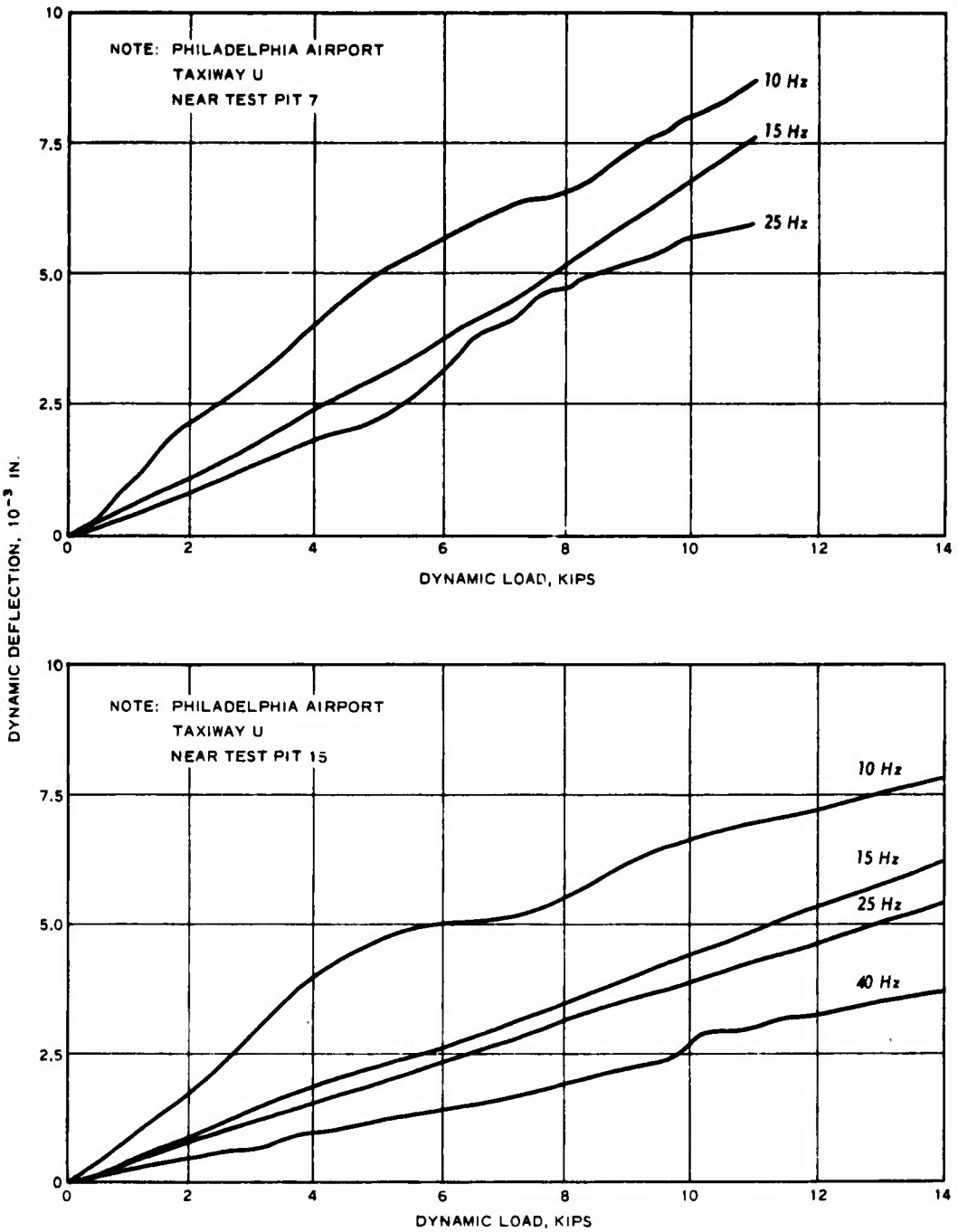

Figure 14. Possible experimental evidence for the existence of a critical frequency value of ≈15 Hz for AC pavement

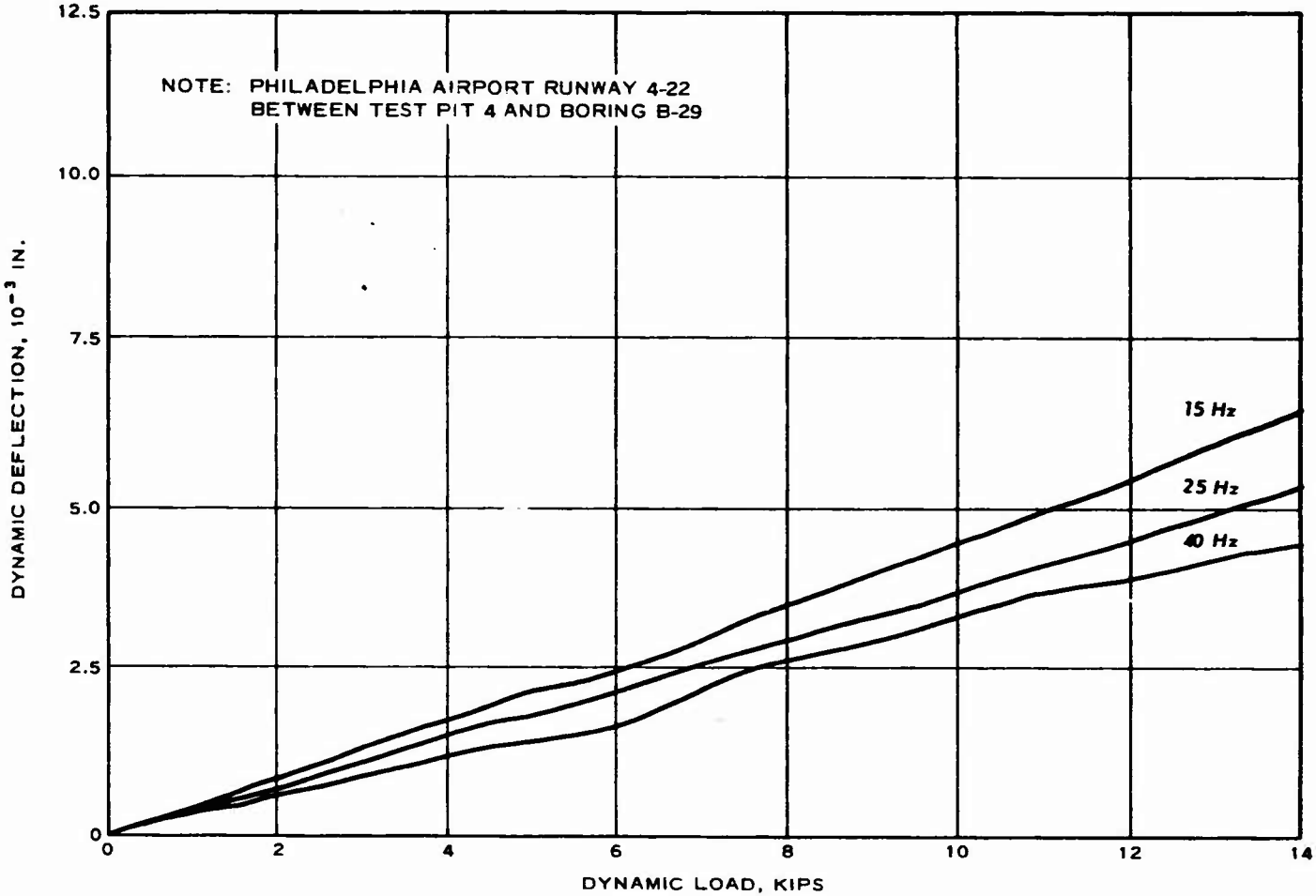

Figure 15. Nearly linear dynamic load-deflection curves obtained at 15 Hz for AC pavements

while other data indicate that for PCC pavements it is about 14.5 Hz. Estimates of the critical frequency, resonance frequency, effective pavement mass, and damping constant that were obtained from the experimental dynamic load deflection curves for rigid and flexible pavements are given in the following tabulation.

Pavement Type	Critical Frequency Hz	Resonance Frequency Hz	Damping Constant kip-sec/in.	Effective Pavement Mass kip-sec^2/in.	Vibrator Mass kip-sec^2/in.
Rigid concrete pavement	14.5	10	35	1.0	0.042
Flexible AC pavement	15.5	8	8	0.33	0.042

4.1.4 EFFECT OF STATIC LOADS

Some experimental work has been done at WES toward determining the dependence of the dynamic load-deflection curves and the dynamic stiffness of a pavement-vibrator system on the static load applied to the pavement. The static load was applied to an AC pavement by a hydraulic system that could apply a static load of 5-50 kips. The vibrator was run at 15 Hz for all of the tests. Dynamic load-deflection curves were measured for a series of static loads that was started at 5 kips and incremented by adding 5-kip lead weights to the vibrator system until a maximum static load of 50 kips was attained. The maximum value of the dynamic load for the case of the 5-kip static load was 4 kips, while the maximum dynamic load for the case of the 50-kip static load was only 10 kips. Therefore, for these experimental tests the maximum value of the dynamic load was considerably less than the value of the static load for which dynamic load-deflection curves were measured. Figure 16 gives the measured dynamic load-deflection curves for several values of the static load, while Figures 17 and 18 show the dependence of the dynamic stiffness on the static and dynamic loads, respectively. The experimental data show that the dynamic stiffness is greatly dependent on the static and dynamic loads, and therefore the dynamic

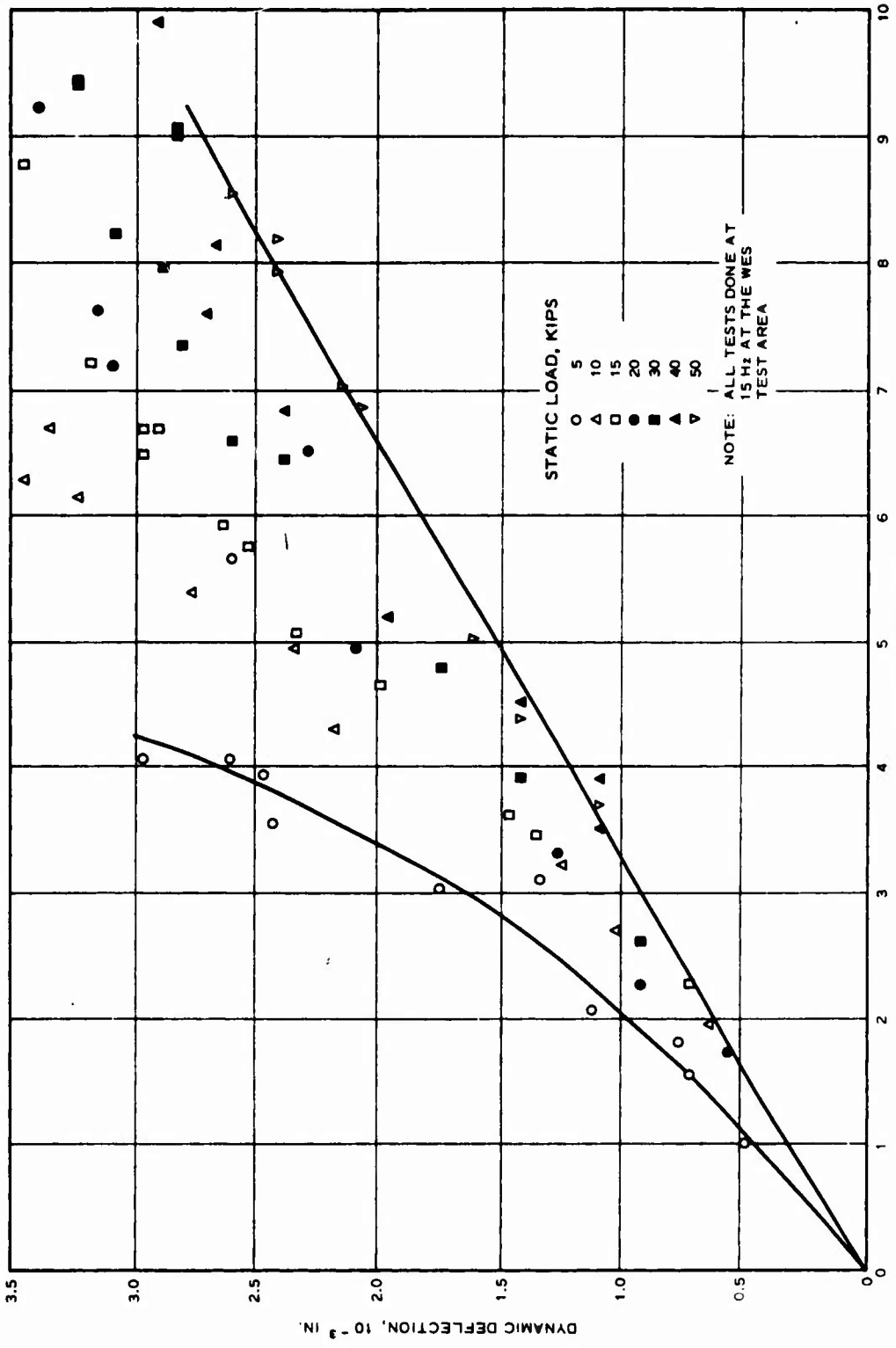

Figure 16. Dynamic load-deflection curves for various static loads on AC pavement

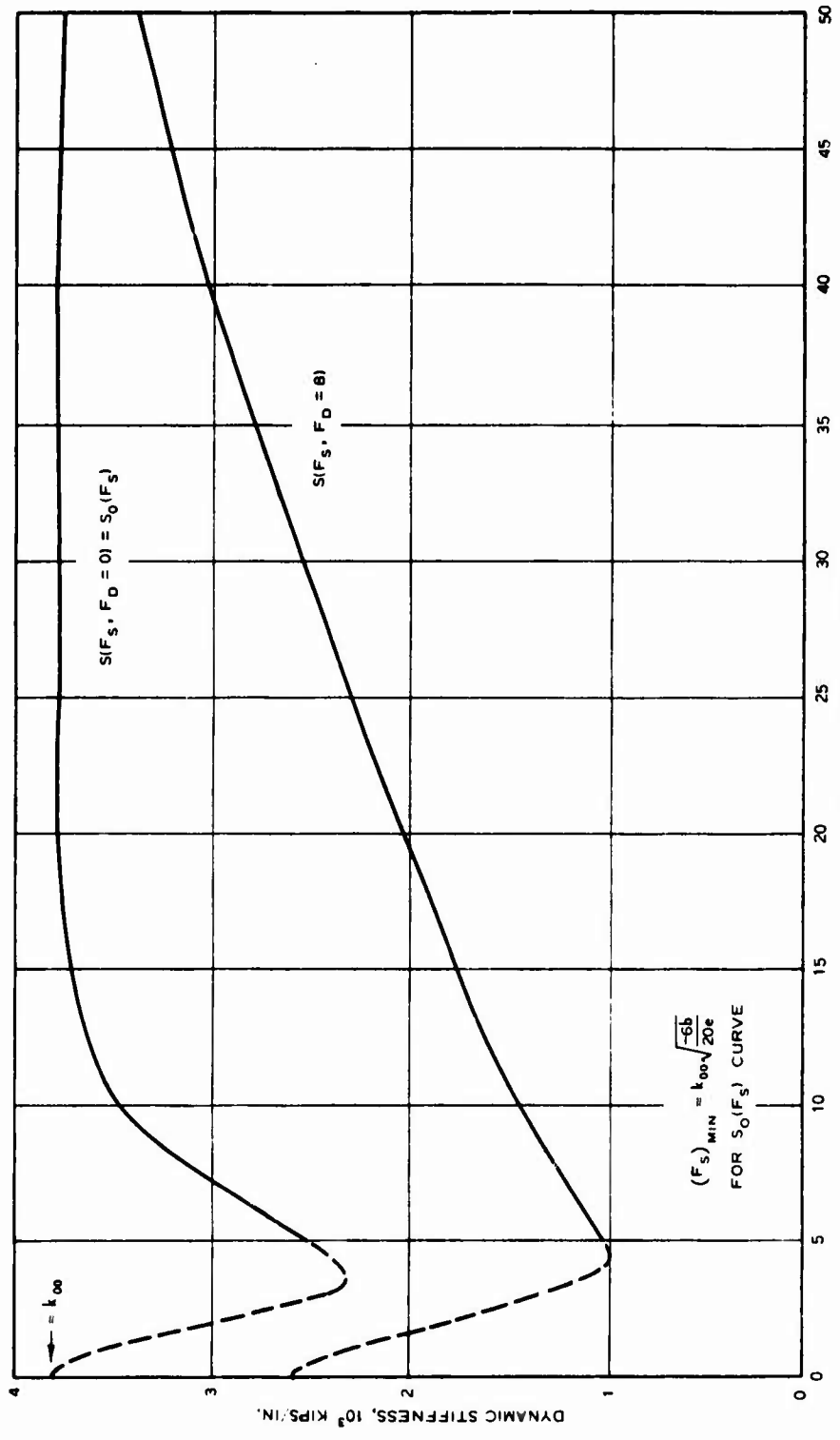

Figure 17. Experimental values of dynamic stiffness versus static load applied by the WES 50-kip vibrator operating at 15 Hz on AC pavement

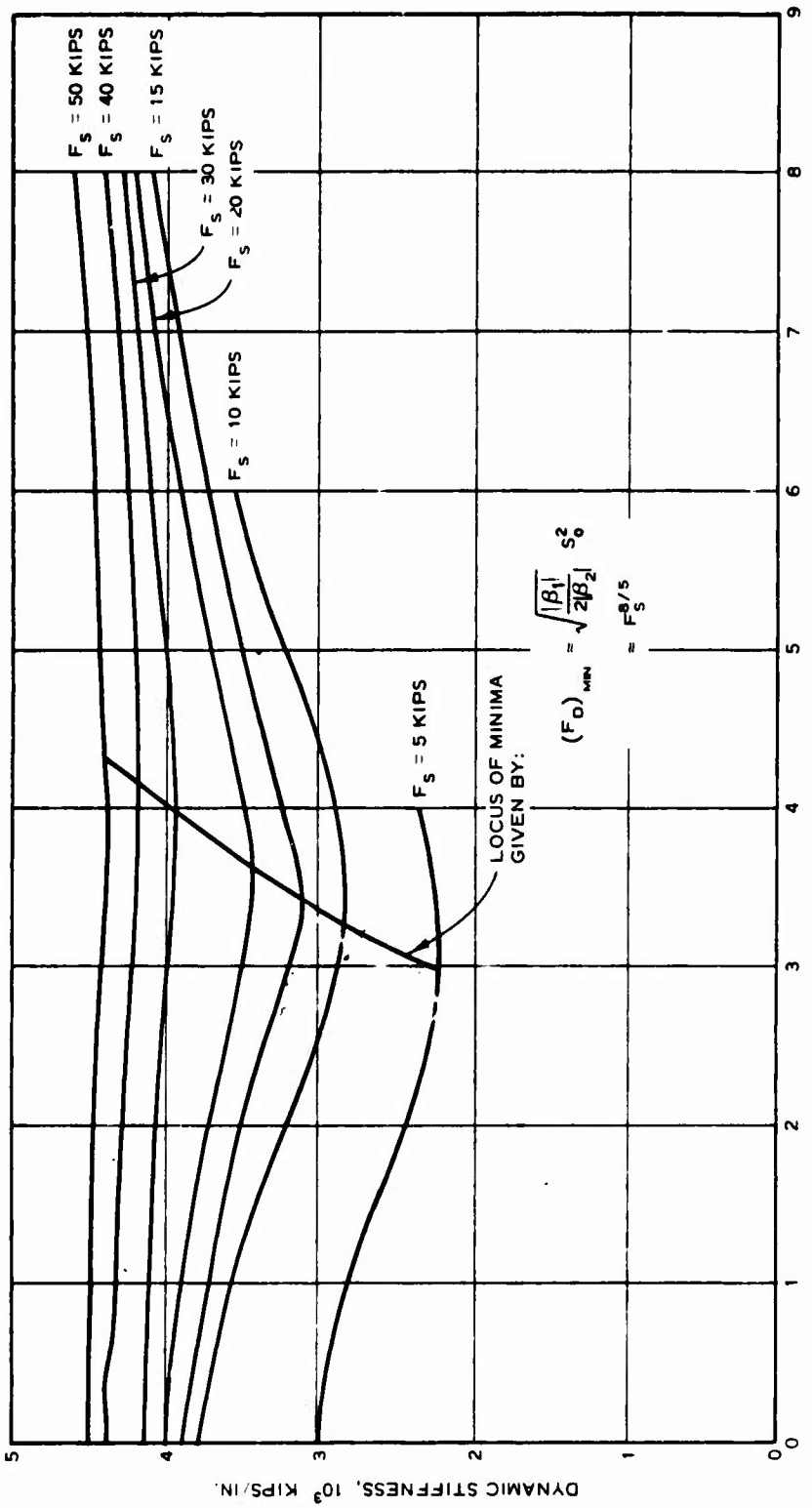

Figure 18. Experimental values of dynamic stiffness versus dynamic load for various values of the static load

stiffness is as much a property of the dynamic characteristics of a vibrator as it is of the strength of the pavement. The experimental data in Figure 16 show that the dynamic stiffness measured by a vibrator tends to increase with the magnitude of the applied static load. The results in Figure 16 also show that the measured dynamic load-deflection curves tend to become more linear with increasing static load. The latter experimental conclusion can be presented only tentatively because the range of the variation of the dynamic load for the experimental tests done with the 50-kip static load was only 0-10 kips. The range of the dynamic load should have been 0-40 kips in order to make a proper comparison with the experimental tests done with the 5-kip static load for which the dynamic load was varied from 0-4 kips.

Figure 17 shows that for the experimental setup used, the dynamic stiffness may exhibit a minimum value for $F_s \sim 5$ kips, but further tests are required to substantiate this conclusion. The results in Figure 18 show that for the experimental setup used, which has $\omega < \omega_c$ and $F_s < F_{sc}$ as operating conditions, there appear to be local minima in the dynamic stiffness as a function of F_D in the range $F_D \sim 3$-4 kips for the WES 50-kip variable static load vibrator operating on AC.

4.1.5 EFFECT OF BASEPLATE RADIUS

Experimental work has been done at WES to determine the dependence of the measured values of the dynamic stiffness on the size of the vibrator baseplate. This experimental work was done in part to confirm the results in Section 3.7.8 regarding the dependence of the theoretically calculated dynamic stiffness on the baseplate radius of the vibrator. The experimental work was also done to establish the existence of the critical radii (Section 3.7.7) and to determine their values for a particular pavement location so that the formulas for calculating the layer thicknesses (Section 3.7.7) and shear modulus of each pavement layer (Section 3.7.9) could be verified.

Experimental measurements of the dynamic load-deflection curves were made for baseplates having diameters of 3, 4, 5, 6, 7, 8, 9, 10, 12, 15, and 18 in. All of the baseplate sizes were used for the tests

on rigid pavements; but for the tests on AC pavements, the 3-, 4-, and 5-in.-diam plates could not be used because the pavement failed by shearing under the 16-kip static load of the vibrator. Figure 19 gives the experimental dynamic load-deflection curves for AC while Figure 20 gives the curves for the case of a rigid pavement. For the rigid pavement, the load-deflection curves for the 5-in.-diam and larger baseplate sizes are very similar, so that only the load-deflection curves for the 5- and 18-in.-diam baseplates are shown in Figure 20. Figure 21 gives the experimental values for the dynamic stiffness of rigid and AC pavements as a function of the baseplate radius. Figure 21 shows that an abrupt change in the slope of the curve giving dynamic stiffness versus baseplate radius occurs at a radius of 2.5 in. for the case of the rigid pavement, and at a radius of 6.0 in. for the AC pavement. The rigid pavement is known to have a thickness of 15 in., while the AC pavement is known to rest on a subgrade the top of which is at a depth of from 28 in. to 42 in.

4.1.6 COMPARISON OF DYNAMIC STIFFNESS VALUES MEASURED BY THE DYNAFLECT AND THE WES 16-KIP VIBRATOR

A comparison of the dynamic stiffness values determined by the WES 16-kip vibrator and by the Dynaflect vibrator on concrete pavements at the same locations is given in Table 2. Table 2 shows that the stiffness values determined by the Dynaflect are considerably higher than those obtained at the same locations using the WES 16-kip vibrator, even though the radius of the WES vibrator is about an order of magnitude larger than the equivalent radius of the Dynaflect operating on a concrete pavement (anomalous behavior). The WES 16-kip vibrator has a baseplate area of 245 sq in. The Dynaflect vibrator makes contact with a pavement through two steel wheels, each having a width of 4 in. and a diameter of 16 in., and therefore the contact area with the pavement varies with the degree of softness of the pavement, being considerably larger for soft asphaltic pavements than for hard concrete pavements. The frequency of operation of the Dynaflect is 8 Hz while that of the WES 16-kip vibrator is 16 Hz. The maximum dynamic load of the Dynaflect

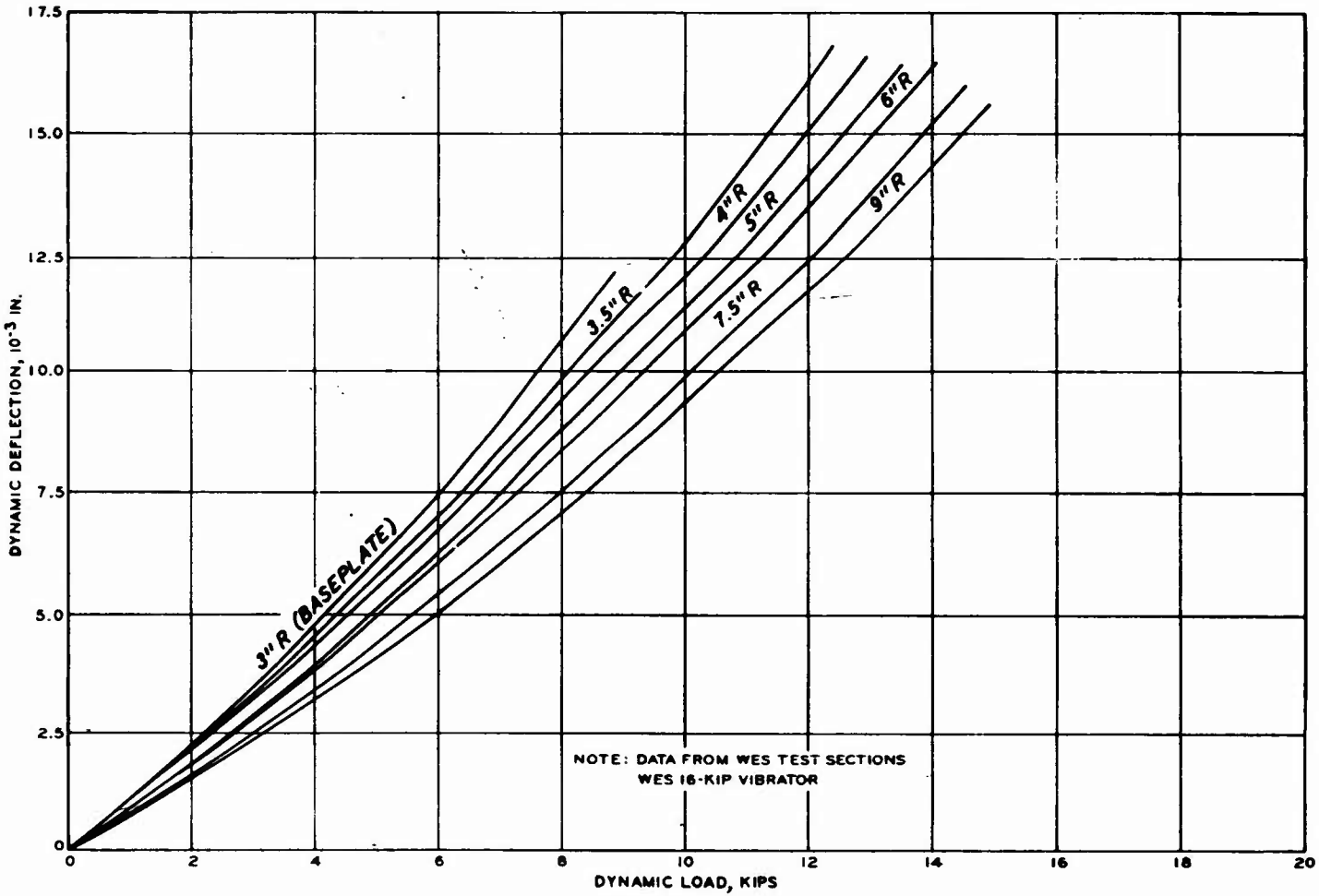

Figure 19. Experimental load-deflection curves for a series of baseplate sizes on AC pavement

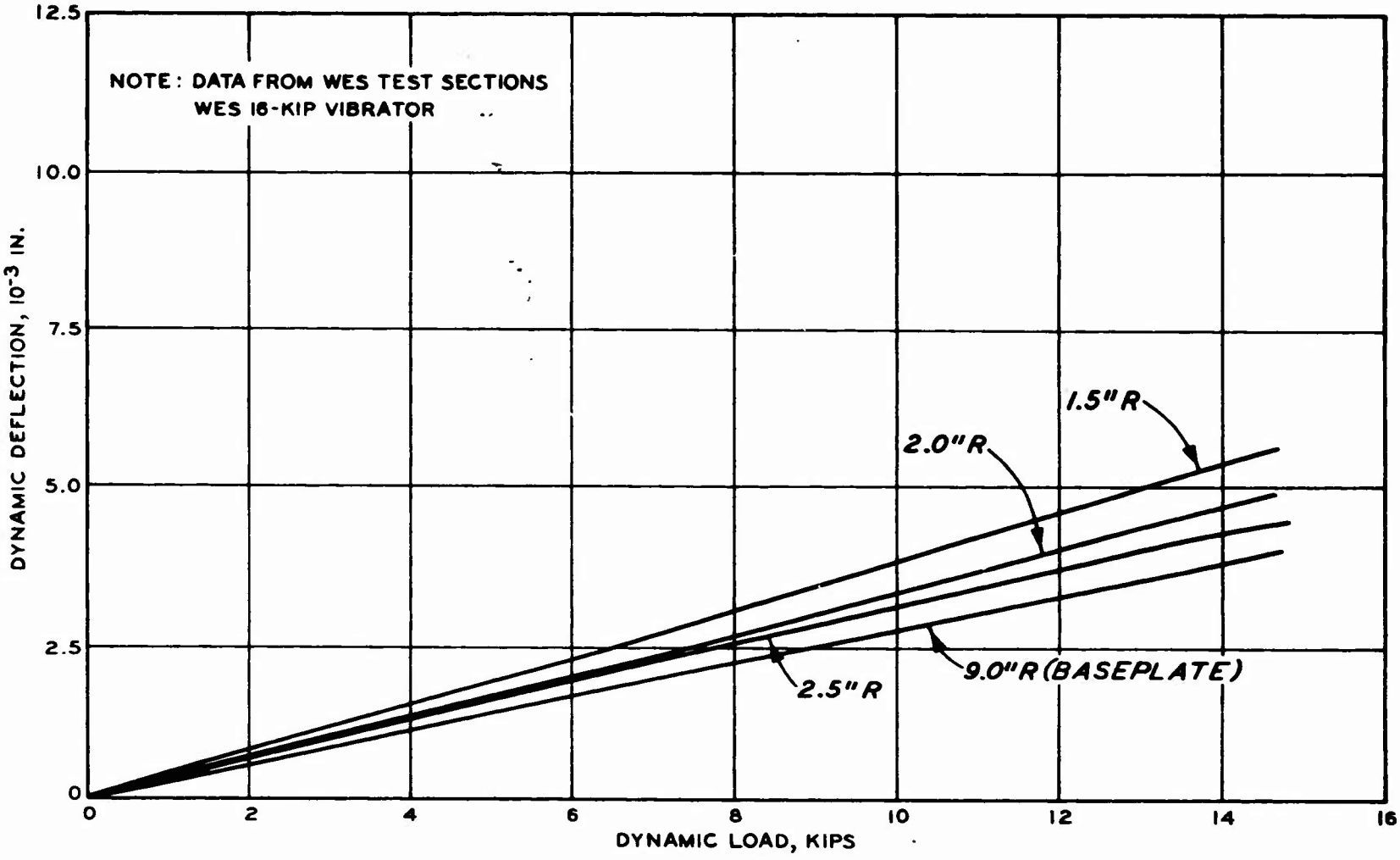

Figure 20. Experimental load-deflection curves for a series of baseplate sizes on rigid pavement

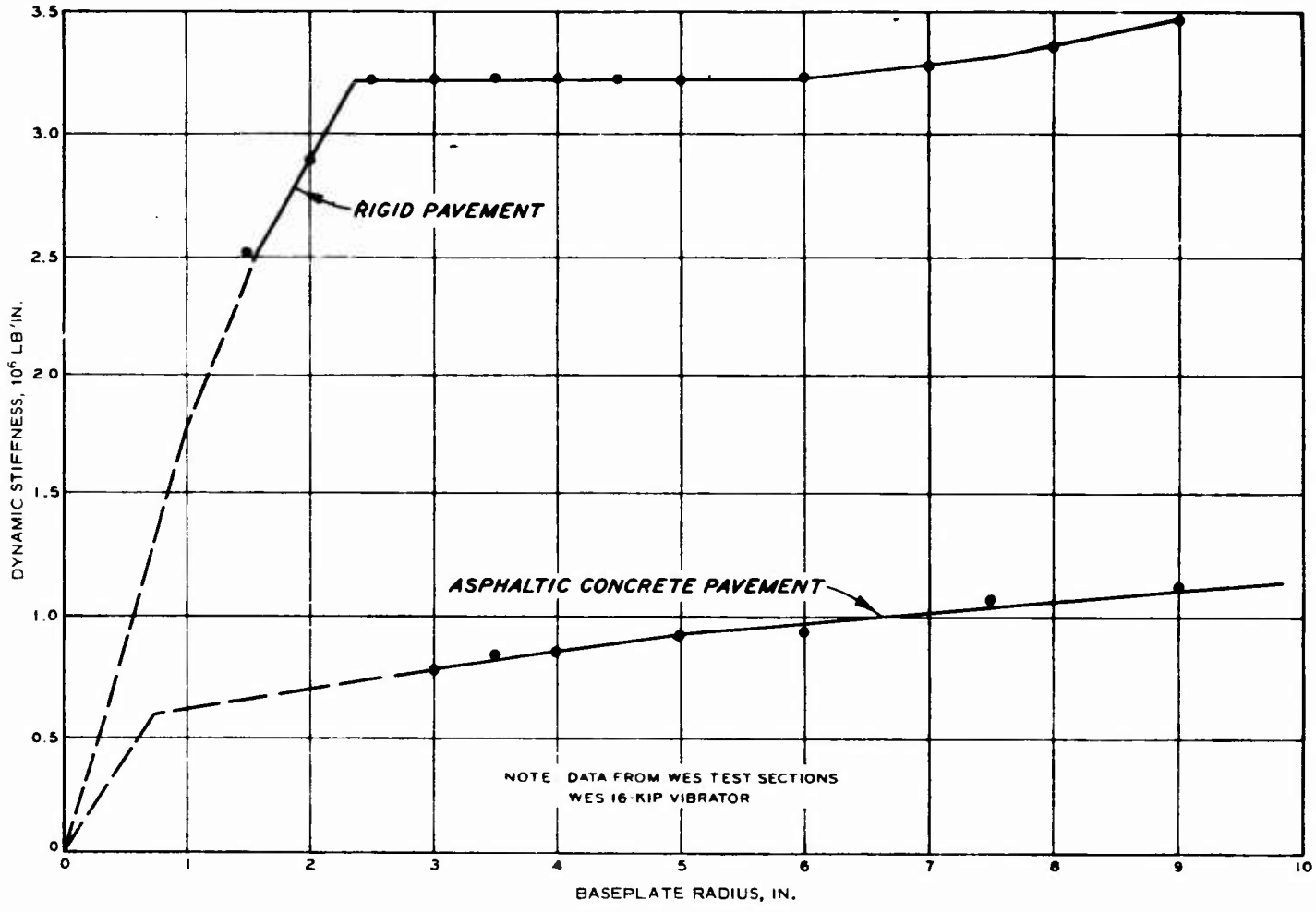

Figure 21. Experimental values of the dynamic stiffness versus the vibrator baseplate radius

Table 2

Comparison of Dynamic Stiffness Values as Measured by the Dynaflect Vibrator and the WES 16-Kip Vibrator (Concrete Pavement)

Palmdale Airfield		O'Hare Airport		Midway Airport		Byrd Field	
WES 16-Kip Vibrator kips/in.	Dynaflect Vibrator kips/in.	WES 16-Kip Vibrator kips/in.	Dynaflect Vibrator kips/in.	WES 16-Kip Vibrator kips/in.	Dynaflect Vibrator kips/in.	WES 16-Kip Vibrator kips/in.	Dynaflect Vibrator kips/in.
6600	7406	2700	2778	3840	4116	1740	4386
5040	7246	3760	3226	3840	3124	5040	5292
4360	5290	3200	3572	2640	2702	3000	4386
4960	5290	3040	1786	2600	3030	3360	4504
6480	7750	3400	2942	2460	2630	4520	5952
4760	7092	3320	2858	2380	2630	5600	6060
3800	8332	2440	2550	2840	2942	3400	4064
5000	8130	1780	1960	2360	2942	3640	4504
4440	5952	2520	2778	1270	1960	3920	3572
3280	7406	2960	3126	1440	2174	4600	4566
3680	7574	2940	2942	2540	2942	4120	4386
4520	6502	3920	3572	2580	3124	4120	4166
4800	6944	2400	2858	2280	2778	3000	4444
4120	5208	2920	3126	2360	2778	3080	4166
4360	5376	2420	2942	2560	2856	3640	4220
2560	6944	3600	3126	3000	3124	3280	3334
3440	7092	3440	3126	1840	2222	3800	3704
4760	7246	3160	3126	2100	2778	4400	4166
5560	7846	3080	4546	1460	1852	4800	4274
4320	7092	2480	3126	2160	3124	5600	5376
4720	7406	3080	3030	1700	2174	--	--
3880	7406	3080	2858	1220	2564	--	--
3760	7574	3000	3030	3200	3448	--	--
4320	7246	1310	1408	3080	3570	--	--
4480	6444	2800	2858	2420	3226	--	--
4640	6802	2480	2500	2720	3334	--	--
3520	6666	2600	2858	--	--	--	--

is 0.5 kips and the static load is 1.5 kips, while the maximum dynamic load of the WES 16-kip vibrator is 15 kips with a static load of 16 kips. The comparatively small size of the Dynaflect is thought to be responsible for the difference between values of the dynamic stiffness measured by the two vibrators at the same pavement location. Volume I of this report[15] gives a complete description of these two vibrators.

4.1.7 COMPARISON OF DYNAMIC STIFFNESS VALUES MEASURED BY ROAD RATER AND WES 16-KIP VIBRATOR

For the same locations, dynamic stiffness measurements were made using the Road Rater and the WES 16-kip vibrator. Measurements were made on both concrete and AC pavements, and the results are tabulated in Table 3. As with the Dynaflect, it was found that the Road Rater generally gives higher values of dynamic stiffness than does the WES 16-kip machine at the same locations. This is true even though the WES 16-kip vibrator has a baseplate radius about 2.5 times larger than the baseplate radius of the Road Rater (anomalous behavior). The Road Rater and the WES 16-kip vibrator have different mechanical characteristics, and this difference is probably responsible for the difference in the measured values of the dynamic stiffness at the same pavement location. The Road Rater is generally operated in the frequency range of 10-40 Hz and has a maximum dynamic load in the range of 1.0 kip and a static load in the range of 3.0 kips, values which are considerably smaller than the corresponding values for the WES 16-kip vibrator. The Road Rater is described in more detail in Volume I of this report.[15]

4.1.8 COMPARISON OF DYNAMIC STIFFNESS VALUES MEASURED BY CERF VIBRATOR AND WES 16-KIP VIBRATOR

Table 4 gives the values of the dynamic stiffness measured at the same locations by the CERF vibrator and the WES 16-kip vibrator.[16,17] The CERF vibrator measures lower values of dynamic stiffness than does the WES vibrator. This behavior of the dynamic stiffness is in accordance with the larger baseplate contact radius of the WES vibrator (normal behavior). The CERF vibrator is more comparable in size with

Table 3

Comparison of Dynamic Stiffness Values Measured by the Road Rater and by the WES 16-Kip Vibrator (Flexible Pavements)

WES Soil Stabilization Test Sections		National Aviation Facilities Experimental Center	
WES 16-Kip Vibrator kips/in.	Road Rater kips/in.	WES 16-Kip Vibrator kips/in.	Road Rater kips/in.
680	1010	3120	4878
1260	2040	2720	3279
700	653	2920	4000
880	653	1140	1220
760	1538	2400	2740
720	531	2960	5000
2920	3846	2460	3077
2200	4347	980	960
720	1265	980	900
800	1123	980	900
400	266	880	862
520	632	880	833
700	840	880	1087
1560	1176	730	909
1960	2000	900	1087
3440	3125	900	1020
--	--	600	633
--	--	600	580
--	--	600	667

Table 4

Comparison of Typical Dynamic Stiffness Values as Measured by the CERF Vibrator and by the WES 16-Kip Vibrator

Webb Air Force Base (Flexible Pavement)		Kelly Air Force Base (Concrete Pavement)	
WES 16-Kip Vibrator kips/in.	CERF Vibrator kips/in.	WES 16-Kip Vibrator kips/in.	CERF Vibrator kips/in.
800	680	4400	2725
940	861	5520	3862
880	783	5440	3026
760	576	4640	2085
780	696	5840	2627
660	587	5440	2875
760	728	4040	1957
740	674	5520	2358
880	779	9200	4895
600	553	4080	2890
780	746	4920	2174
760	645	4920	3650
820	657	5600	4000
780	708	4360	3497
780	698	4560	3129
640	611	2080	1843
760	636	4800	3109
720	723	3880	2909
660	664	1640	1583
960	803	4440	2174
1040	775	4520	3030
700	469	4040	3576
600	503	--	--
720	478	--	--
660	452	--	--

the WES 16-kip vibrator than is either the Dynaflect or the Road Rater. The CERF vibrator is operated in the frequency range of 5-60 Hz and has a maximum dynamic load of 8 kips and a static load of 9 kips. The CERF vibrator is described in more detail in Volume I of this report.[15]

4.2 COMPARISON OF THEORETICAL AND EXPERIMENTAL RESULTS FOR THE DYNAMIC STIFFNESS

4.2.1 DEGREE OF NONLINEARITY

The experimental dynamic load-deflection curves presented in Figures 11 and 12 show that a flexible pavement having a small dynamic stiffness is more nonlinear than a rigid pavement with a large dynamic stiffness. This experimental fact is explained in the selected model by the first nonlinear term in Equation 3.22, which depends on the dynamic stiffness in the manner S_0^{-4}, so that the theory predicts that stiff pavements can be expected to be more linear than flexible pavements.

It has been shown theoretically that for the case when $\omega < \omega_c$ and $F_s < F_{sc}$, for which $\alpha_1 > 0$ in Equations 3.25, 3.31, and 3.35, the dynamic load-deflection curves have a shape such that the dynamic stiffness is a decreasing function of F_D in the range of low values of F_D. For large values of F_D, the dynamic stiffness may continue to be a decreasing function of F_D or may obtain a minimum value and then begin to increase with further increase of the values of F_D. A minimum value for the dynamic stiffness may or may not exist depending on the relative values of the nonlinear parameters b and e. Figures 11 and 13 give cases for which $\alpha_1 > 0$ and for which the dynamic stiffness is a monotonic decreasing function of dynamic load, while Figures 14 and 18 show cases for which $\alpha_1 > 0$ and for which a minimum occurs in the value of the dynamic stiffness at a given value of $F_D \approx 4.0$ kips. For the WES 16-kip vibrator operated at a frequency of 15 Hz, it is found that the flexible AC pavements generally have dynamic load deflection curves for which $\alpha_1 > 0$.

It has also been shown theoretically that for the case when $\omega > \omega_c$ and $F_s > F_{sc}$, for which $\alpha_1 < 0$ in Equations 3.25, 3.31, and

3.35, the dynamic stiffness is an increasing function of the dynamic load in the region of low dynamic load. The 40-Hz curve in Figure 14 may indicate this behavior with $\alpha_1 < 0$. Further experimental verification is necessary.

One of the conclusions of Equation 3.31 is that the dynamic load-deflection curves measured by a vibrator will become essentially linear in the region of small F_D if the vibrator is operated at a characteristic frequency of the vibrator-pavement system which is called the critical frequency. The existence of the critical frequency is suggested by the experimental results in Figures 14 and 15; however, further experimental results on this question are needed. Figures 16 and 17 show conclusively that the dynamic load-deflection curves and the dynamic stiffness depend on the static load present during measurements. Although these curves suggest that the dynamic stiffness attains a minimum value for a certain value of the static load, it cannot be said that this result has been definitely verified experimentally and further tests are necessary.

4.2.2 DETERMINATION OF THE PARAMETERS k_{00}, b, and e

Only a limited amount of numerical analysis has been done toward extracting the parameters k_{00}, b, e, ℓ_0, ℓ_2, and ℓ_4 from the aforementioned experimental data. These parameters depend on the radius of the vibrator baseplate and on the elastic parameters ν and G of the pavement-soil system. Therefore, the measured values of these parameters will depend on the type of vibrator used to make the measurements as well as on the elastic parameters of the pavement-soil system.

The parameters k_{00}, b, and e can be obtained by two methods:

a. If the dynamic load-deflection curves are sufficiently curved so as to allow the direct application of a curve-fit program as in the case of asphalt and weak concrete pavements, the parameters k_{00}, b, and e can be obtained directly from the load-deflection curves. A least-square polynomial fit program was developed which fits the dynamic load-deflection curves with an odd polynomial containing fifth-, third-, and first-order terms. This fitting procedure immediately determines α_1, α_2, and S_0 that appear in

Equation 3.22. The value of k_0 is then obtained from S_0 by using Equation 3.21 and appropriate values for the pavement mass and damping constant. Placing the values of α_1, α_2, S_0, and k_0 into Equations 3.25 and 3.26 immediately gives the values of b and e. The values of k_{00} and x_e are then obtained from a simultaneous solution of Equations 3.4 and 3.15.

b. The dynamic load-deflection curves for very rigid pavements are essentially straight lines. The dynamic load-deflection curves are measured for a series of static loads by using a vibrator with a variable static force. The dynamic stiffness is determined from the slope of the dynamic load-deflection curves. Because the slope is essentially independent of the dynamic load, it follows from Equation 3.23 that $S \approx S_0(\omega,F_s)$, so that the measured dynamic stiffness value immediately determines $S_0(\omega,F_s)$. The function $k_0(F_s)$ is then determined from $S_0(\omega,F_s)$ by using Equation 3.21. The function $k_0(F_s)$ is then fitted to the expression in Equation 3.15 after x_e has been expressed in terms of F_s by using Equation 3.2. This fitting procedure determines k_{00}, b, and e.

Method a can be used for those pavements which have dynamic load-deflection curves that are sufficiently curved to be able to obtain α_1, α_2, and S_0 directly from a least-squares program. This is not generally the case for very strong PCC pavements. For very rigid pavements, method b should be used because the dynamic load-deflection curves are essentially straight lines. Computer programs have been developed which calculate the parameters k_{00}, b, and e directly from the measured dynamic load deflection curves using method a. No numerical work has been done applying method b to the rigid pavement. Figures 22, 23, and 24 give the values of k_{00}, b, and e, respectively, that were determined by method a from the measured dynamic load-deflection curves for a series of baseplate radii. The existence of the first critical radius can be established from the abrupt change in slope of the function $k_{00}(a)$ for $a = a_{c1}$. Method a was applied to the dynamic load-deflection curves of a rigid pavement and a flexible pavement. The considerable scatter in the results for b and e for the rigid and flexible pavements probably reflects the difficulty of determining the curvature of the dynamic load-deflection curves which may contain some experimental error. The large scatter in the experimentally

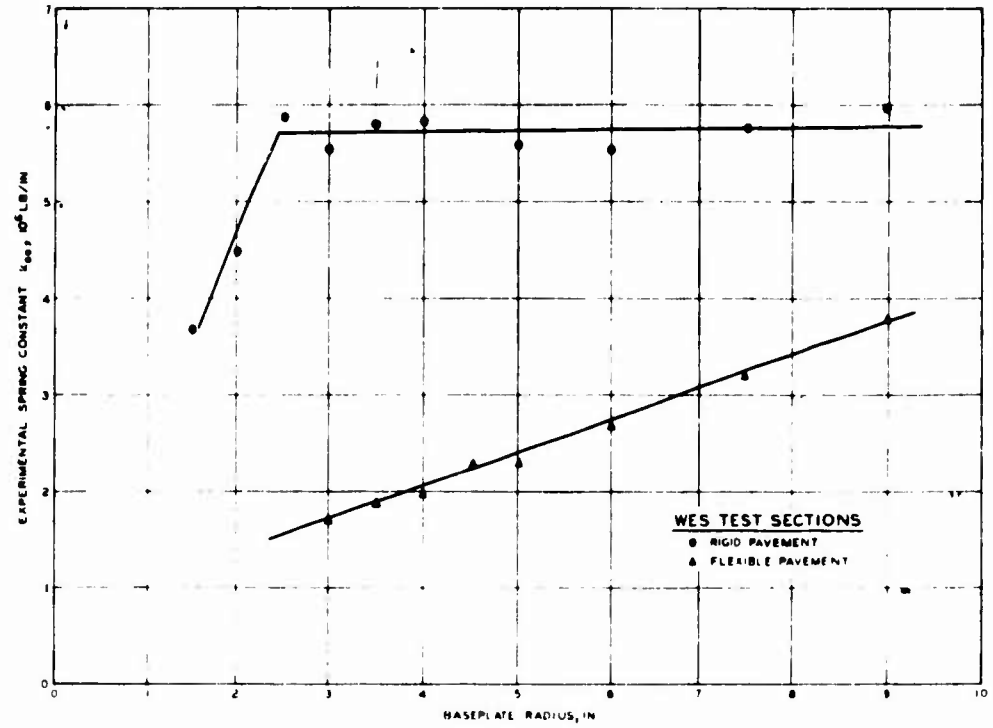

Figure 22. Experimentally derived values of the parameter k_{00} versus baseplate radius

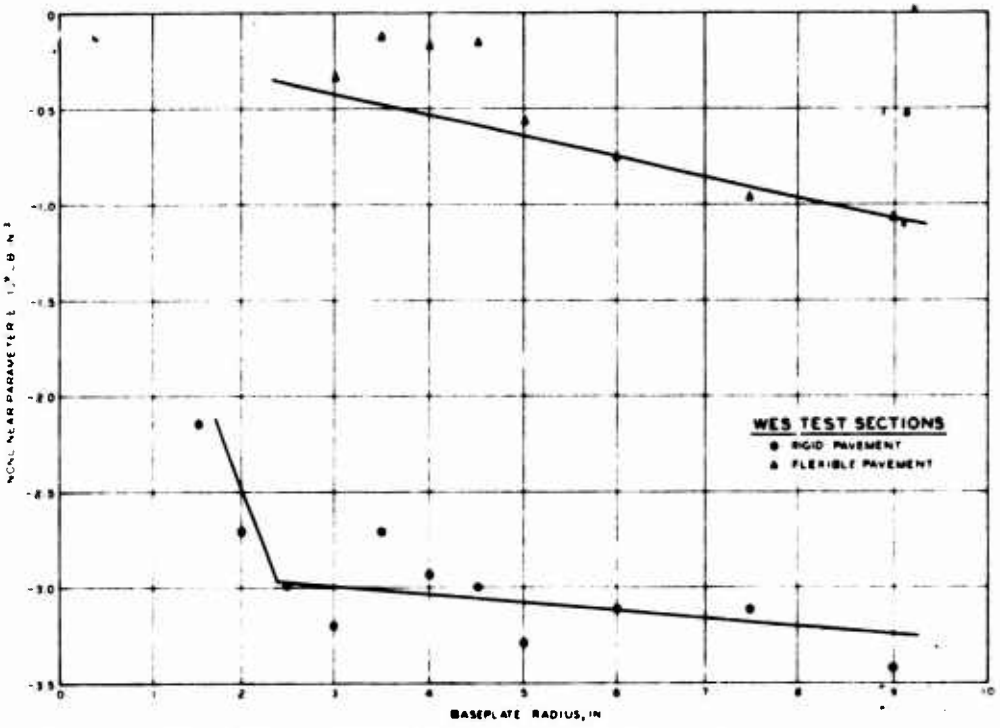

Figure 23. Experimentally derived values of the parameter b versus baseplate radius

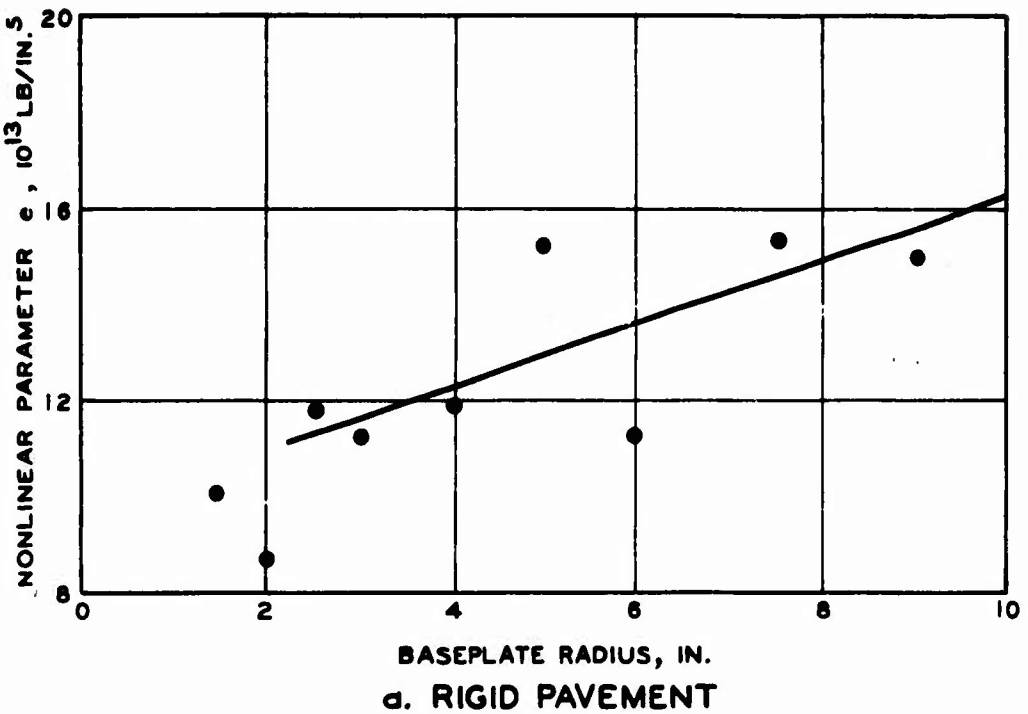

a. RIGID PAVEMENT

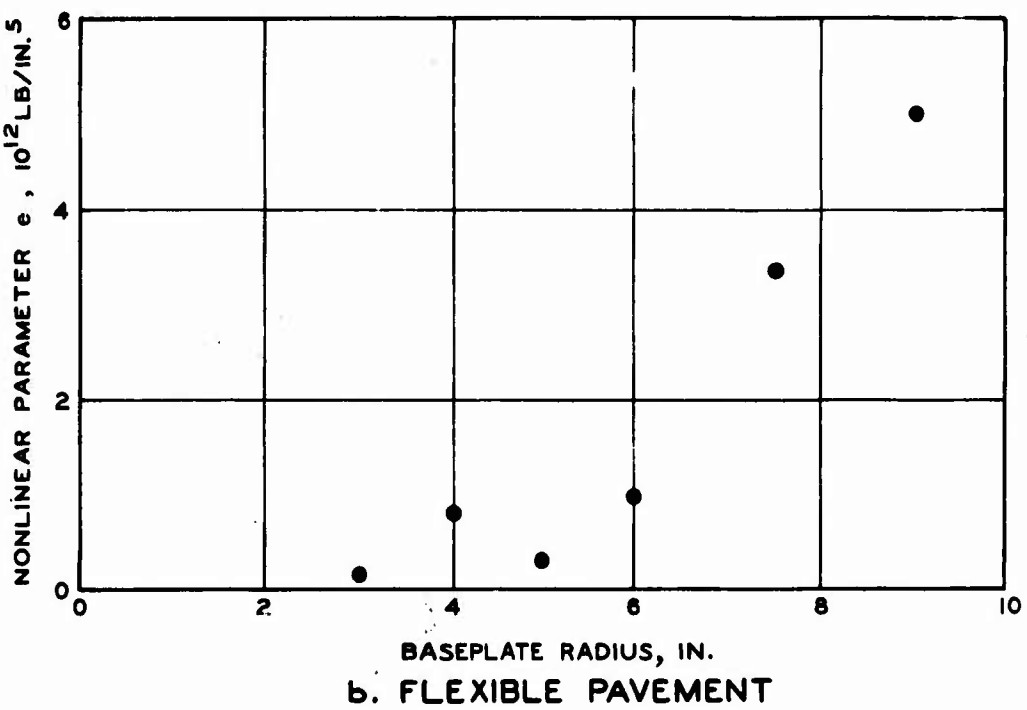

b. FLEXIBLE PAVEMENT

Figure 24 Experimentally derived values of the parameter e versus baseplate radius

derived values of the parameters b and e probably means that only the experimentally derived values of k_{00} for a series of baseplate sizes will be useful for calculating pavement structure.

The values of ℓ_0 can be calculated from Equations 3.103-3.107 provided the Poisson's ratio of each layer of the pavement system is known and provided the values of the critical radii are known. The values of ℓ_2 and ℓ_4 can be obtained in terms of the values of b and e given in Sections 3.7.2-3.7.5, provided the shear modulus and layer thickness are known for each layer contained within the static finite depth of influence. The experimental values of ℓ_0, ℓ_2, and ℓ_4 appear in Figures 25, 26, and 27, respectively. The results in Figure 25 show that ℓ_0 is larger for rigid than for flexible pavements. The large scatter in the values of ℓ_2 and ℓ_4 are probably due to experimental variations in the curvature of the dynamic load-deflection curves. Typical values of k_{00}, b, e, ℓ_0, ℓ_2, and ℓ_4 for the WES 16-kip vibrator with an 18-in.-diam baseplate are given in Table 5.

4.2.3 DETERMINATION OF THE SHEAR MODULI AND THICKNESSES OF PAVEMENT LAYERS

The thickness of each pavement layer can be determined using Equations 3.108-3.110, and the shear modulus of each layer can be determined by using Equations 3.117-3.123. These equations require Poisson's ratio of each pavement layer, the critical radii, and the function $k_{00}(a)$ as input variables. The critical radii are determined by measuring the dynamic load-deflection curves for a series of baseplate sizes and noting the particular values of the baseplate radius at which abrupt changes occur in the slope of the curve showing dynamic stiffness versus baseplate radius. The critical radii can also be obtained by noting the values of the baseplate radius at which abrupt changes in the slope of $k_{00}(a)$ occur. Table 6 gives the values of critical radii, layer thicknesses, and shear moduli corresponding to the experimental data shown in Figure 21. Only the first critical radius was measured experimentally for the rigid pavement, and only the second critical radius was observed

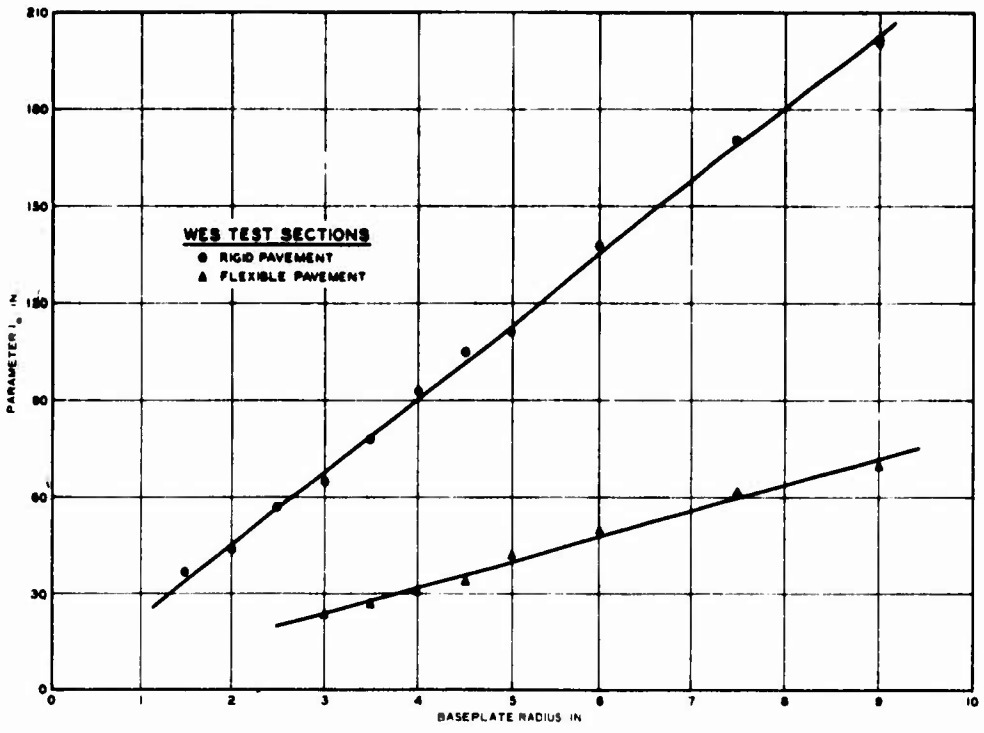

Figure 25. Experimentally derived values of the parameter ℓ_0 versus vibrator baseplate radius

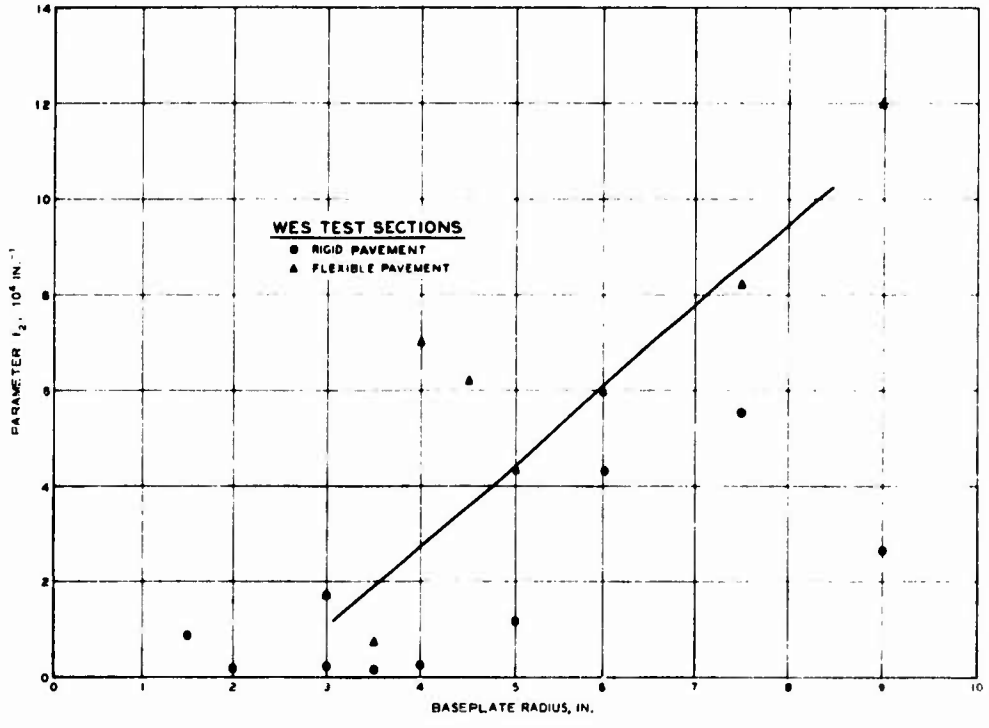

Figure 26. Experimentally derived values of the parameter ℓ_2 versus baseplate radius

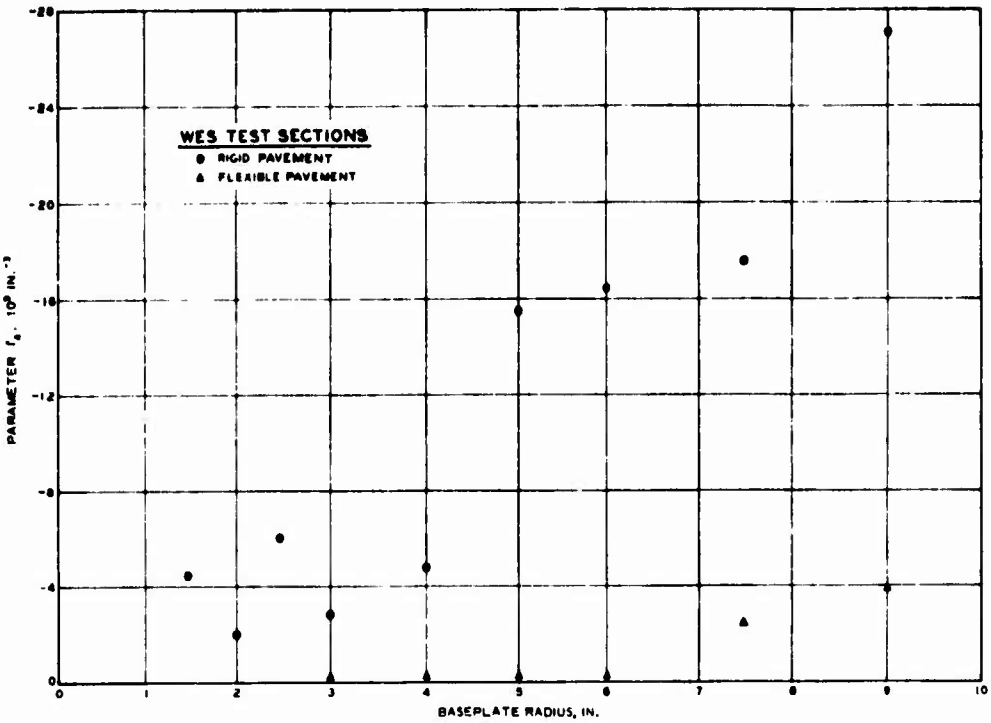

Figure 27. Experimentally derived values of the parameters ℓ_4 versus baseplate radius

Table 5

Approximate Numerical Values of the Parameters Appearing in the Nonlinear Pavement Model (WES 16-Kip Vibrator)

Parameter	Concrete Pavement	Asphaltic Concrete Pavement
k_{00}	8.0×10^6 lb/in.	2.0×10^6 lb/in.
b	-4.0×10^9 lb/in.^{3}	-1.3×10^9 lb/in.^{3}
e	2.0×10^{14} lb/in.^{5}	4.0×10^{12} lb/in.^{5}
ℓ_0	200 in.	72 in.
ℓ_2	1.0×10^5 in.$^{-1}$	2.0×10^4 in.$^{-1}$
ℓ_4	-3.0×10^{10} in.$^{-3}$	-3.5×10^7 in.$^{-3}$

Table 6

Experimental Values of the Parameters Describing the Subsurface Structure of Pavements at the WES Test Area

Parameter	Rigid Pavement	Flexible Pavement
First critical radius, a_{c1}	2.5 in.	Not measured
Second critical radius, a_{c2}	Not measured	6.0 in.
Thickness of pavement, h_1	15.0 in.	33.0 in.
Poisson's ratio, ν_1	0.25	0.35
Shear modulus, G_1	2.4×10^6 psi	3.7×10^4 psi
Compression modulus, E_1	6.0×10^6 psi	1.0×10^5 psi
Volume factor of the frustum of cone of stress, Ψ	3.8	3.8
Ratio of radii of frustum of cone of stress, κ	2.8	2.8

for the flexible pavement. The determination of the thickness of a thin upper layer of a rigid or flexible pavement requires the use of very small baseplate sizes. The shear failure of the flexible pavement prevented any tests using the WES-16 kip vibrator for a baseplate whose diameter was smaller than 3 in., and this prevented the measurement of the first critical radius for the flexible pavement at the WES test section.

The experimental data presented in Section 4.1.5 generally tend to confirm the existence of the critical radii that were introduced in Section 3.7.7. For the case of the rigid pavement shown in Figure 21, the abrupt change in the slope of the dynamic stiffness function for a baseplate radius of 2.5 in. is interpreted to mean that the value of the critical radius is 2.5 in. For this value of the baseplate radius, the zeroth term of the finite depth of influence, ℓ_0, as defined by Equations 3.103 and 3.108, is equal to the depth of the first interface which in this case is 15 in. The condition $\ell_0 = 15$ in. Combined with Equations 3.52, 3.103, and 3.108 give the values of Ψ and κ that appear in Table 6. The shear modulus of the upper pavement layer is calculated from the slope of the experimentally derived function $k_{00}(a)$ that appears in Figure 22 by using Equation 3.117.

4.2.4 ANOMALOUS VALUES OF DYNAMIC STIFFNESS

The difference in the values of the dynamic stiffness measured by the Dynaflect, Road Rater, CERF vibrator, and the WES 16-kip vibrator at the same pavement location is thought to be due to the different baseplate size, static load, and dynamic load used by these vibrators. The difference in the values of the measured dynamic stiffness can be considerable as has been described in Sections 4.1.6-4.1.8 and in Tables 2-4. The nonlinear mechanical model of the dynamic response of pavements to surface loads that was developed in Section 3 implies that the measured values of dynamic stiffness should depend on the baseplate radius, static load, and dynamic load of the vibrator that is used to make these measurements. This nonlinear mechanical model should be sufficient to correlate the different values of dynamic stiffness measured by

different sized vibrators at the same pavement location. However, no numerical studies of this correlation have been performed, and only qualitative results will be described.

Dynamic stiffness measurements were made at the same location using different vibrators in order to determine further the dependence of the measured values of the dynamic stiffness on the type of vibrator used to make the measurements. These measurements produced the unusual result that under some circumstances it is possible at the same pavement site to measure a larger value of dynamic stiffness with a small baseplate than with a large baseplate (Sections 4.1.8-4.1.10 and Tables 4-6). The nonlinear pavement model that was developed in Sections 3.5-3.8 attempts to explain these anomalous experimental results for the dynamic stiffness measurements.

For flexible pavements, a small part of the discrepancy between the values of dynamic stiffness measured by the WES 16-kip vibrator and those measured by the Dynaflect, Road Rater, and CERF vibrators at the same location is due to the fact that the values of dynamic stiffness presented for the WES 16-kip vibrator in Volume I of this report[15] were determined from the slope of the dynamic load-deflection curves in the region of large dynamic load (≈12 kips). These values of dynamic stiffness are considerably lower than the values that would be obtained from the region of lower dynamic load (Figure 11). Better agreement with the Dynaflect, Road Rater, and CERF vibrators would be obtained for flexible pavements if the values of dynamic stiffness measured by the WES 16-kip vibrator were obtained from that portion of the dynamic load-deflection curves where the dynamic load is comparable to the lower value produced by the other vibrators in question. Another contribution to the discrepancy between the values of dynamic stiffness measured by different vibrators at the same locations is due to the difference in operating frequency as indicated in Table 1.

Actually, the dependence of the measured values of the dynamic stiffness on the magnitude of the dynamic load of the vibrator plays only a part in the explanation of the anomalous dynamic stiffness measurements. This explanation of the anomalous values of the dynamic

stiffness measurements does not apply to strong rigid pavements whose dynamic load-deflection curves are essentially linear (Figure 12). In this case the dynamic stiffness is essentially independent of the magnitude of the dynamic load, and the explanation of the higher values of dynamic stiffness measured by a vibrator with a small baseplate contact radius (about 1 in. in the case of Dynaflect) compared to those measured using a vibrator with a large baseplate contact radius (about 9 in. in the case of the WES 16-kip vibrator) depends on the two nonlinear effects shown in Figure 4a and described in Section 3.8.2:

a. The spring constant k_0 is a function of F_s which has a local minimum value for a specific value of F_s.

b. The parameter k_{00} is not a linear function of baseplate contact radius for the case of a layered pavement structure which has a finite depth of influence, but is a very slowly increasing function of baseplate radius when the baseplate radius is larger than the first critical radius.

4.2.5 CALCULATION OF AVERAGED PARAMETERS FOR A NON-HOMOGENEOUS PAVEMENT

The static and dynamic stress and strain distribution in the pavement beneath the vibrator baseplate is three-dimensional in nature. The average values that are calculated in Equation 3.66 are based on an assumed one-dimensional distribution of strain in the pavement. Some experimental evidence on the relatively large surface deflection of pavements associated with an applied static load suggests that the average values that appears in Equation 3.66 should more properly be volume averages. To account for the volume averages, it is a simple matter to insert volume ratio factors for each layer thickness that appears in Equation 3.66. Each pavement layer is associated with a strain distribution which can be represented by a frustum of a cone. The ratios of the volume of the frustum of the cone in each pavement layer to the volume of the complete frustum of the cone of strain in the pavement and subgrade are the volume ratio factors that should replace the one-dimensional average that appears in Equations 3.66-3.99. The volume average tends to increase the effect of the subgrade as compared to that of the upper

pavement layers, and thereby gives a somewhat smaller net spring constant for a pavement than would be predicted by the one-dimensional average.

5. SUMMARY, CONCLUSIONS, AND RECOMMENDATIONS

5.1 SUMMARY

A nonlinear mechanical model describing the dynamic properties of a pavement-vibrator system has been developed which describes the nonlinear dynamic response of a pavement to a sinusoidal loading applied to the pavement surface. Theoretical expressions are developed for the dynamic stiffness of a pavement measured by a mechanical vibrator which are expressed in terms of the static load, dynamic load, and vibrator baseplate size and in terms of the linear and nonlinear pavement parameters. The nonlinear mechanical model gives an analytical correlation among the values of the dynamic stiffness measured by different vibrators at the same pavement location. The nonlinear parameters that characterize the dynamic pavement-restoring force are calculated in terms of the layered structure of the pavement-soil system and in terms of the finite depth of influence of the static load of the vibrator. The basic nonlinearity of the pavement system is used to determine the shear modulus and thickness of each pavement layer from the measured values of the dynamic stiffness for a series of baseplate sizes. Experimental tests were done to determine the validity of the theoretical pavement response model. The experimental and theoretical results are in good agreement.

5.2 CONCLUSIONS

The nonlinear mechanical model developed in this report gives the following conclusions:

a. Third- and fifth-order nonlinear terms in the displacement are required to describe the dynamic load-deflection response of actual pavement systems (Section 3.2).

b. The theoretical nonlinear oscillator model of pavement response to a dynamic loading shows that stiff pavements have a more linear dynamic load-deflection curve than flexible pavements (Section 3.5.3).

c. At specific critical frequencies the dynamic load-deflection curves become essentially linear at low values of the dynamic force (Section 3.5.4).

d. An explanation of the nonlinear response of pavement and soil systems requires a departure from linear elasticity and a finite depth of influence for a static load applied to the surface of a pavement (Section 3.6).

e. The linear and nonlinear parameters of the nonlinear pavement-restoring force, k_{00}, b, and e, can be described in terms of the elastic constants and thicknesses of the pavement layers. In general, b and e are discontinuous functions of the vibrator baseplate radius and have the properties $b < 0$ and $e > 0$, while k_{00} is a continuous and increasing function of the baseplate radius (Section 3.7).

f. The anomalous values of the dynamic stiffness wherein a vibrator with a small baseplate and a small static load can measure a larger dynamic stiffness value than a vibrator with a large baseplate and a large static load is explained in terms of the penetration of the finite depth of influence through the successive layers of the pavement system and in terms of the dependence of the dynamic stiffness on the static load (Section 3.8.2).

g. The measured value of the dynamic stiffness is not entirely a property of the pavement because it also depends on the size of the dynamic load, static load, and baseplate radius of the vibrator that is used to make the measurement. (Sections 3.4 and 3.5).

h. Critical values of the baseplate radius of the vibrator are expected to exist for which the dominant term of the static finite depth of influence passes through the various interfaces of the pavement layers. Abrupt changes in the slope of the dynamic stiffness versus baseplate radius function are expected to occur at the critical radii (Sections 3.7.7 and 3.7.8).

i. The variation of the dynamic stiffness with the vibrator baseplate radius is less rapid than is predicted by the linear elastic theory. For rigid pavements the dynamic stiffness is roughly independent of baseplate radius when the baseplate radius is larger than the first critical radius (Sections 3.7.8 and 3.8.2).

j. A determination of the elastic constants of each layer in a pavement system may be possible from dynamic stiffness measurements, but requires that the vibrator have the capability of varying the radius of its baseplate (Sections 3.7.7, 3.7.8, and 3.7.9).

k. The thickness of each pavement layer can be calculated in terms of the critical radii (Section 3.7.7).

A comparison of the theoretical and experimental results for the

dynamic load-deflection curves and the dynamic stiffness yields the following conclusions:

a. Some of the experimental dynamic load-deflection curves of pavements are nonlinear. This is especially true of more flexible AC pavements. The stiffer PCC pavements exhibit dynamic load-deflection curves that are only slightly nonlinear (Section 4.1).

b. Generally speaking, stiff pavements have dynamic load deflection curves which are more linear than those corresponding to more flexible pavements (Section 4.1.2 and Figure 11).

c. There is some evidence that the critical frequency exists and that it has a value of about 15 Hz for AC and PCC pavements (Sections 3.5.4, 3.5.5, and 4.1.3 and Figures 11, 14, and 15).

d. The value of the dynamic stiffness of a given pavement depends on the magnitude of the dynamic force static load, and baseplate size of the vibrator (Sections 3.4, 3.5, 3.8, 4.1.2, 4.1.4, 1.5, Figures 16-19, and Tables 2-4).

e. The measurement of dynamic load-deflection curves for a series of baseplate sizes allows the critical radii to be determined. The shear modulus and thickness of each pavement layer can be determined in terms of the critical radii, the measured values of dynamic stiffness in the intervals between the critical radii, and the assumed value of Poisson's ratio for each pavement layer (Sections 3.7.7, 3.7.9, and 4.1.7).

5.3 RECOMMENDATIONS

The positive conclusions of this report regarding the usefulness of a mechanical vibrator for determining the strength of pavements and their subsurface structure suggest that a more detailed study of the measured dynamic stiffness function be made.

5.3.1 DETERMINATION OF SUBSURFACE STRUCTURE

In this report only one case of a rigid pavement and one case of a flexible pavement were used for the determination of the shear modulus and thickness of each pavement layer directly from the values of the dynamic load-deflection curves that were measured at the pavement surface using a mechanical vibrator with a variable baseplate size. It is suggested that many different test sites of known subsurface structure be tested with the purpose of validating the method of subsurface structure

determination which employs a variable baseplate size that is presented in Sections 3.7.7 and 3.7.9.

5.3.2 CORRELATION OF DYNAMIC STIFFNESS VALUES MEASURED BY DIFFERENT VIBRATORS

This report has determined the theoretical dependence of the dynamic stiffness values on the size of the dynamic load, static load, and baseplate radius that are used during the measurement of the dynamic stiffness of a pavement. This theoretical dependence enables the values of the dynamic stiffness measured by different vibrators to be compared. A more detailed numerical study should be performed to validate the capability of analytically correlating the values of the dynamic stiffness measured by different vibrators at the same pavement location.

5.3.3 SELECTION OF VIBRATOR

The mechanical vibrators that are used to evaluate pavements nondestructively should be viewed as scientific instruments that are used to determine the nature and structure of pavement systems. Each pavement and its corresponding operational traffic will require its own specific vibrator characteristics if the nondestructive testing is to be accomplished optimally. From the conclusions of this report it follows that optimal operating conditions can be obtained only if the vibrator has the capability of:

a. Applying a series of static loads.

b. Generating a series of dynamic loads over a range of constant frequencies.

c. Operating in a frequency range which includes the critical frequency.

d. Applying a series of baseplate sizes to the pavement.

It is recommended that the construction of a new vibrator should include the capability of easy changes of baseplate size and magnitude of the static and dynamic loads applied to the pavement surface.

REFERENCES

1. Hall, J. W., Jr., "Nondestructive Testing of Pavements: Tests on Multiple-Wheel Heavy Gear Load Sections at Eglin and Hurlburt Airfields," Technical Report No. AFWL-TR-71-64, Mar 1972, Air Force Weapons Laboratory, Kirtland Air Force Base, N. Mex.

2. _____, "Nondestructive Testing of Pavements: Final Test Results and Evaluation Procedure," Technical Report No. AFWL-TR-72-151, Jun 1973, Air Force Weapons Laboratory, Kirtland Air Force Base, N. Mex.

3. Balakrishna Rao, H. A., "Nondestructive Evaluation of Airfield Pavements (Phase I)," Technical Report No. AFWL-TR-71-75, Dec 1971, Air Force Weapons Laboratory, Kirtland Air Force Base, N. Mex.

4. Lysmer, J., "Vertical Motion of Rigid Footings," Contract Report No. 3-115, Jun 1965, U. S. Army Engineer Waterways Experiment Station, CE, Vicksburg, Miss.; prepared by University of Michigan under Contract No. DA-22-079-eng-340.

5. Rocard, Y., General Dynamics of Vibrations, Ungar Publishing Co., New York, 1960.

6. McLachlan, N. W., Theory of Vibrations, Dover Publications, New York, 1951.

7. Turnbull, H. W., Theory of Equations, Interscience, New York, 1957.

8. Harr, M. E., Foundations of Theoretical Soil Mechanics, McGraw-Hill, New York, 1966.

9. Jumikis, A. R., Theoretical Soil Mechanics, Van Nostrand, New York, 1969.

10. Rostovtsev, N. A. and Khranevskaia, I. E., "The Solutions of the Boussinesq Problem for a Half-Space Whose Modulus of Elasticity Is a Power Function of the Depth," PMM, Vol 35, No. 6, 1971, pp 1000-1009.

11. Brown, P. T. and Gibson, R. E., "Surface Settlement of a Deep Elastic Stratum Whose Modulus Increases Linearly with Depth," Canadian Geotechnical Journal, Vol 9, 1972, pp 467-476.

12. Sneddon, I. E., Fourier Transforms, McGraw-Hill, New York, 1951.

13. Westergaard, H. M., Theory of Elasticity and Plasticity, Harvard University Press, Cambridge, 1952.

14. Sommerfeld, A., Lectures on Theoretical Physics; Mechanics of Deformable Bodies, Vol 2, Academic Press, New York, 1950.

15. Green, J. L. and Hall, J. W., "Nondestructive Vibratory Testing of Airport Pavements, Volume I: Experimental Test Results and Development of Evaluation Methodology and Procedure," Technical Report FAA-RD-73-205-I, in preparation, Department of Transportation,

Federal Aviation Administration, Systems Research and Development Service, Washington, D. C.

16. Balakrinshna Rao, H. A., "Results of Nondestructive Tests at Kelly Air Force Base (W.O.6.16C)," Letter Report IV, University of New Mexico, Albuquerque, N. Mex.

17. _____, "Results of Nondestructive Tests at Webb Air Force Base (W.O.6.16C)," Letter Report III, University of New Mexico, Albuquerque, N. Mex.

GPO 891-033